三重水研報　第 31 号　令和 7 年 2 月
Bull. Mie Pref. Fish. Res. Inst. **31** 1–66 (2025)

Stock assessment of the *Ammodytes japonicus* population in Ise Bay using a model integrating catch and body length data

KAZUHIRO HANYU

Keywords: Bayes estimation, fishing gear efficiency, high water temperature, Kuroshio path, recruits

SUMMARY

1. This study examined the following four issues of the *Ammodytes japonicus* fishery in Ise Bay: (1) the development of an integrated model to estimate the stock abundance accounting for the effects of recruitment during the fishing season and daily variations in fishing gear efficiency, (2) re-estimation of the initial and final stock abundances in each year using the integrated model and comparison with published estimates, (3) analysis of the effects of environmental factors, such as condition factor (feeding environment), water temperature, dissolved oxygen concentration, and the Kuroshio path, on the stock fluctuation, and (4) exploring prospects for the stock assessment and management.
2. DeLury's and Phiri's models, which have been used to estimate published estimates, tend to overestimate the final stock abundance under conditions of daily variation in fishing gear efficiency and large recruits during the fishing season, as observed in the *A. japonicus* fishery in Ise Bay. However, the integrated model in this study tended to be less biased under such conditions.
3. Although published estimates of the final stock abundance exceeded the reference point (2 billion fish) over many years, those estimated using the integrated model were less than 2 billion fish. Despite the sharp decline in *A. japonicus* stock abundance since 2015, several years before 2015 revealed lower final stock abundance than in 2014 and 2015. In addition, the Ricker and Beverton–Holt reproductive relationships models did not fit well with the integrated model estimates, making it difficult to identify an appropriate reference point. Therefore, the current reference points may lack validity.
4. The effects of water temperature and the Kuroshio path on *A. japonicus* stock fluctuations were detected. The declining and non-recovering trend of stock abundance in Ise Bay since the 2010s may be attributed to high water temperatures and Kuroshio path changes.
5. Current stock assessment and management measures may not have the expected management effects owing to the low accuracy of stock abundance estimation, high fishing pressure, and ambiguous reproduction relationships. In the future, as environmental conditions improve and a stock recovery trend is observed, revising stock assessment and management measures based on the results of this study is necessary.

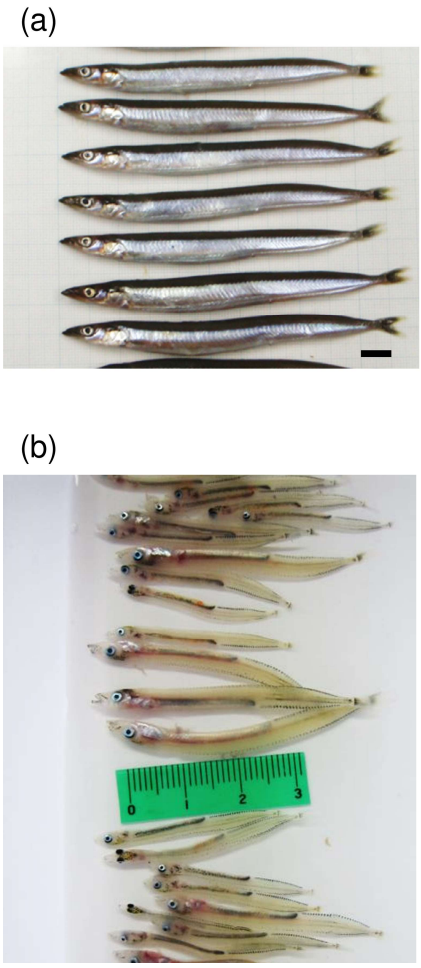

Fig. 1. Photographs of *Ammodytes japonicus* in Ise Bay. Photo (a): adults; Scale bar: 1 cm; Date: January 12, 2010. Photo (b): juveniles; Scale unit: cm; Date: March 8, 2016.

INTRODUCTION

The sand lance *Ammodytes japonicus* in Ise Bay (Fig. 1) is an important target species for fisheries in the Mie and Aichi prefectures. *A. japonicus* young (including juveniles) have been captured from February to May over several years (Funakoshi 1991; Itokawa 1983). The young inhabit Ise Bay, migrating outside the bay after the fishing season. They estivate in the sandy bottoms near the mouth of the bay (habitat names: Deyama, Segiyose, and Tainoshima; Fig. 2) to avoid high water temperatures in summer. During this period, the young mature at the bottom and do not feed until the end of estivation. Spawning occurs around the bottom of the bay at the beginning of winter (Itokawa 1978a, 1978b, 1983; Nishimura et al. 1991; Yamada 2011). Fisheries relationships have managed the remains of young abundance using DeLury's model (DeLury 1947) or Phiri's model (Phiri et al. 1999) daily during the fishing season every year (Yamamoto et al. 2019).

The reference point for the stock abundance remaining on the day after the final day of the fishing season in each year (final stock abundance) was 10 oku fish (1 billion fish) until 2006, which has been 20 oku fish since 2007 (Yamamoto et al. 2019). The reference point was determined assuming Ricker's model (Ricker 1954) and Beverton–Holt's model (Beverton and Holt 1957) between the adults and the young of the following year (Funakoshi et al. 1997; Itokawa 1983; Yamada 2011). This has been accepted and practiced by fisheries relations for many years. However, stock abundance has declined since 2015. No trend of recovery in abundance has been observed, although fisheries relations have banned catching *A. japonicus* since 2016.

Published estimates of the final stock abundances in 2014 and 2015 were 48 and 33 oku fish, respectively (Yamamoto et al. 2019), which were higher than the reference values. Additionally, the survival rates of *A. japonicus* estivating Deyama were low in both years (Nakamura et al. 2017). Therefore, the cause of the decline was not likely overfishing but some environmental factors (high water temperature, Kuroshio path, and predation) that may have prevented the estivating fish from oversummering, thereby disrupting their reproductive relationships (Nakamura et al. 2017).

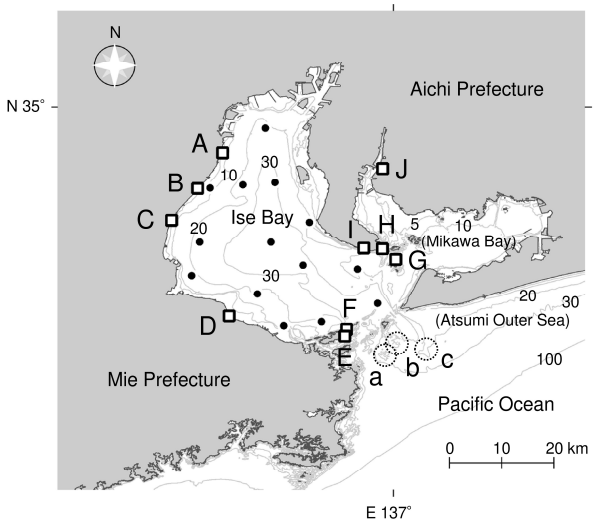

Fig. 2. Locations of fishing ports, *Ammodytes japonicus* estivation areas, and water temperature and dissolved oxygen concentration measurement points in Ise Bay, central Japan. Rectangles represent fishing ports: Kusu (A); Shiroko (B); Shiratsuka (C); Oizu (D); Toshi (E); Waguura (F); Shinojima (G); Morozaki (H); Toyohama (I); Ohama (J). Dotted circles represent estivation areas of *A. japonicus* in Ise Bay: Tainoshima (a); Segiyose (b); Deyama (c). Solid circle represents the water temperature and dissolved oxygen concentration measurement point. Solid line and number: water depth.

However, some studies have highlighted the following issue related to stock assessment and management based on the reference point (Funakoshi et al. 1997; Yamada 2011; Yamada et al. 1995): the reference point is tentative because the reproductive relationship is unclear; therefore, to accelerate stock recovery, it is recommended to immediately initiate stock management, even if the reference point is tentative, and the validity of the reference point should be evaluated. However, previous studies have not comprehensively examined the effect of reference points on stock assessment and management. To examine the validity of the reference point, I collected original data to calculate the published estimates. Consequently, the following three issues were identified in published estimates from 1979 to 2015:

The first issue was the ambiguity in the correction of fishing efforts based on fishing hours. The stock abundances for 2014 and 2015 were estimated based on fishing efforts (number of vessels) corrected for fishing

hours. However, whether the published estimates were corrected for hours before 2013 is unknown. Published estimates may contain biases caused by the estimation method. Therefore, determining the environmental factors affecting stock abundance based on interannual changes in the published estimates may be challenging.

The second issue was the difficulty in considering the effect of recruits during the fishing season. DeLury's model assumes that there is no recruitment during the fishing season and that a proportional relationship exists between stock abundance and catch per unit effort (CPUE) (DeLury, 1947). However, the body length composition of fish caught in Ise Bay in 1988 and 1998 changed from unimodal in February to multimodal in March (Mukai et al. 1988; Tomiyama and Nakamura 1998; Tsumoto and Itokawa 1989). These changes in length composition may represent the process by which a portion of unrecruited fish is recruited to the target stock during the fishing season. Descriptions such as 'main group,' 'first group,' and 'late group' are found in the published reports from other years (Hayashi 1985; Nakajima et al. 1986; Nishimura et al. 1993; Yamada et al. 1999b; Yamada et al. 2001). Therefore, assuming that there are numerous recruits after the first day of the fishing season in the *A. japonicus* fishery in Ise Bay is reasonable. In 1988, the body length of fish caught in the middle of the fishing season was shorter than that of fish caught on the first fishing day, and the CPUE varied widely during the fishing season, indicating that many fish were recruited during the fishing season (Tsumoto and Itokawa 1989). Because the recruitment period was divided into the first and second halves of the fishing season in 1988, the analysis period was divided into the first and second halves, and the initial and final stock abundances were estimated using DeLury's model for each half-period (Tsumoto and Itokawa 1989). However, the timing of recruitment could not be easily identified for other years. Whether the published estimates were overestimated (or underestimated) due to recruitment during the fishing season in most years is unknown.

Third, the confidence intervals of the published estimates were unclear. The initial stock abundances of *A. japonicus* fishery in Ise Bay from 1979 to 2003 were estimated using Phiri's model, and their confidence intervals were determined (Yamada 2011). When the caught fish abundance is known, the confidence interval of the final stock abundance can be calculated by subtracting the cumulative catch from the confidence interval of the initial stock abundance for each year. In contrast, for 2004 and later years, descriptions of confidence intervals in the published reports (Fujita et al. 2006, 2007, 2009; Fujiwara et al. 2010, 2011, 2012; Fujiwara and Simizu 2013; Hayashi et al. 2014, 2015, 2016, 2017; Kamiya et al. 2008; Tsumoto et al. 2005) and their unpublished materials could not be confirmed. Whether the lower confidence interval limit for the final stock abundance has been confirmed in reference point operations since 2004 remains unclear.

Although the above problems were identified, two additional types of observed data have not been used in conventional analysis. The first includes data on the number of fishing vessels and catches by prefecture. As fishing time is affected by the distance to the fishing grounds (their locations vary with time), the variation in the catches by prefecture may contain information on fishing time (Hayashi et al. 2014), which could be valuable in correcting fishing efforts. The second was the body length composition of the caught fish. As mentioned above, body length compositions provide recruitment information, and their use can help identify recruits during the fishing season. In this study, a model was developed to solve the problem of estimation bias owing to daily variation in fishing effort and recruits during the fishing season, which integrates these additional observed data to estimate stock abundances. Second, the initial and final stock abundances of *A. japonicus* fishery in Ise Bay were estimated using an integrated model, and the estimates were compared with published estimates. Third, the relationships between the estimates using the integrated model and the values of environmental factors were analyzed. Finally, stock assessment and management were explored.

MATERIALS AND METHODS

1. Data collection

Data were collected on *A. japonicus* catches and the number of fishing vessels operating daily in Ise Bay from 1993 to 2015 from the Mie Prefecture Fisheries Research Institute and the Aichi Fisheries Research Institute. The

landing ports in Mie Prefecture were Kusu, Shiroko, Shiratsuka (including Kawage), Oizu, Toshi, and Waguura, and those in Aichi Prefecture were Shinojima, Morozaki, Toyohama, and Ohama (Fig. 2). The catches and number of fishing vessels used in this study were based on data from all of these landing ports, which were aggregated in the Mie and Aichi prefectures. Additionally, unpublished data on body length composition and mean body weight for the catches was obtained from the Mie Prefecture Fisheries Research Institute and the Mie Prefecture Tsu Agriculture, Forestry, and Fisheries Office. The composition and weight data were obtained from a portion of the catch that landed at the ports of Shiroko and Shiratsuka (Table 1). The two ports have landings on almost all fishing days, accounting for most landings in Mie Prefecture. These data were treated as representative of *A. japonicus* catches in Ise Bay.

Table 1. Summary of collected data for the *Ammodytes japonicus* fishery in Ise Bay from 1993 to 2015

Year	First fishing date	Last fishing date	Days of fishing season	Fishing days		Maximum number of fishing vessels per day[*1]		Survey[*2]	
				Mie	Aichi	Mie	Aichi	Number of sampled buckets	Measured fish number per bucket
1993	Feb. 12	May 9	87	41	34	97	168	125	100
1994	Feb. 27	Apr. 29	62	25	15	99	166	112	100
1995	Mar. 29	May 14	47	20	11	90	160	111	100
1996	Mar. 3	May 19	78	39	24	85	163	323	100
1997	Mar. 6	Apr. 30	56	27	20	88	163	295	100
1998	Feb. 22	Mar. 30	37	12	11	84	156	175	100
1999	Mar. 7	May 13	68	31	24	93	161	264	100
2000	Mar. 6	Mar. 31	26	7	7	81	131	127	100
2001	Mar. 6	May 24	80	39	35	89	134	380	100
2002	Feb. 24	May 30	96	40	41	93	129	503	100
2003	Feb. 22	Apr. 29	67	29	15	85	127	313	100
2004	Mar. 4	May 28	86	36	34	78	125	259	100
2005	Mar. 8	May 29	83	39	18	75	125	229	100
2006	Mar. 9	Jun. 18	102	50	30	78	125	419	100
2007	Feb. 27	Apr. 30	63	34	31	67	121	373	100
2008	Mar. 2	Apr. 30	60	20	26	66	123	293	100
2009	Mar. 8	Mar. 25	18	4	4	58	117	75	100
2010	Mar. 3	Jun. 9	99	54	43	59	116	532	100
2011	Mar. 11	May 26	77	29	28	58	116	255	100
2012	Mar. 8	Jun. 7	92	40	30	53	113	397	100
2013	Feb. 28	Jun. 2	95	35	15	49	114	401	100
2014	Mar. 2	May 15	75	36	27	49	114	274	50
2015	Mar. 6	Mar. 31	26	10	7	43	111	121	50

[*1] Unit: tou. [*2] The surveys were conducted by the Mie Prefecture Fisheries Research Institute and Mie Prefecture Tsu Agriculture, Forestry and Fisheries Office.

2. Modeling

An integrated model was developed that modified DeLury's and Phiri's models. In the following section, the conventional models are outlined, and then the integrated model is described. Variables and parameters are shown in italics, and their vectors and matrices are shown in italics bold gothic.

1) DeLury's model

Assume that the catch on day t (c_t) reduces the stock abundance immediately before fishing on day t (N_t) and that the remainder represents the stock abundance immediately before fishing on day $t + 1$ (N_{t+1}). This process can be expressed as follows:

$$N_{t+1} = N_t - c_t. \tag{1}$$

Equation (1) can be rewritten using the stock abundance immediately before the fishing on day $t = 1$ (i.e., initial stock abundance, λ_1) as follows:

$$N_{t+1} = \lambda_1 - \sum_{j=1}^{t} c_j, \tag{2}$$

where c_j is the catch on day j, and the second term on the right side is the cumulative catch from day 1 to t.

Substituting Equation (1) into Equation (2), Equation (2) can also be expressed as follows:

$$N_t = \lambda_1 - \sum_{j=1}^{t-1} c_j. \tag{3}$$

Assuming that the stock abundance index on day t (U_t) has the following relationship with stock abundance (N_t):

$$U_t = \theta N_t, \tag{4}$$

where θ is a proportionality coefficient and is assumed to be positive.

Equation (3) is substituted into Equation (4), and the coefficients are replaced as follows:

$$U_t = b_0 + b_1 I_t, \tag{5}$$

where $b_0 = \theta\lambda_1$, $b_1 = -\theta$, $I_t = \sum_{j=1}^{t-1} c_j$.

When the effort on day t (x_t) and catch on day t (c_t) are known, the CPUE is c_t / x_t. Assume that c_t / x_t is available as an observed value of U_t (u_t) and that u_t follows a normal distribution with the mean U_t and the variance σ_U^2 as follows:

$$u_t \sim \text{Normal}\left(U_t, \sigma_U^2\right). \tag{6}$$

Assuming that σ_U^2 is constant regardless of U_t, b_0 and b_1 are obtained by the least square, maximum likelihood, or Bayesian methods based on Equation (6). In addition, λ_1 is obtained by the following equation.

$$\lambda_1 = -b_0 / b_1, \tag{7}$$

where, $b_1 < 0$ and therefore $b_0 > 0$.

If day T is the last day of fishing in a year, the final stock abundance in the year is N_{T+1}, which is the stock abundance immediately before fishing on day $T + 1$, and is determined using Equation (2) as follows:

$$N_{T+1} = \lambda_1 - \sum_{j=1}^{T} c_j. \tag{8}$$

In the stock assessment of *A. japonicus* young in Ise Bay, the number of buckets (Fig. 3) containing fish on day t (o_t), the mean weight of fish caught on day t ($\overline{w}_t$, unit: g), and the number of fishing vessels on day t (x_t, unit: tou) were observed in the Mie and Aichi prefectures. These were used to convert c_t (unit: oku fish, which equals 100 million fish) and x_t into c_t / x_t, and c_t / x_t was used as u_t in Equation (6):

Fig. 3. Photograph of buckets used to hold fish caught by the *Ammodytes japonicus* fishery in Mie Prefecture. Each bucket, called 'oke' in Japanese, contains 30 kg of fish.

$$u_t = c_t / x_t, \quad (9)$$

$$c_t = \left(\frac{30\, o_{t,\mathrm{Mie}}}{\overline{w}_{t,\mathrm{Mie}}} + \frac{18\, o_{t,\mathrm{Aichi}}}{\overline{w}_{t,\mathrm{Aichi}}} \right) \frac{10^3}{10^8}, \quad (10)$$

$$x_t = x_{t,\mathrm{Mie}} + x_{t,\mathrm{Aichi}}, \quad (11)$$

where 30 and 18 are the weights (kg) of catches per bucket in the Mie and Aichi prefectures, respectively. $\overline{w}_{t,\mathrm{Mie}}$ and $\overline{w}_{t,\mathrm{Aichi}}$ are the means per day based on the mean fish body weight per bucket (in Mie Prefecture, the means of 50–100 fish) and are known. Until 2002, the weight per bucket in Aichi Prefecture was 30.

Fishing hours in 2014 fluctuated daily, ranging from the minimum of 2.5 hours to the maximum of 5.5 hours. The initial stock abundance published in 2014 was estimated using DeLury's model based on the following corrected fishing effort:

$$x_t = \left(x_{t,\mathrm{Mie}} + x_{t,\mathrm{Aichi}} \right) \frac{3.5}{s_t}, \quad (12)$$

where s_t is a fishing time on day t and is known.

The estimate of the initial stock abundance using DeLury's model in 2014 was 310 oku fish based on Equation (11), and 279 oku fish in this study were based on Equation (12). The difference was 31 oku fish. In this study, the numbers based on Equations (11) and (12) for 2015 were estimated to be 135 and 84 oku fish, respectively. The difference was 51 oku fish. Thus, the presence or absence of corrections for fishing efforts by fishing time significantly affected the estimates. However, it may be insufficient to correct the fishing effort among the prefectures because the distances from ports to fishing grounds differ between prefectures (Hayashi et al. 2014). In addition, s_t is unknown for several years; the correction based on Equation (12) cannot be applied.

2) Phiri's model

Typically, the DeLury's model assumes an equal variance in observed CPUE (σ_U^2). However, the assumption of equal variances may not be valid for the *A. japonicus* fishery in Ise Bay because the observed CPUE often deviates significantly from the estimate, particularly at the beginning of the fishing season (Yamada 2011). Phiri's model assumes that such unequal variances are due to the spatial distribution of fish and that the variance of catch ($\sigma_{C_t}^2$) is related to C_t as follows, based on the Taylor's power law (Phiri et al. 1999; Yamada 2011):

$$\sigma_{C_t}^2 = \alpha C_t^{\beta}, \quad (13)$$

where α is the proportionality coefficient, and β is the degree of concentration of the fish distribution (Taylor 1961).

For C_t, assume the following (Yamada 2011):

$$C_t = N_t E_t, \quad (14)$$

$$E_t = 1 - \exp(-F_t), \quad (15)$$

$$F_t = q x_t, \quad (16)$$

where N_t is the stock abundance on day t in Equation (3), E_t is the exploitation rate on day t, F_t is the fishing coefficient on day t, and q is fishing gear efficiency. The x_t is the number of fishing vessels on day t and is known.

Assuming the observed catch (c_t) follow an appropriate distribution, such as a normal distribution with mean C_t and variance $\sigma_{C_t}^2$, it is possible to estimate α, β, q, and λ_1 by the maximum likelihood method or the Bayesian method. However, because Equation (13) is an exponential function of C_t, it is challenging to select the initial values at which the calculation converges using the maximum likelihood method. Therefore, C_t was transformed into the following variables (Phiri et al. 1999):

$$\mathrm{f}(C_t) = C_t^{1-\beta/2}. \quad (17)$$

Assuming that c_t follows a normal distribution with a mean C_t and variance $\sigma_{C_t}^2$, then, approximately, $c_t^{1-\beta/2}$ follows a normal distribution with a mean $C_t^{1-\beta/2}$ and variance $\sigma_{C_t^{1-\beta/2}}^2$ (Phiri et al. 1999; Yamada 2011):

$$C_t^{1-\beta/2} = (N_t E_t)^{1-\beta/2} - \frac{\alpha\beta(1-\beta/2)}{4\,(N_t E_t)^{1-\beta/2}}, \quad (18)$$

$$\sigma^2_{C_t^{1-\beta/2}} = \alpha(1-\beta/2)^2, \quad (19)$$

$$c_t^{1-\beta/2} \sim (1-\beta/2)c_t^{-\beta/2} \times \text{Normal}\left(C_t^{1-\beta/2}, \sigma^2_{C_t^{1-\beta/2}}\right). \quad (20)$$

Because the variance is constant in Equation (19), a more stable estimation can be expected than that in Equation (13). The maximum likelihood method or the Bayesian method based on Equation (20) can be used to estimate α, β, q, and λ_1. The final stock abundance can also be obtained using Equation (8). In the Bayesian estimation in this study, the prior distributions of α, β, q, and λ_1 were assumed to follow uniform distributions under constraints that $0 < \alpha$, $0 < \beta < 2$, $0 < q < 1$, and $0 < \lambda_1 < 10^4$, respectively. The upper limit of q was set to 1 for convenience as a sufficiently large value due to the convergence of the calculation. The upper limit of λ_1 was set to 10^4 for convenience as a value sufficiently larger than the maximum published estimate due to computational stability.

3) Integrated model

The integrated model is a state-space model with multiple states and observed processes (Fig. 4). In conventional models, the initial stock abundance is sometimes denoted as 'recruits' because it is assumed that there is no recruitment during the fishing season. In contrast, in the integrated model, recruitment is defined as the fish becoming the fishing target. Thus, the initial stock abundance included fish that were not targeted on the first fishing day, and the recruits on day t were the number of fish added to the target stock on day t (Fig. 5). In the integrated model, initial stock abundance and recruits have different meanings.

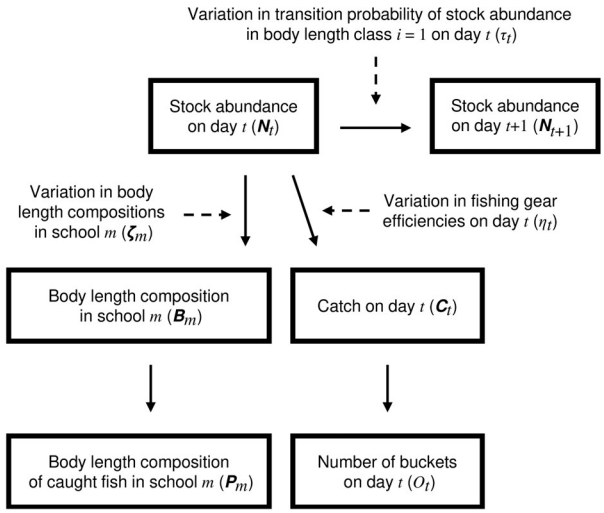

Fig. 4. State processes in the integrated model. Text: explanation of parameter; Solid arrow: transformation of parameters; Dotted arrow: insertion of a process variation.

(a) State process

Stock abundance by body length: The maximum body length of caught fish in *A. japonicus* fishery in Ise Bay from 1993 to 2015 was 117 mm (unpublished data). Therefore, I divided the body length from 0 to 120 mm in 10 mm increments and defined the stock abundance by

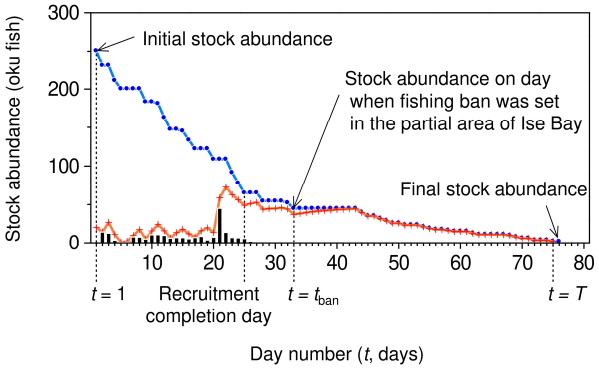

Fig. 5. Schematic diagram of the stock abundance definition in this study. Circle with blue line: stock abundance on day t (N_t); Cross with orange line: fishing target stock abundance on day t ($N_{t,\text{Target}}$); Bar: recruits on day t (R_t); t = 1: first fishing day; t = T: last fishing day; Recruitment completion day: a day when the accumulative recruitment rate exceeds 95%. Initial stock abundance: stock abundance on the day t = 1 (λ_1); Final stock abundance: stock abundance immediately after the last fishing day (N_{T+1}). The target stock abundance increases with the daily recruitment and decrease with fishing. The difference between N_t and $N_{t,\text{Target}}$ represents the abundance of non-target stock on day t ($N_{t,\text{Non-target}}$). These stock abundances were estimated using the integrated model. The abundances in the diagram show the actual estimates in 2014 for the *Ammodytes japonicus* fishery in Ise Bay.

body length immediately before fishing on the first day t = 1 ($\boldsymbol{N}_1$) as follows:

$$\boldsymbol{N}_1 = \begin{bmatrix} N_{1,1} \\ N_{2,1} \\ \vdots \\ N_{12,1} \end{bmatrix} = \lambda_1 \boldsymbol{\varphi}_1, \tag{21}$$

$$\boldsymbol{\varphi}_1 = \begin{bmatrix} \varphi_{1,1} \\ \varphi_{2,1} \\ \vdots \\ \varphi_{12,1} \end{bmatrix}, \tag{22}$$

where the first subscript term of each element in $\boldsymbol{N}_1$ (1–12), is a body length class number, λ_1 is the initial stock abundance (unit: oku fish), and $\boldsymbol{\varphi}_1$ is a composition of the initial stock abundance by body length. As mentioned above, note that $\boldsymbol{N}_1$, λ_1, and $\boldsymbol{\varphi}_1$ include the unrecruited fish.

The prior distribution of λ_1 in Equation (21) was assumed to follow a uniform distribution:

$$\lambda_1 \sim \text{Uniform}(0, 10^4). \tag{23}$$

The elements of Equation (22) were assumed to follow a Dirichlet distribution:

$$\boldsymbol{\varphi}_1 \sim \text{Dirichlet}(\boldsymbol{\pi}), \tag{24}$$

$$\boldsymbol{\pi} = \begin{bmatrix} \pi_1 \\ \pi_2 \\ \vdots \\ \pi_{12} \end{bmatrix} = \begin{bmatrix} 1 \\ 1 \\ \vdots \\ 1 \end{bmatrix}. \tag{25}$$

Stock abundance was assumed to decrease gradually with fishing, and the body length composition of $\boldsymbol{N}_t$ changed with growth. This process is expressed as follows:

$$\boldsymbol{N}_{t+1} = \begin{bmatrix} N_{1,t+1} \\ N_{2,t+1} \\ \vdots \\ N_{12,t+1} \end{bmatrix} = \boldsymbol{G}_t \left\{ \left(\begin{bmatrix} 1 \\ 1 \\ \vdots \\ 1 \end{bmatrix} - \boldsymbol{E}_t \right) \circ \boldsymbol{N}_t \right\}, \tag{26}$$

where $\boldsymbol{E}_t$ is a vector of exploitation rates by body length on day t and $\boldsymbol{G}_t$ is the transition probability matrix of body length compositions on day t. The ◦ denotes the multiplication of the elements of the vectors before and after the symbol (the Adamar product).

Exploitation rate by body length: $\boldsymbol{E}_t$ in Equation (26) is defined as follows:

$$\boldsymbol{E}_t = \begin{bmatrix} E_{1,t} \\ E_{2,t} \\ \vdots \\ E_{12,t} \end{bmatrix} = A_t \begin{bmatrix} D_1 \\ D_2 \\ \vdots \\ D_{12} \end{bmatrix}, \tag{27}$$

where A_t is the maximum exploitation rate on day t ($0 \leq A_t \leq 1$) and D_i is a selection probability in body length class i ($0 \leq D_i \leq 1$).

Based on Equations (15) and (16), A_t is defined as:

$$A_t = 1 - \exp\left(-F_{t,\text{Mie}} - F_{t,\text{Aichi}}\right), \tag{28}$$

where $F_{t,\text{Mie}}$ and $F_{t,\text{Aichi}}$ are the fishing coefficients on day t for fishing vessels in the Mie and Aichi prefectures, respectively.

The integrated model assumed that the fishing gear efficiency q in Equation (16) varied daily. That is, $F_{t,\text{Mie}}$ and $F_{t,\text{Aichi}}$ can be expressed as follows:

$$F_{t,\text{Mie}} = q_{t,\text{Mie}} x_{t,\text{Mie}}, \tag{29}$$

$$F_{t,\text{Aichi}} = q_{t,\text{Aichi}} x_{t,\text{Aichi}}, \tag{30}$$

$$q_{t,\text{Mie}} = \exp\left(\eta_0 + \eta_{t,\text{Mie}}\right), \tag{31}$$

$$q_{t,\text{Aichi}} = \exp\left(\eta_0 + \eta_{t,\text{Aichi}}\right), \tag{32}$$

where $q_{t,\text{Mie}}$and $q_{t,\text{Aichi}}$ are a fishing gear efficiency on day t for each prefecture, $\exp(\eta_0)$ is a mean gear efficiency, and $\eta_{t,\text{Mie}}$ and $\eta_{t,\text{Aichi}}$ are an effect of daily variation in the fishing gear efficiencies in each prefecture.

The η_0, $\eta_{t,\text{Mie}}$ and $\eta_{t,\text{Aichi}}$ in Equations (31) and (32) were assumed to follow prior distributions:

$$\eta_0 \sim \text{Uniform}(-\infty, 0), \tag{33}$$

$$\eta_{t,\text{Mie}} \sim \text{Normal}(0, \sigma_\eta^2), \tag{34}$$

$$\eta_{t,\text{Aichi}} \sim \text{Normal}(0, \sigma_\eta^2), \tag{35}$$

$$\sigma_\eta \sim \text{Cauchy}(0, 10)\ , \quad (\sigma_\eta > 0), \tag{36}$$

where σ_η is a parameter that controls the variation in the fishing gear efficiencies. The upper limit of η_0 was set to zero for convenience as a sufficiently large value due to computational stability.

The D_i in Equation (27) was obtained from the mesh selection model (Tokai and Mitsuhashi 1998) as follows:

$$D_i = \left\{1 + \exp\left[-\left(\frac{2\log(3)}{\sigma_l}\right)\mu_l + \left(\frac{2\log(3)}{\sigma_l}\right)l_i\right]\right\}^{-1}, \quad (37)$$

where μ_l is a body length (unit: mm) with a selection probability of 0.50, σ_l is a range (unit: mm) from selection probability 0.25 to 0.75. l_i is the median value (mm) for body length class i (1–12) in increments of 10 mm as follows:

$$l_i = 5 + 10 \times (i - 1). \quad (38)$$

The μ_l and σ_l in Equation (37) were assumed to follow a prior distribution, respectively:

$$\mu_l \sim \text{Uniform}(0, 120), \quad (39)$$
$$\sigma_l \sim \text{Uniform}(0, 120). \quad (40)$$

The exploitation rates by body length for each prefecture ($\boldsymbol{E}_{t,\text{Mie}}$ and $\boldsymbol{E}_{t,\text{Aichi}}$) were calculated by proportionally dividing Equation (27) by the fishing coefficient for each prefecture, as follows:

$$\boldsymbol{E}_{t,\text{Mie}} = \begin{bmatrix} E_{1,t,\text{Mie}} \\ E_{2,t,\text{Mie}} \\ \vdots \\ E_{12,t,\text{Mie}} \end{bmatrix} = \frac{F_{t,\text{Mie}}}{F_{t,\text{Mie}} + F_{t,\text{Aichi}}}\boldsymbol{E}_t, \quad (41)$$

$$\boldsymbol{E}_{t,\text{Aichi}} = \begin{bmatrix} E_{1,t,\text{Aichi}} \\ E_{2,t,\text{Aichi}} \\ \vdots \\ E_{12,t,\text{Aichi}} \end{bmatrix} = \frac{F_{t,\text{Aichi}}}{F_{t,\text{Mie}} + F_{t,\text{Aichi}}}\boldsymbol{E}_t. \quad (42)$$

Catches by body length for each prefecture ($\boldsymbol{C}_{t,\text{Mie}}$ and $\boldsymbol{C}_{t,\text{Aichi}}$) were determined using Equations (26), (41), and (42) as follows:

$$\boldsymbol{C}_{t,\text{Mie}} = \begin{bmatrix} C_{1,t,\text{Mie}} \\ C_{2,t,\text{Mie}} \\ \vdots \\ C_{12,t,\text{Mie}} \end{bmatrix} = \begin{bmatrix} N_{1,t}E_{1,t,\text{Mie}} \\ N_{2,t}E_{2,t,\text{Mie}} \\ \vdots \\ N_{12,t}E_{12,t,\text{Mie}} \end{bmatrix}, \quad (43)$$

$$\boldsymbol{C}_{t,\text{Aichi}} = \begin{bmatrix} C_{1,t,\text{Aichi}} \\ C_{2,t,\text{Aichi}} \\ \vdots \\ C_{12,t,\text{Aichi}} \end{bmatrix} = \begin{bmatrix} N_{1,t}E_{1,t,\text{Aichi}} \\ N_{2,t}E_{2,t,\text{Aichi}} \\ \vdots \\ N_{12,t}E_{12,t,\text{Aichi}} \end{bmatrix}. \quad (44)$$

Transition probability in body length composition: $\boldsymbol{G}_t$ in Equation (26) is defined as follows:

$$\boldsymbol{G}_t = \begin{bmatrix} G_{1,t} & 0 & \cdots & 0 \\ 1 - G_{1,t} & G_{2,t} & \cdots & 0 \\ 0 & 1 - G_{2,t} & \cdots & 0 \\ \vdots & \vdots & \cdots & \vdots \\ 0 & 0 & \cdots & 1 \end{bmatrix}, \quad (45)$$

where $G_{i,t}$ is the probability that body length does 'not' change from class i to the next class $i + 1$ during the transition from day t to day $t + 1$.

The transition probability due to the growth in $\boldsymbol{G}_t$ was assumed to be constant during the fishing season. However, the stock abundance in class $i = 1$ (body length range: 0–10 mm) may also include larvae transported to the bay after the first fishing day (Funakoshi et al. 1997). Therefore, the body length composition in class $i = 1$ was assumed to change because of transport. Based on these assumptions, $G_{i,t}$ is defined as follows:

for $i = 1$,
$$G_{i,t} = [1 + \exp(\omega_0 - \omega_i + \tau_t)]^{-1}, \quad (46)$$

for $2 \le i \le 11$,
$$G_{i,t} = [1 + \exp(\omega_0 - \omega_i)]^{-1}, \quad (47)$$

where $G_{i,t}$ is in the form of such a logistic curve, ω_0 is a growth coefficient common to all classes, and ω_i is a class difference in the growth. The τ_t is a coefficient for the larvae transported.

The ω_0, ω_i, and τ_t in Equations (46) and (47) were assumed to follow prior distributions:

$$\omega_0 \sim \text{Uniform}(-\infty, \infty), \quad (48)$$
$$\omega_i \sim \text{Normal}(0, \sigma_\omega^2), \quad (49)$$
$$\sigma_\omega \sim \text{Cauchy}(0, 10), \ (\sigma_\omega > 0). \quad (50)$$
$$\tau_t \sim \text{Normal}(0, \sigma_\tau^2), \quad (51)$$
$$\sigma_\tau \sim \text{Cauchy}(0, 10), \ (\sigma_\tau > 0). \quad (52)$$

Body length composition in school: The actual observations of the body length compositions of the caught fish followed the three-step sampling procedure described below.

First step: 1–25 fishing vessels were randomly selected for each fishing day.
Second step: one bucket was randomly selected from the buckets landed by each selected vessel (the total number of buckets was not recorded for each vessel).
Third step: from each selected bucket, 50–100 fish were randomly sampled, and their body lengths were measured with an accuracy of 1 mm.

Some of the observed body length compositions differed significantly among fishing vessels even though they were observed on the same day. This may be due to the differences in the selected fish schools by vessel and their length composition. Additionally, a vessel might have caught several schools, and their body length compositions differed among buckets. The latter effect was difficult to detect because only one bucket was sampled during the second sampling step. I assumed that the former effect was large and defined the state process variation in the selection of a school as follows:

First, based on Equation (26), the mean body length composition of the stock on day t ($\boldsymbol{H}_t$) was assumed to be

$$\boldsymbol{H}_t = \begin{bmatrix} H_{1,t} \\ H_{2,t} \\ \vdots \\ H_{12,t} \end{bmatrix} = \frac{1}{\sum_{i=1}^{12} N_{i,t}} \begin{bmatrix} N_{1,t} \\ N_{2,t} \\ \vdots \\ N_{12,t} \end{bmatrix}. \quad (53)$$

Second, the body length composition of school m selected by vessel ($\boldsymbol{B}_m$) was set as follows:

$$\boldsymbol{B}_m = \begin{bmatrix} B_{1,m} \\ B_{2,m} \\ \vdots \\ B_{12,m} \end{bmatrix} = \frac{1}{\sum_{i=1}^{12} \exp(V_{i,m})} \begin{bmatrix} \exp(V_{1,m}) \\ \exp(V_{2,m}) \\ \vdots \\ \exp(V_{12,m}) \end{bmatrix}, \quad (54)$$

where Equation (54) is in the form of a softmax function. $V_{i,m}$ is $\boldsymbol{H}_t$ transformed by the inverse of the softmax function with process variation as follows:

for $i = 1$,
$$V_{1,m} = 0, \quad (55)$$

for $2 \le i \le 12$,
$$V_{i,m} = \log(H_{i,t_m}) - \log(H_{1,t_m}) + \zeta_{i,m}, \quad (56)$$

where $\zeta_{i,m}$ is a variation of body length composition in class i of school m. t_m is the fishing day t when the school m was caught.

$\zeta_{i,m}$ in Equation (56) was assumed to follow a prior distribution:

$$\zeta_{i,m} \sim \text{Normal}(0, \sigma_\zeta^2), \quad (57)$$
$$\sigma_\zeta \sim \text{Cauchy}(0, 10), \ (\sigma_\zeta > 0), \quad (58)$$

where, σ_ζ is a standard deviation of the body length compositions between schools in the stock, which controls $\zeta_{i,m}$.

(b) Observation process

Body length composition of caught fish: Assuming that the fish in school m were caught at the exploitation rate on day t_m ($\boldsymbol{E}_{t_m}$), the body length composition of caught fish in school m ($\boldsymbol{P}_m$) was expressed by the following equation:

$$\boldsymbol{P}_m = \begin{bmatrix} P_{1,m} \\ P_{2,m} \\ \vdots \\ P_{12,m} \end{bmatrix} = \frac{1}{\sum_{i=1}^{12} (B_{i,m} E_{i,t_m})} \begin{bmatrix} B_{1,m}E_{1,t_m} \\ B_{2,m}E_{2,t_m} \\ \vdots \\ B_{12,m}E_{12,t_m} \end{bmatrix}. \quad (59)$$

The observed values for the body length composition

of the school m ($\boldsymbol{p}_m$), were the count numbers obtained by the three-step sampling mentioned above. This was assumed to follow a multinomial distribution.

$$\boldsymbol{p}_m \sim \text{Multinomial}(\boldsymbol{P}_m), \tag{60}$$

$$\boldsymbol{p}_m = \begin{bmatrix} p_{1,m} \\ p_{2,m} \\ \vdots \\ p_{12,m} \end{bmatrix}. \tag{61}$$

Bucket numbers: As shown in Equation (10), to estimate the stock abundance using conventional models, the numbers of buckets were converted to catches with units of oku fish using the mean body weights of the caught fish, which were considered as observed values. However, the actual observed values are the numbers of buckets, and catches in units of oku fish are unknown. By contrast, in the integrated model, the total number of fish landed at the ports of Mie Prefecture on day t ($C_{t,\text{Mie}}$) were estimated as $\sum_{i=1}^{12} C_{i,t,\text{Mie}}$, which is the sum of the elements in Equation (43). Therefore, in the integrated model, variables $C_{t,\text{Mie}}$ were converted into the number of buckets ($O_{t,\text{Mie}}$) using the following equation:

$$O_{t,\text{Mie}} = \overline{W}_{t,\text{Catch}} C_{t,\text{Mie}}\ 10^5\ 30^{-1}, \tag{62}$$

where $\overline{W}_{t,\text{Catch}}$ is the mean body weight of the caught fish (unit: g).

For $\overline{W}_{t,\text{Catch}}$ in Equation (62), the estimate from the following equation was used:

$$\overline{W}_{t,\text{Catch}} = \frac{\sum_{i=1}^{12} \left[\exp\left(\gamma_1 + \gamma_2 \log(l_i)\right) H_{i,t} E_{i,t}\right]}{\sum_{i=1}^{12} \left(H_{i,t} E_{i,t}\right)}, \tag{63}$$

where $\exp\left(\gamma_1 + \gamma_2 \log(l_i)\right)$ is a conversion equation from the median body length in class i to its body weight, where γ_1 and γ_2 are unknown parameters. $E_{i,t}$ is the element of $\boldsymbol{E}_t$ in Equation (27), $H_{i,t}$ is the element of $\boldsymbol{H}_t$ in Equation (53), and $H_{i,t}E_{i,t}$ is the coefficient used to obtain the weighted mean.

In actual observations by the Mie Prefecture, the mean weight of the fish caught by school m ($\overline{w}_{m,\text{Catch}}$) was measured in the third step of the aforementioned three-step sampling of body length composition. Therefore, in this study, γ_1 and γ_2 in Equation (63) could be estimated in advance by the Bayesian method, assuming that $\overline{w}_{m,\text{Catch}}$ follows the following normal distribution. The medians of the Markov Chain Monte Carlo (MCMC) samples were treated as fixed parameter values.

$$\log\left(\overline{w}_{m,\text{Catch}}\right) \sim \text{Normal}\left(\log\left(\frac{\sum_{i=1}^{12}\left[\exp\left(\gamma_1 + \gamma_2 \log(l_i)\right) p_{i,m}\right]}{\sum_{i=1}^{12}\left(p_{i,m}\right)}\right), \sigma^2_{\log\overline{W}}\right), \tag{64}$$

$$\gamma_1 \sim \text{Uniform}(-\infty, \infty), \tag{65}$$

$$\gamma_2 \sim \text{Uniform}(0, \infty), \tag{66}$$

$$\sigma_{\log\overline{W}} \sim \text{Uniform}(0, \infty), \tag{67}$$

where $p_{i,m}$ is the element of $\boldsymbol{p}_m$ in Equation (61) and $\sigma_{\log\overline{W}}$ is a conversion error from the body length composition to the mean body weight on a log scale.

The variance $\sigma^2_{O_{t,\text{Mie}}}$ in Equation (62) was approximated by the delta method as follows:

$$\sigma^2_{O_{t,\text{Mie}}} = \left(C_{t,\text{Mie}}\ 10^5\ 30^{-1}\right)^2 \sigma^2_{\overline{W}_{t,\text{Catch}}} + \left(\overline{W}_{t,\text{Catch}}\ 10^5\ 30^{-1}\right)^2 \sigma^2_{C_{t,\text{Mie}}}, \tag{68}$$

where $\sigma^2_{\overline{W}_{t,\text{Catch}}}$ is a variance of $\overline{W}_{t,\text{Catch}}$ and $\sigma^2_{C_{t,\text{Mie}}}$ is a variance of $C_{t,\text{Mie}}$.

Equation (68) was simplified as follows: $C_{t,\text{Mie}}$ in the integrated model is the value after going through the various state processes on day t. Therefore, first, $\sigma^2_{C_{t,\text{Mie}}}$ was defined as follows, assuming that $C_{t,\text{Mie}}$ follows a Poisson distribution:

$$\sigma^2_{C_{t,\text{Mie}}} = C_{t,\text{Mie}}. \tag{69}$$

Second, assuming that $\sigma_{\log\overline{W}}$ in Equation (64) is approximately equal to the coefficient of variation of $\overline{W}_{t,\text{Catch}}$, we define $\sigma^2_{\overline{W}_{t,\text{Catch}}}$ as follows.

$$\sigma^2_{\overline{W}_{t,\text{Catch}}} = \left(\overline{W}_{t,\text{Catch}}\,\sigma_{\log\overline{W}}\right)^2. \quad (70)$$

Substituting Equations (69) and (70) into Equation (68), we obtain:

$$\sigma^2_{O_{t,\text{Mie}}} = O^2_{t,\text{Mie}}\sigma^2_{\log\overline{W}} + O_{t,\text{Mie}}\overline{W}_{t,\text{Catch}}\,10^{-3}\,30^{-1}. \quad (71)$$

Finally, the number of buckets observed by the Mie Prefecture ($o_{t,\text{Mie}}$) was assumed to approximate the following normal distribution:

$$o_{t,\text{Mie}} \sim \text{Normal}\left(O_{t,\text{Mie}}, \sigma^2_{O_{t,\text{Mie}}}\right). \quad (72)$$

Similarly, the number of buckets observed by the Aichi Prefecture ($o_{t,\text{Aichi}}$) was assumed to follow a normal distribution with $O_{t,\text{Aichi}}$ and $\sigma^2_{O_{t,\text{Aichi}}}$ as follows:

$$O_{t,\text{Aichi}} = \overline{W}_{t,\text{Catch}}C_{t,\text{Aichi}}\,10^5\,18^{-1}, \quad (73)$$

$$\sigma^2_{O_{t,\text{Aichi}}} = O^2_{t,\text{Aichi}}\sigma^2_{\log\overline{W}} + O_{t,\text{Aichi}}\overline{W}_{t,\text{Catch}}\,10^{-3}18^{-1}, \quad (74)$$

$$o_{t,\text{Aichi}} \sim \text{Normal}\left(O_{t,\text{Aichi}}, \sigma^2_{O_{t,\text{Aichi}}}\right), \quad (75)$$

where the value 18 in Equations (73) and (74) is the weight (kg) of caught fish per bucket in Aichi Prefecture. For calculations involving data prior to and including 2002, this value is replaced with 30.

(c) Unobserved number of fishing vessels

On April 27, May 4, and May 7, 1995, the number of fishing vessels in Aichi Prefecture was unobserved. The unobserved vessel number ($\Gamma_{t,\text{Aichi}}$) were set as parameters according to the following prior distribution:

$$\Gamma_{t,\text{Aichi}} \sim \text{Uniform}(0, 160), \quad (76)$$

where 160 is the maximum number of fishing vessels in Aichi Prefecture observed in 1995 (Table 1).

(d) Generating stock abundance indices

Stock abundances determined by conventional models are scalars, which can be easily handled as stock abundance indices. However, stock abundances estimated using the integrated model are vectors or matrices that are complicated to handle. Therefore, various scalar abundance indices were converted from the estimates using the integrated model as follows:

Final stock abundance: Based on elements of $\boldsymbol{N}_{T+1}$, the final stock abundance (N_{T+1}) was obtained using the following equation:

$$N_{T+1} = \sum_{i=1}^{12} N_{i,T+1}. \quad (77)$$

Recruits and annual recruitment rate: Recruitment in the integrated model was defined as fish becoming fishing targets. Therefore, whether a fish is targeted is determined by the selection probability D_i in Equation (37). The non-target and target stock abundances immediately before fishing on day t ($N_{t,\text{Non-target}}$ and $N_{t,\text{Target}}$) are expressed as follows:

$$N_{i,t,\text{Non-target}} = N_{i,t}(1 - D_i), \quad (78)$$

$$N_{t,\text{Non-target}} = \sum_{i=1}^{12} N_{i,t,\text{Non-target}}, \quad (79)$$

$$N_{t,\text{Target}} = N_t - N_{t,\text{Non-target}}. \quad (80)$$

Under the assumptions of the integrated model, the non-target stock abundance between day $t-1$ and t is reduced by recruitment. The change in non-target stock abundance from $t-1$ to t represents recruits during the period. Equation (79) was used to obtain the recruits on day t (R_t), as follows:

$$R_t = N_{t-1,\text{Non-target}} - N_{t,\text{Non-target}}, \quad (81)$$

where recruits on the first fishing day, $t = 1$ (R_1), when the amount of change cannot be defined, is set to zero.

The maximum value of R_t was determined for each year and defined as the peak of recruitment. Based on Equation (81), the annual recruits (R) were determined using the following equation:

$$R = \sum_{t=1}^{\text{T}} R_t. \quad (82)$$

The annual recruitment rate (K) during the fishing season was determined as follows:

$$K = R / \lambda_1. \quad (83)$$

Mean body length in stock and its daily changes: The mean body length in the stock ($\bar{L}_t$), including non-target fish, was calculated using the following equation:

$$\bar{L}_t = \frac{\sum_{i=1}^{12}(L_i H_{i,t})}{\sum_{i=1}^{12} H_{i,t}}. \quad (84)$$

$\bar{L}_t - \bar{L}_{t-1}$ was defined as the daily change on day t (mm/day). The maximum daily changes for each year and date were identified.

Mean body length of caught fish: The mean body length of the caught fish ($\bar{L}_{t,\mathrm{Catch}}$) was obtained using the following equation:

$$\bar{L}_{t,\mathrm{Catch}} = \frac{\sum_{i=1}^{12}(L_i H_{i,t} E_{i,t})}{\sum_{i=1}^{12}(H_{i,t} E_{i,t})}. \quad (85)$$

According to Equation (85), the mean body length denotes the mean body length, which was excluded from the body lengths of non-target fish from those in the stock using the exploitation rates. The effects of size selection on the mean body length of the caught fish were examined by comparing $\bar{L}_t$ and $\bar{L}_{t,\mathrm{Catch}}$.

Catch, annual catch rate, and CPUE: The catch on day t (C_t) was calculated as follows:

$$C_t = \sum_{i=1}^{12}\left(C_{i,t,\mathrm{Mie}} + C_{i,t,\mathrm{Aichi}}\right). \quad (86)$$

The annual catch (C) and exploitation rate (E) were obtained as follows:

$$C = \sum_{t=1}^{T} C_t, \quad (87)$$
$$E = C / \lambda_1. \quad (88)$$

Using x_t in Equation (11) and C_t in Equation (86), the CPUE on day t (U_t) was obtained as follows:

$$U_t = C_t / x_t. \quad (89)$$

Cumulative catch during a period when fishing was banned in partial areas of Ise Bay: Fishing bans were set from the middle of the fishing season every year to protect adults in some areas of Ise Bay since 1993 (Tomiyama 2002; Tomiyama et al. 2005). The partial ban area was mainly at the mouth of the bay, and its coverage varied from year to year (Appendix Table 1). Ban areas are set when the body length becomes too large to meet market demand (Tomiyama 2003) or when the stock abundance of young decreases to 40 oku fish (mainly in April) (Nakamura, M.[1], personal communication). The stock abundance on the day when the fishing ban was first set ($N_{t_{\mathrm{ban}}}$) and the cumulative catch during the period from the first day of the partial ban to the last fishing day (C_{ban}) were obtained as follows:

$$N_{t_{\mathrm{ban}}} = \sum_{i=1}^{12} N_{i,t_{\mathrm{ban}}}, \quad (90)$$
$$C_{\mathrm{ban}} = \sum_{t=t_{\mathrm{ban}}}^{T} C_t, \quad (91)$$

where t_{ban} is the day on which the partial ban was first implemented each year. $N_{t_{\mathrm{ban}}} - C_{\mathrm{ban}} = N_{T+1}$. Therefore, the effects of the fishing ban on the protection of adults were inferred by comparing $N_{t_{\mathrm{ban}}}$ and C_{ban} for each year.

Reproductive efficiency and relative reproductive efficiency: The following equation was used to obtain the reproductive efficiency in year y (r_y):

$$r_y = \lambda_{1,y+1} / N_{T+1,y}. \quad (92)$$

Note that the reproductive efficiency in 2015 (r_{2015}) cannot be calculated because the initial stock abundance in 2016 ($\lambda_{1,2016}$) is unknown.

The expected initial stock abundance for *A. japonicus* stock management in Ise Bay was 300 oku fish (Nakamura et al. 2017). The reproductive efficiency in year y when the initial abundance in year $y+1$ becomes 300 oku fish, is obtained as 300 per $N_{T+1,y}$ based on Equation (92) (hereafter $r_{300,y}$). The r_y of *A. japonicus* in Ise Bay fluctuated around $r_{300,y}$ and tended to deviate

[1] Aichi Prefecture Fisheries Institute

downward from $r_{300,\,y}$ because of environmental deterioration (Nakamura et al. 2017). In this study, this process was expressed as the relative reproductive efficiency (relative-r_y):

$$\text{relative-}r_y = \frac{r_y}{r_{300,\,y}} = \frac{\frac{\lambda_{1,\,y+1}}{N_{T+1,\,y}}}{\frac{300}{N_{T+1,\,y}}} = \frac{\lambda_{1,\,y+1}}{300}. \quad (93)$$

Equation (93) shows that the estimate and its variation in relative-r_y are specified by the initial stock abundance in year $y + 1$.

3. Estimation of the parameters

Although the catch weight per bucket in Aichi Prefecture has been rounded from 18 to 20 kg since 2004, it was unified to 18 kg in this study.

The parameters were estimated using DeLury's, Phiri's, and integrated models for each year using the Bayesian method. R version 4.3.3 (R Core Team 2024) and rstan version 2.32.6 (Stan Development Team 2024) were used for the estimation program. The iterations were set to 80000, warmup to 70000, thinning to 20, and chains to 4. Calculations converged when the Rhats for all parameters were less than 1.1 (Gelman et al. 2013). Additionally, estimates (medians) and their 90% credible intervals were estimated based on the MCMC samples. A list of the parameters in the integrated model is presented in Table 2.

Table 2. Parameters in the integrated model

Parameter	Description
λ_1	Stock abundance on day $t = 1$ (i.e., initial stock abundance)
$\varphi_{i,1}$	Composition of stock abundances of body length class i on day $t = 1$
η_0	Mean of log transformed fishing gear efficiency
$\eta_{t,\text{Mie}}$, $\eta_{t,\text{Aichi}}$	Variation in log transformed fishing gear efficiency in the Mie and Aichi prefecture ships on day t
σ_η^2	Variance controls $\eta_{t,\text{Mie}}$ and $\eta_{t,\text{Aichi}}$
μ_l	Body length with selectivity probability 0.50
σ_l	Difference between body length with a selectivity probability of 0.25 and body length with a selectivity probability of 0.75
ω_0	Mean of softmax transformed transition probability of stock abundance
ω_i	Variation in softmax transformed transition probability of stock abundance in each body length class i
σ_ω^2	Variance controls ω_i
τ_t	Variation in transition probability of stock abundance in body length class $i = 1$ on day t
σ_τ^2	Variance controls τ_t
$\zeta_{i,m}$	Variation in body length composition in body length i of school m
σ_ζ^2	Variance controls $\zeta_{i,m}$
$\Gamma_{t,\text{Aichi}}$	Number of ships in Aichi Prefecture on day $t = 30$, 37, and 40 in 1995 (i.e., missing data)

The parameters followed the prior probability distributions shown in the text.

4. Model diagnostics

1) Actual catch data

(a) Mean percentage error and root mean square percentage error

The mean percentage error (MPE) and root mean square percentage error (RMSPE) for bucket numbers and mean body lengths were calculated to assess the goodness of fit of the integrated model to the observed data. Posterior prediction *p*-values (PPP) (Gelman et al. 2013) were also obtained. Calculations for DeLury's and Phiri's models were excluded.

(b) Prediction interval of the mean body length of caught fish in selecting new schools

To evaluate the model's fit to the observations, new schools were additionally selected to measure the mean body lengths by simulation and to calculate 90% prediction intervals for their mean body lengths. Calculations for DeLury's and Phiri's models were excluded.

(c) Comparing with the published estimates

I verified whether the published estimates of the initial stock abundance, final stock abundance, annual catch rate, and reproductive efficiency were included in the credible intervals of the estimate using the integrated model. The consistency of the pattern of interannual trend between the published estimates and the estimates using the integrated model was also verified using scatter plots and Spearman's correlation coefficients (ρ). The ratios of the published estimates to the estimates using the integrated model were used as indicators of discrepancy in their estimates, and the relationships between these ratios and daily variation in fishing gear efficiencies and between these ratios and annual recruitment rates were evaluated using scatter plots. Estimates of the initial and final stock abundances, which were estimated using DeLury's and Phiri's models in this study, were also compared with published estimates.

2) Simulation data

To confirm the robustness of the models, simulations under various scenarios generated the initial and final stock abundances, and their true values were compared to the estimates obtained by the model. Simulation data were generated for eight scenarios with small or large recruitment abundance during the fishing season, no or large daily variation in fishing gear efficiency, and large or small sample sizes (number of fishing days). A total of 100 simulation datasets were generated for each scenario. Detailed parameter settings for the simulations are shown in Supplement A. The ratios of the estimate in each model to the true value were obtained from the dataset. The closer the ratio is to 1.0, the smaller the bias in the estimate. The percentages of the true values included in the 90% credible interval of the estimate were also obtained. The closer the percentage is to 90%, the smaller the bias in the credible interval. We expected estimates using DeLury's or Phiri's models to be unbiased under scenarios of small recruits and no daily variation in fishing gear efficiency during the fishing season and that estimates using the integrated model would be unbiased under all scenarios.

5. Stock assessment

1) Interannual trends in stock indices from the 1990s to the 2010s

The presence or absence of long-term trends in the aforementioned stock indices was confirmed by the lower-side test of the runs using DescTools version 0.99.54 (Signorell 2024) based on the estimates (the medians of the MCMC samples). Reproductive relationships were confirmed by a scatter plot based on the final stock abundance in year y as adults and the initial stock abundance in year $y + 1$ as young. Riker's and Beverton–Holt's models were fitted to the reproductive relationships using the nonlinear least-squares method. In addition, fitness to the Nakamura model (Nakamura et al. 2017) was confirmed using a scatter plot.

2) Interannual trends in environmental factors from the 1990s to the 2020s

Interannual trends in the following four environmental factors were confirmed by the lower-side test of the runs based on the estimates (the medians of MCMC samples). The relationships between these factors and the relative reproductive efficiency were confirmed using scatter plots.

(a) Condition factor

The condition factor of *A. japonicus* is a valuable index of food availability (Hashiguchi et al. 2021; Sekiguchi et al. 1976; Yamada 2011). The lower limit of the condition factor required for sexual maturity is 4.2 (Yamada et al. 1999a). Using the parameters of Equation (64), a mean condition index at 75 mm body length (Y_{75}), which is close to the body length of yearlings during the transition to estivation (Yamada et al. 1999a), was obtained using the following equation for each year from 1993 to 2015:

$$Y_{75} = \exp\left(\gamma_1 + \gamma_2 \log(75)\right) 75^{-3} 10^6. \quad (94)$$

The mean condition index after 2016 was unknown due to the fishing ban.

(b) Water temperature

A. japonicus in Ise Bay begins to estivate when the water temperature increases to approximately 21 °C (approximately from May to August) (Itokawa 1983; Nishimura et al. 1991; Yamada 2011). Water temperature immediately before the fishing season affects the recruitment and growth of *A. japonicus* in Ise Bay (Tomiyama and Komatsu 2006). The mean water temperatures in Ise Bay were estimated based on the water temperatures observed by the Mie Prefecture Fisheries Research Institute at depths of 0, 10, and 20 m at the largest 14 points in Ise Bay once a month yearly from 1993 to 2022 (Fig. 2; Supplement B). However, this study did not examine water temperatures from January to July 1993 because of a change in the observation methods, although observations were conducted. The mean water temperatures at 0, 10, and 20 m for each month and year were estimated using the Bayesian method, assuming normal distributions. The topography of Ise Bay is bowl-shaped, with the deepest point at 37 m in the center of the bay (Fig. 2). Depths of 0, 10, and 20 m corresponded to the upper, middle, and lower depth zones, respectively. A large volume of water was found in the upper and middle depth zones of Ise Bay (Table 3).

(c) Dissolved oxygen concentration

Large hypoxic water masses occur every summer in the Ise Bay and affect various marine benthic communities (Amakawa and Sekiguchi 2015). The effect of hypoxic water masses on the *A. japonicus* population is unknown; however, its occurrence period overlaps with the estivation transition period in *A. juponicus*. Depth zones were identified where the mean dissolved oxygen concentration was below 4 mg/L, which is generally unsuitable for habitats of fish (Kakuta 2006) based on the dissolved oxygen concentrations observed by the Mie Prefecture Fisheries Research Institute simultaneously with the aforementioned water temperatures (Fig. 2; Supplement B). The mean DO at 0, 10, and 20 m for each month and year was estimated using the Bayesian method, assuming normal distributions with positive means.

Table 3. Percentage of water volumes in each depth zone of Ise Bay

Depth zone (m)	Ise Bay excluding Mikawa Bay	Mikawa Bay	Ise Bay including Mikawa Bay
0–5	19	6	25
5–10	17	5	21
10–15	15	3	18
15–20	13	1	14
20–25	10	0	11
20–30	7	0	7
30–100	4	0	4
Total	85	15	100

The boundary of Ise Bay followed Achiha (2008). Percentages were obtained from Digital Bathymetric Chart Japan M7002 version 2.3 (Japan Hydrographic Association) and Digital National Land Information (Ministry of Land, Infrastructure, Transport and Tourism, https://nlftp.mlit.go.jp/ksj/) using QGIS version 3.28.12 and SAGA GIS 7.8.2 in this study.

(d) Kuroshio path

The distance from Ise Bay to the Kuroshio path affects initial stock abundance in the *A. japonicus* fishery in Ise Bay (Funakoshi et al. 1997; Narita et al. 2002). The difference in the daily mean sea level of Kushimoto minus that of Uragami is useful as a path index, which is small along the path away from Ise Bay (Fujita 2002; Moriyasu 1958; Yoshida et al. 2006). These differences were observed by the Japan Meteorological Agency (https://www.data.jma.go.jp/kaiyou/data/shindan/b_2/kuroshio_stream/kuroshio_stream.html; Accessed February 29, 2024).

RESULTS

1. Model diagnostics

1) Actual catch data

(a) MPE and RMSPE

The observed catches (bucket numbers) showed large daily fluctuations, and the trends differed from prefecture to prefecture (Fig. 6). All observed values were included in each prediction interval (Fig. 6). The minimum and maximum MPE for the bucket numbers were −3.0% and −0.2%, respectively and their PPP ranged from 0.43 to 0.65 (Appendix Table 2). The minimum and maximum RMSPE values for the bucket numbers were 4.6% and 17.9%, respectively, and their PPP ranged from 0.31 to 0.54 (Appendix Table 2). Observed mean body lengths notably varied between different schools and across various days (Fig. 7). Prediction intervals of the mean body length of each school were in good agreement with the observations (intervals not shown in Fig. 7). The MPE for the mean body length were approximately zero, and their PPP ranged from 0.66 to 0.88 (Appendix Table 3). The minimum and maximum RMSPE for mean body length were 1.0% and 1.9%, respectively, and their PPP ranged from 0.04 to 0.74 (Appendix Table 3). Therefore, the MPE and RMSPE were small, and most of the PPP ranged from 0.05 to 0.95.

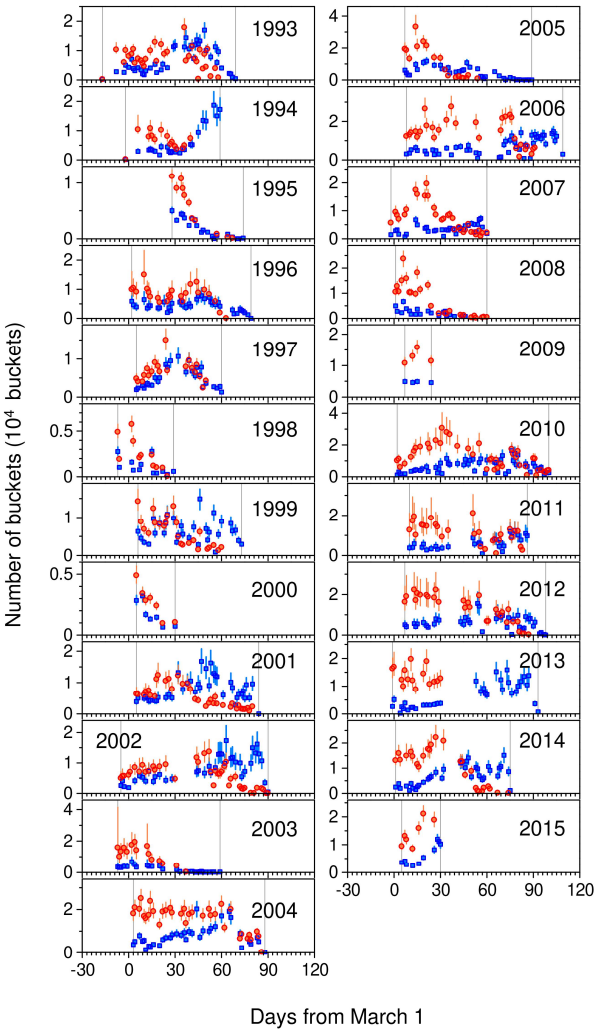

Fig. 6. The catches in the *Ammodytes japonicus* fishery in Ise Bay from 1993 to 2015 and their 90% prediction intervals using the integrated model. Rectangle: observed catch in Mie Prefecture; Circle: observed catch in Aichi Prefecture; Vertical line with rectangle or circle: prediction interval based on the Markov chain Monte Carlo samples; Vertical line: the first and last fishing day; Number in panel: year. Each bucket in Mie Prefecture contains 30 kg of fish. In Aichi Prefecture, each bucket contained 30 kg of fish until 2002, but since 2003, each bucket contains 18 kg of fish.

(b) Prediction interval of the mean body length when selecting new schools

The maximum prediction interval of the mean body length in 1993 was extensive compared to the others, but no such wide prediction intervals were identified in other years (Fig. 7; Appendix Table 4). Most observations were included in the 90% prediction interval, and some were not (Fig. 7; Appendix Table 4).

(c) Comparisons with the published estimates

The published estimates of the initial stock abundance for 2014 and 2015 were above the upper limit of the 90% credible interval obtained using the integrated model (Fig. 8a). In many other years, the published estimates exceeded each upper limit of the credible interval using the integrated model (Fig. 8a). In contrast, a correlation coefficient (ρ) between the published estimates and the estimates using the integrated model was 0.974 ($p < 0.001$, $n = 23$), indicating a good agreement between the interannual trend (Fig. 8a). The ratios of the published estimates to the estimates obtained using the integrated model positively correlated with daily variations in fishing gear efficiency (Fig. 9a). The correlation between the ratios and annual recruitment rates was weak; no ratio above 1.0, indicating overestimation, was identified in years when the annual recruitment rates were less than 0.1 (Fig. 9b).

Published estimates of the final stock abundances in 2014 and 2015 were above the upper limit of the 90% credible intervals obtained using the integrated model (Fig. 8b). In many other years, the published estimates exceeded the upper limit of the 90% credible interval using the integrated model (Fig. 8b). The number of years in which the final stock abundance using the integrated model exceeded 20 oku fish (the reference point after 2007) was 3 out of 23 years based on the estimates and 2 out of 23 years based on their lower limits of the 90% credible interval (Fig. 8b). However, the number based on published estimates was 16 out of 23 years (Fig. 8b). Therefore, evaluations in stock management notably differed between the estimates using the integrated model and the published estimates. The correlation coefficient between the published estimates and estimates obtained using the integrated model was 0.479 ($p = 0.021$, $n = 23$). The ratios of the published estimates to the estimates

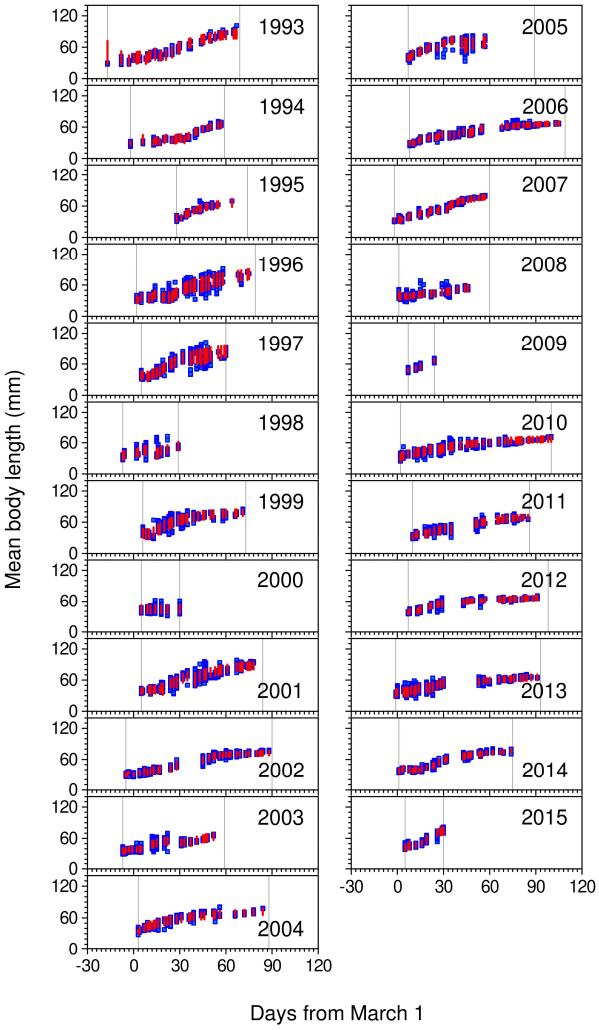

Fig. 7. The mean body lengths of fish caught in the *Ammodytes japonicus* fishery in Ise Bay from 1993 to 2015 and their 90% prediction intervals using the integrated model. Rectangle: observed mean body length in Mie Prefecture; Red vertical line: prediction interval based on the Markov chain Monte Carlo samples of the mean body length of caught fish; Vertical line: first and last fishing day; Number in panel: year.

obtained using the integrated model positively correlated with daily variations in fishing gear efficiency and annual recruitment rates during the fishing season (Fig. 9c, d).

The published catch estimate in 2014 was below the lower limit of the 90% credible interval using the integrated model (Fig. 8c). In many other years, the published estimates were below the lower limit of the credible interval using the integrated model (Fig. 8c). However, the correlation coefficient between the

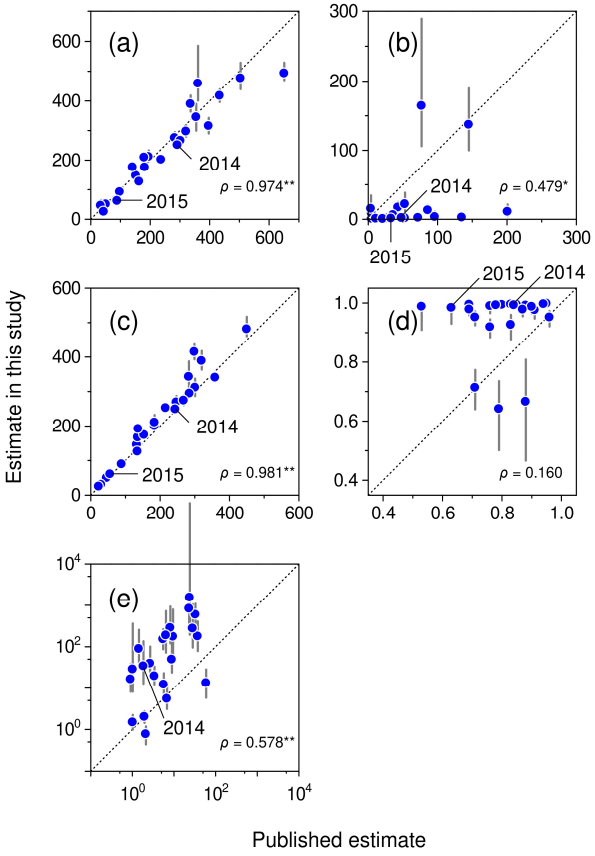

Fig. 8. Comparisons between the published and integrated model estimates for stock indices in the *Ammodytes japonicus* fishery in Ise Bay from 1993 to 2015. (a) initial stock abundance (unit: oku fish), (b) final stock abundance (unit: oku fish), (c) annual catches (unit: oku fish), (d) annual exploitation rate, (e) reproductive efficiency. Circle: median of the Markov chain Monte Carlo samples; Vertical line: 90% credible interval; Dotted line: 1:1 relationship; Number in panel: year. Published estimates without their credible intervals, based on Yamamoto et al. (2019). Unit oku represents 100 million; ρ: Spearman's correlation coefficient; *: $p < 0.05$; **: $p < 0.01$; $n = 23$ in panel a–d; $n = 22$ in panel e.

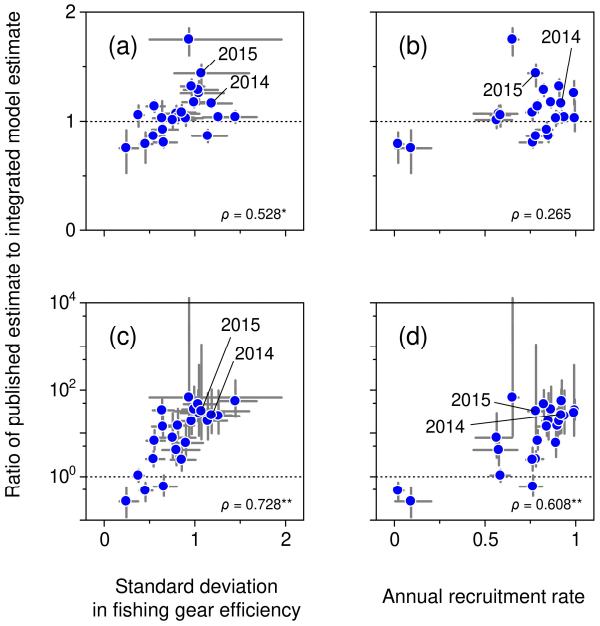

Fig. 9. Effects of the variation in fishing gear efficiencies and annual recruitment rates on ratio of the published estimates to the initial stock abundance and the final stock abundance estimates using the integrated model in the *Ammodytes japonicus* fishery in Ise Bay from 1993 to 2015. (a) and (b) initial stock abundance, (c) and (d) final stock abundance. Circle: median of the Markov chain Monte Carlo samples using the integrated model; Vertical and horizontal lines: 90% credible interval; Dotted line: ratio = 1.0 (unbiased); Number in panel: year; ρ: Spearman's correlation coefficient; *: $p < 0.05$; **: $p < 0.01$; $n = 23$. Published estimates are based on Yamamoto et al. (2019). The standard deviation represents σ_η in the text.

published estimates and the estimates using the integrated model was 0.981 ($p < 0.001$, $n = 23$), indicating good agreement between these interannual trends. The correlation between the ratios of the published estimates to the estimates obtained using the integrated model and the daily variations in fishing gear efficiency was weak (Plate 1a). The correlation between these ratios and the annual recruitment rates was weak (Plate 1b).

The published estimates of the annual exploitation rates for 2014 and 2015 were below the lower limit of the 90% credible interval obtained using the integrated model (Fig. 8d). In many other years, the published estimates were below the lower limit of the credible interval using the integrated model (Fig. 8d). The correlation coefficient between the published estimates and the estimates obtained using the integrated model was 0.160 ($p = 0.465$, $n = 23$), indicating a lack of agreement between these interannual trends. The ratios of the published estimates to the estimates obtained using the integrated model negatively correlated with daily

variations in fishing gear efficiency and annual recruitment rates during the fishing season (Plate 1c, d).

The estimated reproductive efficiency published in 2014 was below the lower limit of the 90% credible interval when the integrated model was used (Fig. 8e). In many other years, the published estimates were below the lower limit of the 90% credible interval using the integrated model (Fig. 8e). The correlation coefficient between the published estimates and the estimates obtained using the integrated model was 0.578 ($p = 0.005$, $n = 22$). The ratios of the published estimates to the estimates obtained using the integrated model negatively correlated with daily variations in fishing gear efficiency and annual recruitment rates during the fishing season (Plate 1e, f).

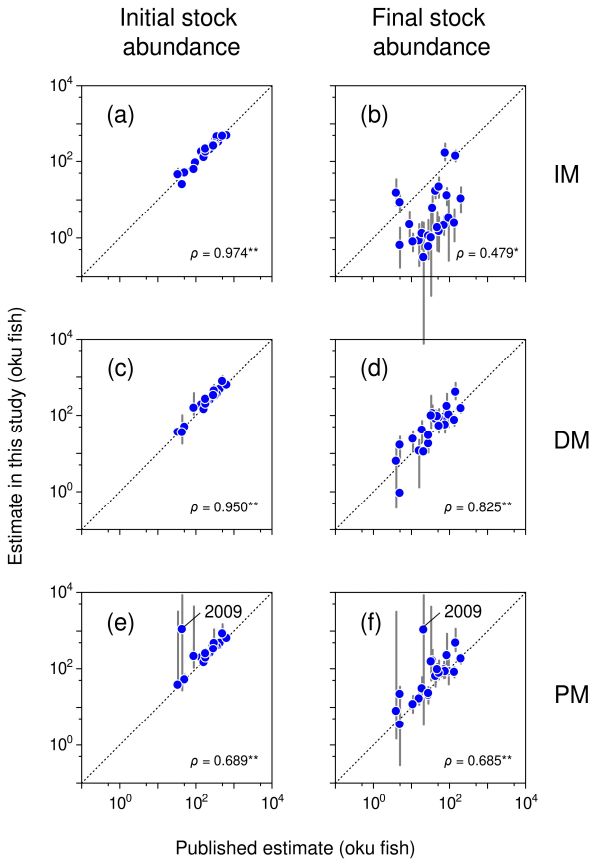

Fig. 10. Comparisons between published and this study's estimates of the initial stock abundance and final stock abundance in the *Ammodytes japonicus* fishery in Ise Bay from 1993 to 2015. (a) and (b) estimates using the integrated model in this study (IM); (c) and (d) estimates using DeLury's model in this study (DM); (e) and (f) estimates using Phiri's model in this study (PM). Circle: median of the Markov chain Monte Carlo samples; Vertical line: 90% credible interval. Published estimates were estimated using the DeLury's or Phiri's models, without their credible intervals and based on Yamamoto et al. (2019). Unit oku represents 100 million. Dotted line: 1:1 relationship; Number: year; ρ: Spearman's correlation coefficient; *: $p < 0.05$; **: $p < 0.01$; $n = 23$ in IM; $n = 22$ in DM and PM.

Estimates of initial and final stock abundances using DeLury's and Phiri's models in this study were not consistent with the published estimates because the data used in this study were not the same, and the estimation method differed (Fig. 10c–f). The estimates in 2009 using Phiri's model in this study differed significantly from the published ones (Fig. 10e, f), whose sample size was smallest from 1993 to 2015 (Table 1). However, the correlations between the estimates in this study and published estimates were high (Fig. 10c–f). In this study, the number of years in which estimates of the final stock abundance exceeded 20 oku fish was 17 out of 22 years when using DeLury's model (Fig. 10d) and 18 out of 22 years when using Phiri's model (Fig. 10f). The number of years in which the lower limit of the 90% credible interval of the final stock abundance exceeded 20 oku fish was 15 out of 22 years (DeLury's model) (Fig. 10d) and 13 out of 22 years (Phiri's model) (Fig. 10f). Those using published estimates were 16 out of 23 years, as mentioned above. Consequently, the stock management evaluations were mostly consistent with the estimates using the conventional models in this study and the published estimates.

2) Simulation data

(a) Integrated model

The median ratios of the integrated model estimate to the true initial stock abundance ranged from 0.98 to 1.00 (Table 4b). The percentages of the true value included in the 90% credible interval for the initial stock abundance ranged from 75% to 95% (Table 4b). The median ratios of the integrated model estimate to the true final stock abundance ranged from 1.00 to 2.14 (Table 4c). The percentage of the true value included in the 90% credible interval for the final stock abundance ranged from 73% to 94% (Table 4c). The estimates of the final stock abundance were greater than the true values in scenarios with large recruits during the fishing season and/or daily variations in fishing gear efficiency (Table 4c). However, the bias decreased as the sample size increased (Table. 4c; Fig. 11a, b).

Table 4. Scenarios of recruitment, variation in fishing gear efficiency, and sample size to generate datasets in simulation, and summary of estimates using the integrated, DeLury's, and Phiri's models in each scenario

	Scenario							
	i	ii	iii	iv	v	vi	vii	viii
(a) Condition to generate simulation data								
Recruitment	Small				Large			
Variation in fishing gear efficiency	None		Some		None		Some	
Sample size	Large	Small	Large	Small	Large	Small	Large	Small
(b) Initial stock abundance								
Median of ratios of initial stock abundance estimate to its true value in each model								
Integrated model	0.99	0.99	0.99	0.99	1.00	0.98	0.99	1.00
DeLury's model	0.98	0.97	0.98	1.02	1.15	1.26	1.20	1.26
Phiri's model	0.97	0.98	0.99	1.02	1.01	1.12	1.02	1.23
Percentage of true initial stock abundances included in 90% credible interval of estimate in each model								
Integrated model	75	88	78	79	86	89	91	95
DeLury's model	24	27	69	73	39	80	70	86
Phiri's model	1	5	25	56	34	71	50	45
(c) Final stock abundance								
Median of ratios of the final stock abundance estimate to its true value in each model								
Integrated model	1.01	1.03	1.14	1.88	1.00	1.07	1.54	2.14
DeLury's model	2.23	2.24	3.35	4.05	11.52	34.90	21.29	40.09
Phiri's model	1.04	1.22	1.70	5.06	2.18	14.08	4.93	41.40
Percentage of true final stock abundances included in 90% credible interval of estimate in each model								
Integrated model	94	88	89	73	92	86	83	80
DeLury's model	80	99	94	91	10	67	71	83
Phiri's model	98	95	81	73	32	31	41	19

Medians and percentages were obtained based on 100 datasets in each scenario. Results based on high-density intervals are shown in Appendix Table 5.

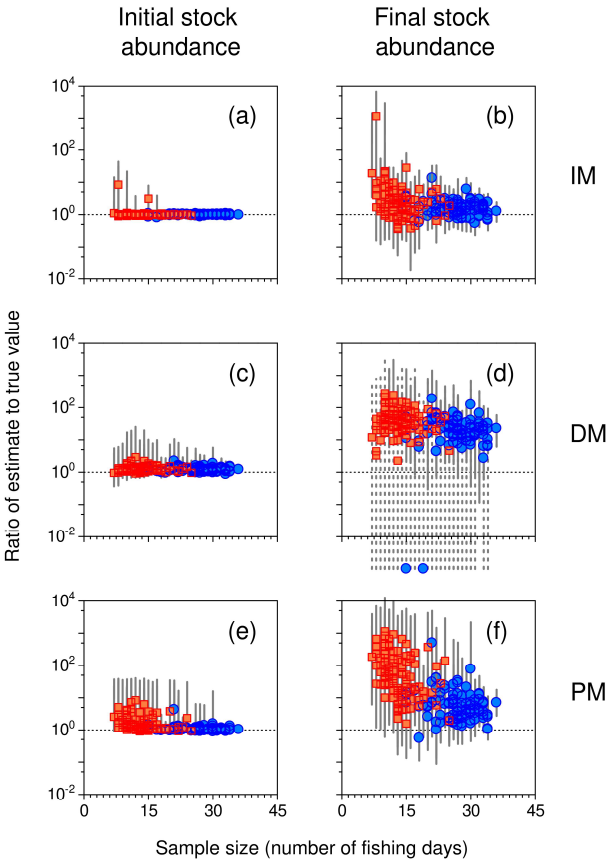

Fig. 11. Relationships between sample size and the ratio of stock abundance estimate to its true value in simulations. The simulation conditions were established with a large recruitment rate and some variation in fishing gear efficiency (Scenario vii and viii in Table 4). (a) and (b) estimates using the integrated model (IM), (c) and (d) estimates using DeLury's model (DM), (e) and (f) estimates using Phiri's model (PM). Rectangle: median of the Markov chain Monte Carlo (MCMC) samples of the ratio in the small sample size (Scenario viii in Table 4); Circle: median of MCMC samples of the ratio for the large sample size (Scenario vii in Table 4); Circle outside frame: median of the ratio less than 0; Solid vertical line: 90% credible interval; Dotted vertical line: 90% credible interval with lower limit less than 0. Horizontal dotted line: ratio = 1.0 (unbiased). Results for other scenarios are shown in Plate 2, 3, and 4.

(b) DeLury's model

The median ratios of DeLury's model estimate to the true initial stock abundance ranged from 0.97 to 1.26 (Table 4b). The percentages of the true value included in the 90% credible interval for the initial stock abundance ranged from 24% to 86% (Table 4b). The median ratios of DeLury's model estimate to the true value for the final stock abundance ranged from 2.23 to 40.09 (Table 4c). The percentage of the true value included in the 90% credible interval for the final stock abundance ranged from 10% to 99% (Table 4c). The estimates of the final stock abundance were greater than the true values in scenarios with large recruits during the fishing season and/or daily variations in fishing gear efficiency (Table 4c). The biases of the estimates decreased as the sample size increased; however, the validity of the 90% credible intervals in some scenarios worsened as the sample size increased (Table 4b, c; Fig. 11c, d). The biases of DeLury's model estimates were more extensive than those of the integrated model estimates (Tables 4b, c; Fig. 11a–d).

(c) Phiri's model

The median ratios of Phiri's model estimate to the true initial stock abundance ranged from 0.97 to 1.23 (Table 4b). The percentages of the true value included in the 90% credible interval for the initial stock abundance ranged from 1% to 71% (Table 4b). The median ratios of Phiri's model estimate to the true final stock abundance ranged from 1.04 to 41.40 (Table 4c). The percentages of the true value included in the 90% credible interval for the final stock abundance ranged from 19% to 98% (Table 4c). The final stock abundance estimates were greater than the true values in scenarios with large recruits during the fishing season and/or daily variations in fishing gear efficiency (Table 4c). The estimate biases decreased as the sample size increased; however, the validity of the 90% credible intervals worsened in some scenarios (Table 4b; Fig. 11e). The biases of Phiri's model estimates were greater than those of the integrated model estimates (Tables 4b, c; Fig. 11a, b, e, and f).

2. Stock assessment

1) Interannual trends in stock indices

(a) Body length to body weight conversion equation

The minimum, maximum, and median intercepts were −15.3 in 2012, −13.4 in 2005, and −14.3, respectively (Appendix Table 6). No long-term decreasing or increasing trends were detected (run test, $p = 0.507$; $n = 23$; Appendix Table 6). The minimum, maximum, and median slopes were 3.25 in 2005, 3.68 in 2012, and 3.46, respectively (Appendix Table 6). No long-term decreasing or increasing trends were detected (run test, $p = 0.665$; $n = 23$; Appendix Table 6). The minimum, maximum, and median of the standard deviations were 4.71×10^{-2} in 1995, 16.6×10^{-2} in 2003, and 8.02×10^{-2}, respectively (Appendix Table 6). No long-term decreasing or increasing trends were detected (run test, $p = 0.335$; $n = 23$; Appendix Table 6).

(b) Initial stock abundance

The minimum, maximum, and median initial stock abundances were 25.1 oku fish in 2009, 493.2 oku fish in 2006, and 211.2 oku fish, respectively (Fig. 12). No long-term decreasing or increasing trends were detected (run test, $p = 0.507$; $n = 23$; Fig. 12). The initial stock abundance declined sharply after 2015.

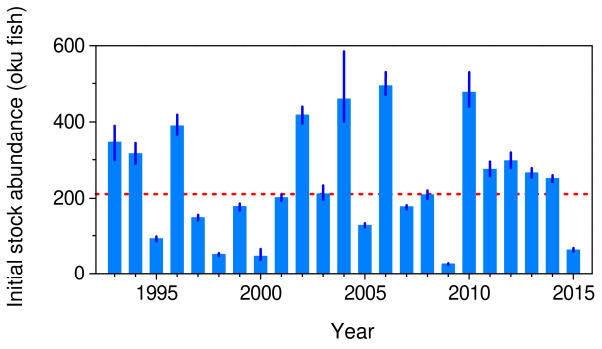

Fig. 12. The initial stock abundance in the *Ammodytes japonicus* fishery in Ise Bay from 1993 to 2015. Bar: median of the Markov chain Monte Carlo samples using the integrated model; Vertical line: 90% credible interval; dotted line: median of the medians. Unit oku represents 100 million. The data are shown in Appendix Table 7.

(c) Recruits and annual recruitment rate

Recruitment was most common during the first half of the fishing season (Fig. 13). The maximum daily recruits in each year were defined as the peak of the recruits; the minimum, maximum, and median of the peaks were 0.504 oku fish in 2000, 135.282 oku fish in 2012, and 21.639 oku fish, respectively (Fig. 13). The earliest, last, and median dates observed for the peaks were February 23, 2003, April 6, 2006, and March 11, respectively (Fig. 13). Peaks were observed within 10 days of the first fishing day in most years, whereas in some years (1993, 2006, 2007, 2010, and 2014), they were observed 20 days

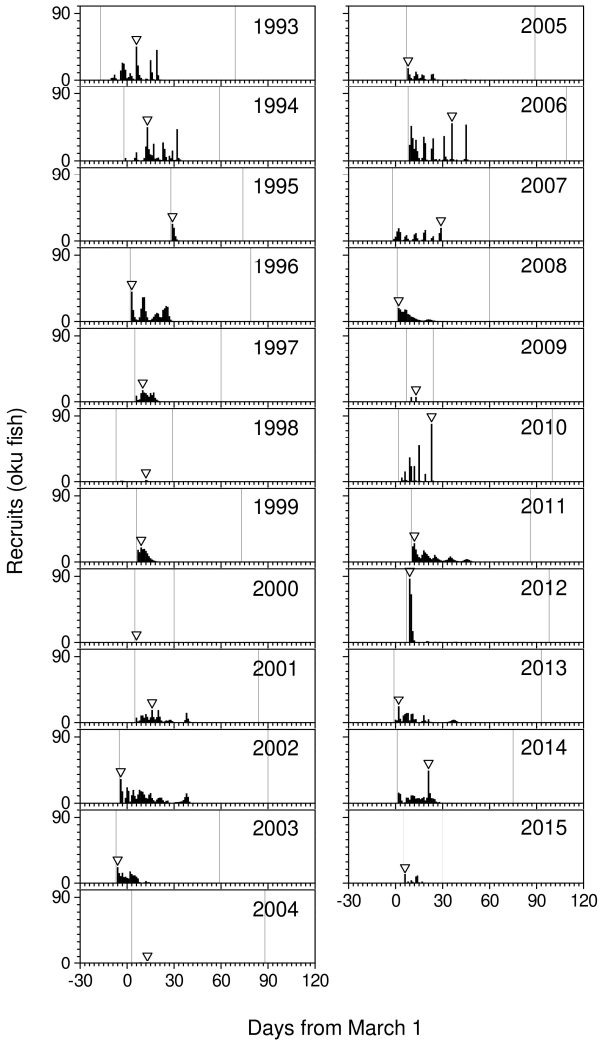

Fig. 13. The recruits in the *Ammodytes japonicus* fishery in Ise Bay from 1993 to 2015. Bar: median of the Markov chain Monte Carlo samples using the integrated model; Triangle: maximum daily recruits; Vertical line: first and last fishing day; Number in panel: year. Unit oku represents 100 million.

after the first fishing day (Fig. 13). No long-term decreasing or increasing trends were detected for the peak dates (run test, p = 0.900; n = 23; Fig. 13). The minimum, maximum, and median annual recruits were 4.39 oku fish in 2000, 447.97 oku fish in 2006, and 174.33 oku fish, respectively (Fig. 14a). No long-term decreasing or increasing trend was detected for the recruits (run test, p = 0.202; n = 23; Fig. 14a). The minimum, maximum, and median annual recruitment rates during the fishing season were 0.0211 in 2004, 0.9954 in 1993, and 0.8250, respectively (Fig. 14b). No long-term decreasing or increasing trend was detected in the rates (run test, p = 0.507, n = 23; Fig. 14b).

(d) Parameters in the selection model

The minimum, maximum, and median of the body lengths for a selection probability of 0.50 were 11.5 mm in 2010, 34.9 mm in 2005, and 25.2 mm, respectively (Appendix Table 8). No long-term decreasing or increasing trend was detected for the parameters (run test, p = 0.809; n = 23; Appendix Table 8). The minimum, maximum, and median of the body lengths for a selection probability of 0.25–0.75 were 0.878 mm in 2009, 6.519 mm in 2005, and 2.814 mm, respectively (Appendix Table 8). No long-term decreasing or increasing trends were detected in the parameters (run test, p = 0.665; n = 23; Appendix Table 8).

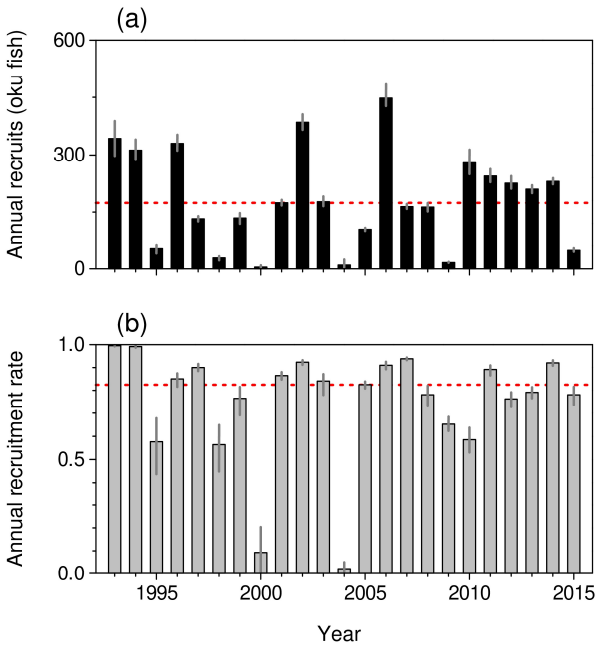

Fig. 14. The annual recruits and annual recruitment rates in the *Ammodytes japonicus* fishery in Ise Bay from 1993 to 2015. (a) annual recruits, (b) annual recruitment rates. Bar: median of the Markov chain Monte Carlo samples using the integrated model; Vertical line: 90% credible interval; dotted line: median of medians. Unit oku represents 100 million.

(e) Mean body length

The minimum, maximum, and median of the mean body lengths in the stock on the first fishing day were 5.18 mm in 1993, 35.81 mm in 2000, and 12.31 mm, respectively (Fig. 15). The minimum, maximum, and median of the mean body lengths of caught fish on the first fishing day were 27.2 mm in 1994, 46.9 mm in 2009, and 35.7 mm, respectively (Fig. 15). The minimum, maximum, and median of the mean body lengths in the stock on the last fishing day were 30.4 mm in 2000, 89.8 mm in 2001, and 69.3 mm, respectively (Fig. 15). The minimum, maximum, and median of the mean body lengths of caught fish on the last fishing day were 42.4 mm in 2000, 89.8 mm in 2001, and 69.3 mm, respectively (Fig. 15). The difference between the mean lengths of the stock and caught fish gradually decreased over time. The latest date when the body length class of the stock and that of the caught fish first matched was April 24, 2005 (vertical dotted lines in Fig. 15). After April 25, the mean body length class in the stock and the mean body length class of the catches matched in each year (Fig. 15). The correlation coefficients between the date when the body length class in the stock and those of the caught fish first matched and the date when the cumulative recruits exceeded 80%, 85%, 90%, 95%, and 99% of the annual recruits were 0.677, 0.678, 0.676, 0.749, and 0.680, respectively. Based on these results, the date when the cumulative recruits exceeded 95% was defined as the date when recruitment was completed (triangles in Fig. 15). The minimum, maximum, and median number of days from the first fishing day to the recruitment completion day were 5 days in 1995, 45 days in 2002, and 24 days, respectively (Fig. 15). The latest dates of recruitment completion were April 15, 2006, and 2011 (Fig. 15). The minimum, maximum, and median daily change peaks in the mean body length of the stock during the fishing season were 0.372 mm/day in 2000, 9.710 mm/day in 2007, and 6.878 mm/day, respectively. The earliest, last, and median peak dates were March 5, 2004, April 15, 2006, and March 25, respectively (rectangles in Fig. 15). These dates were earlier than April 25. The interannual trend was similar to that of the recruitment completion dates (Fig. 15). The minimum, maximum, and median of the mean body lengths in the stock on April 25 of each year were 56.4 mm in 2008, 83.6 mm in

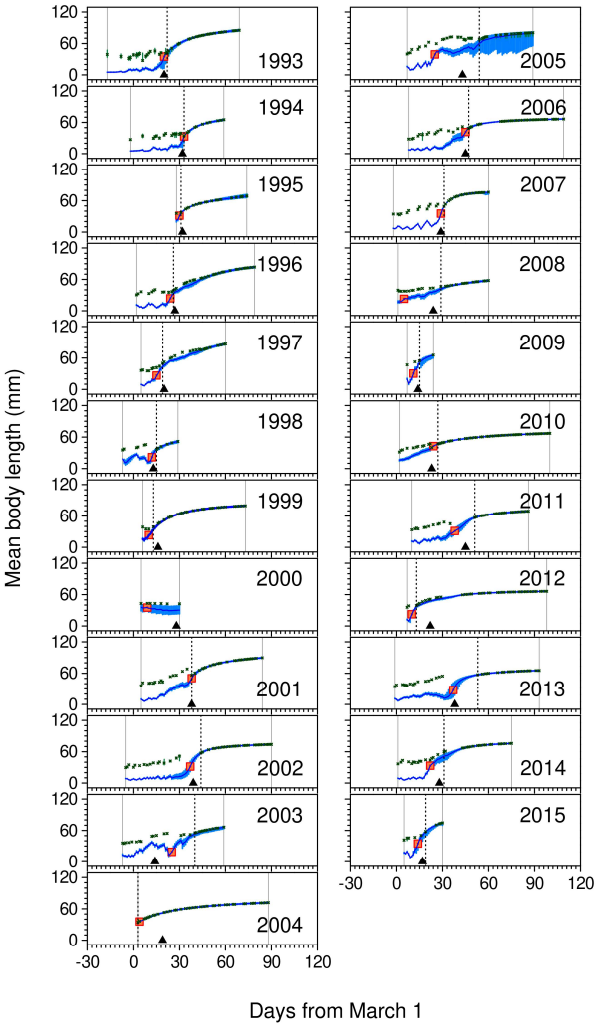

Fig. 15. The mean body lengths in the *Ammodytes japonicus* fishery in Ise Bay from 1993 to 2015. Cross: median of the Markov chain Monte Carlo (MCMC) samples of the mean body length of caught fish using the integrated model; Vertical line with cross: 90% credible interval; Blue line: median of MCMC samples of the mean body length in the stock using the integrated model; Vertical line with blue line: 90% credible interval; Rectangle: the maximum daily change of the length; Triangle: recruitment completion day; Vertical solid line: first and last fishing day; Vertical dotted line: day when the mean body length class of the stock and caught fish matched; Number in panel: year.

1997, and 64.2 mm, respectively (Fig. 16a). The minimum, maximum, and median standard deviations of body length composition in the stock were 0.911 in 2014, 1.722 in 1996, and 1.227, respectively (Fig. 16b). The

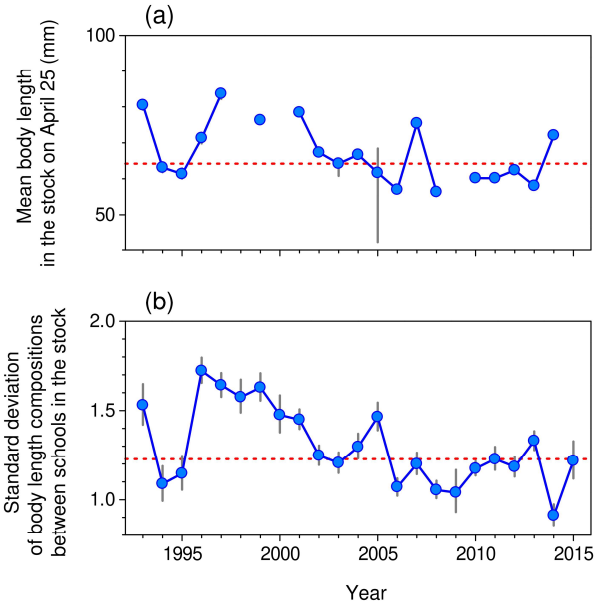

Fig. 16. The mean body length in the stock on April 25 and standard deviation of the body length compositions between schools in the *Ammodytes japonicus* fishery in Ise Bay from 1993 to 2015. (a) the mean body length in the stock on April 25, (b) the standard deviation of the body length compositions between schools in the stock. Circle: median of Markov chain Monte Carlo samples using the integrated model; Vertical line: 90% credible interval; Dotted line: median of the medians. The standard deviation represents σ_ζ in the text.

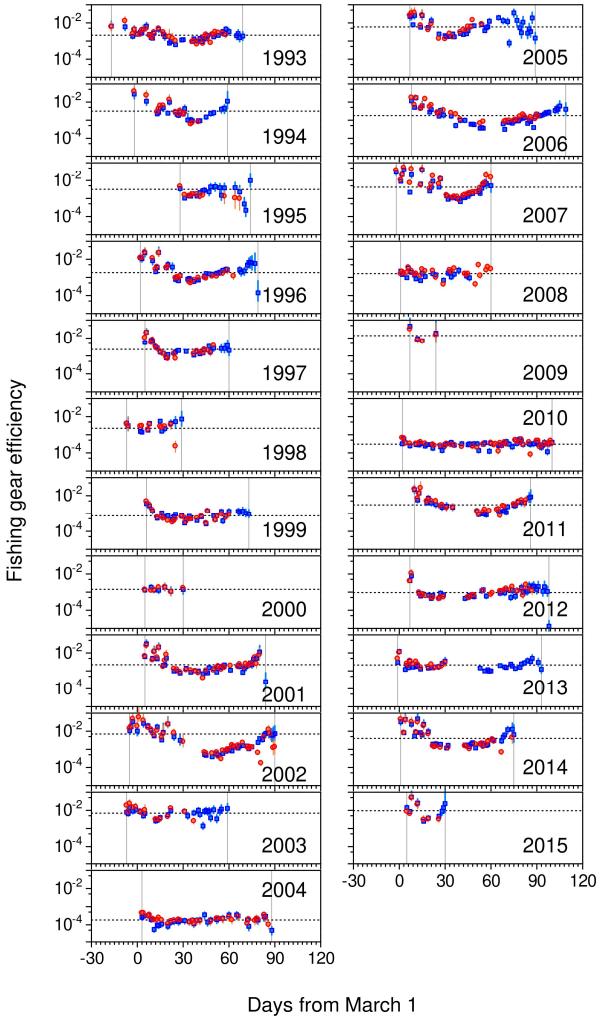

Fig. 17. The fishing gear efficiency in the *Ammodytes japonicus* fishery in Ise Bay from 1993 to 2015. Blue rectangle: median of the Markov chain Monte Carlo (MCMC) samples of the fishing gear efficiency for Mie Prefecture using the integrated model; Red circle: median of MCMC samples for Aichi Prefecture; Vertical line with rectangle or circle: 90% credible interval; Horizontal dotted line: mean of the fishing gear efficiencies; Vertical solid line: first and last fishing day; Number in panel: year.

standard deviations decreased from the 1990s through the 2010s (run test, $p = 0.044$; $n = 23$; Fig. 16b) and positively correlated with the median mean body lengths in the stock in April 25 ($\rho = 0.560$, $p = 0.014$, $n = 18$).

(f) Fishing gear efficiency

In most years, the fishing gear efficiencies were higher at approximately the first and last fishing days (Fig. 17). The minimum, maximum, and median of the mean fishing gear efficiencies were 0.184×10^{-3} in 2004, 13.9×10^{-3} in 2009, and 2.29×10^{-3}, respectively (Appendix Table 9). No long-term decreasing or increasing trend was detected for efficiency (run test $p = 0.959$; $n = 23$; Appendix Table 9). The correlation coefficient between the mean fishing gear efficiencies and the initial stock abundances was weakly negative ($\rho = -0.398$, $p = 0.061$, $n = 23$). The minimum, maximum, and median standard deviations in daily fishing gear efficiency were 0.245 in 2000, 1.45 in 2002, and 0.856, respectively (Appendix Table 9). No long-term decreasing or increasing trend was detected for the standard deviations ($p = 0.809$; $n = 23$; Appendix Table 9).

(g) Catches, annual exploitation rate, and CPUE

If the maximum daily catches in each year were defined as a peak of the fishing, the minimum, maximum, and median of the peaks were 7.8 oku fish in 2000, 59.1 oku fish in 1996, and 27.8 oku fish, respectively (Fig. 18). Peaks were observed on the first fishing day in most years (Fig. 19). The minimum, maximum, and median annual catches were 24.6 oku fish in 2009, 481 oku fish in 2006, and 210 oku fish, respectively (Fig. 20a). The minimum, maximum, and median annual catch rates were 0.641 in 2000, 0.998 in 1996, and 0.987, respectively (Fig. 20b). No long-term decreasing or increasing trend was detected for the rates (run test, p = 0.809, n = 23; Fig. 20b). In most years, the CPUE declined toward the end of the fishing season (Fig. 21). The 90% credible intervals of CPUE tended to be wider and closer to the first fishing day in most years (Fig. 21).

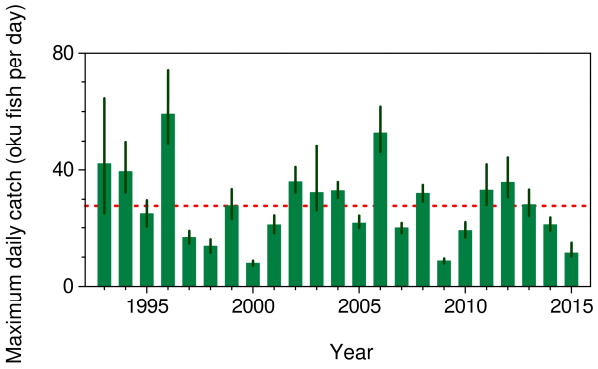

Fig. 18. The maximum daily catch in the *Ammodytes japonicus* fishery in Ise Bay from 1993 to 2015. Bar: median of the Markov chain Monte Carlo samples using the integrated model; Vertical line: 90% credible interval; Dotted line: median of the medians. Unit oku represents 100 million.

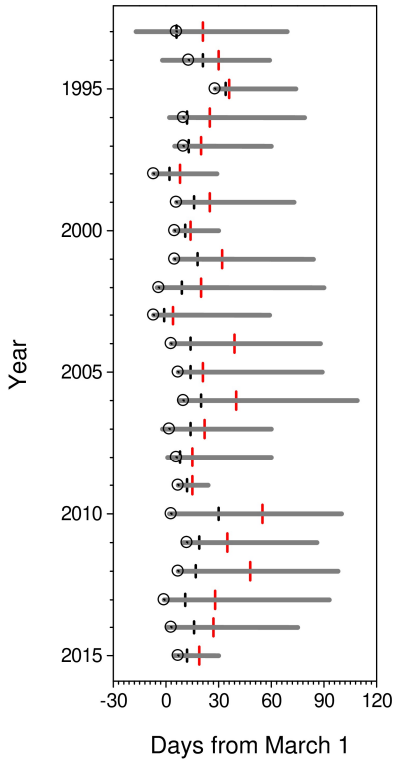

Fig. 19. Day when the maximum daily catch was observed, day when the cumulative catch reached 50% of the annual catch, and day when the cumulative catch reached 75% of the annual catch in the *Ammodytes japonicus* fishery in Ise Bay from 1993 to 2015. Horizontal line: fishing season; Circle: the maximum daily catch day; Black line: 50% cumulative catch day; Red line: 75% cumulative catch day.

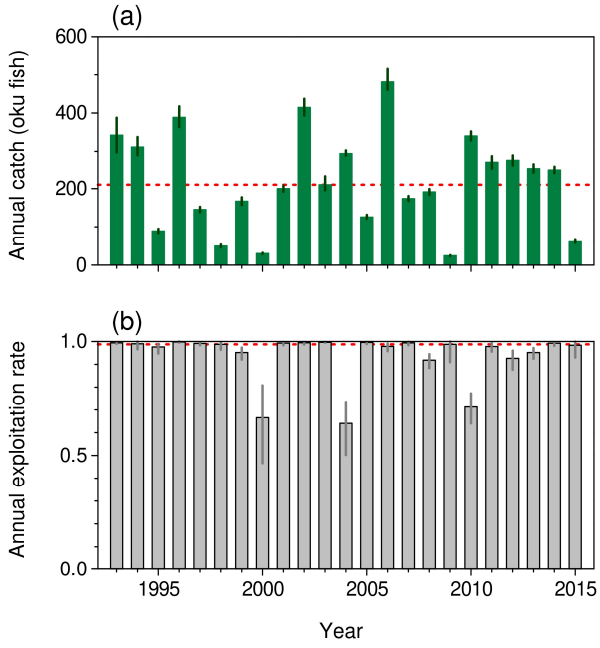

Fig. 20. The annual catch and exploitation rate in the *Ammodytes japonicus* fishery in Ise Bay from 1993 to 2015. (a) the annual catch, (b) annual exploitation rate. Bar: median of the Markov chain Monte Carlo samples using the integrated model; Vertical line: 90% credible interval; Dotted line: median of the medians. Unit oku represents 100 million.

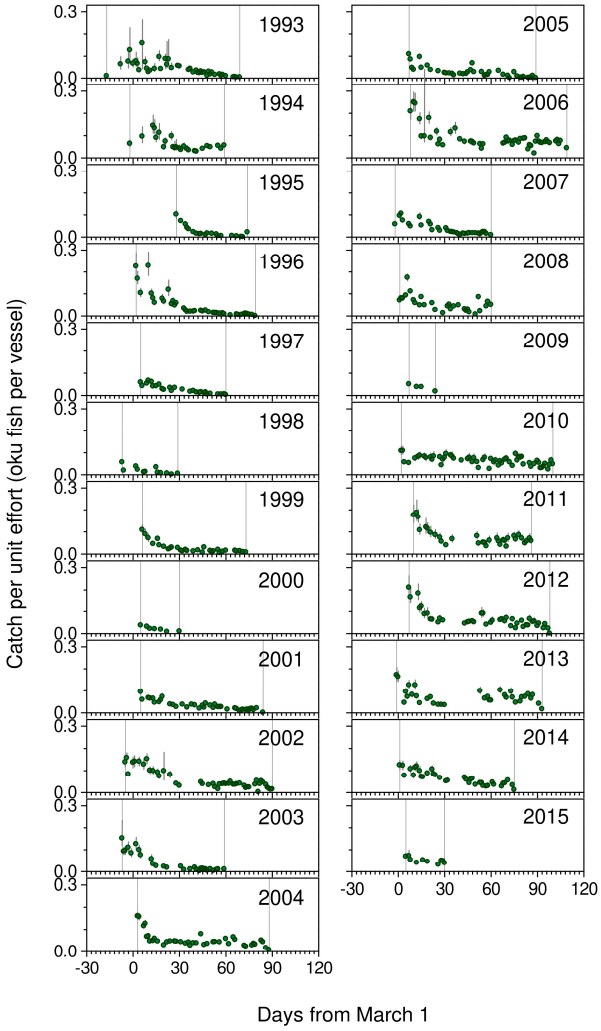

Fig. 21. The catch per unit effort (CPUE) of the *Ammodytes japonicus* fishery in Ise Bay from 1993 to 2015. Circle: median of the Markov chain Monte Carlo samples of the CPUE using the integrated model; Vertical line with the circle: 90% credible interval; Vertical line: first and last fishing day; Number in panel: year. Unit oku represents 100 million.

(h) Final stock abundance

The minimum, maximum, and median abundances of the final stock were 0.310 oku fish in 2009, 164.211 oku fish in 2004, and 2.200 oku fish, respectively (Fig. 22). No long-term decreasing or increasing trend was detected in abundance (run test, p = 0.901; n = 23; Fig. 22). The rankings of the final stock abundance medians in 2014 and 2015 were 14 and 18 out of 23 years, respectively (Fig. 22).

(i) Stock abundance on the day when the fishing ban was first set in the partial area

The minimum, maximum, and median stock abundances on the fishing ban day were 2.2 oku fish in 1998, 261.3 oku fish in 2010, and 32.6 oku fish, respectively (Fig. 23). No long-term decreasing or increasing trend was detected in abundance (run test, p = 0.665; n = 23; Fig. 23). The stock abundance on the day of the fishing ban was less than 20 oku fish in some years before 2009, but not after 2010 (Fig. 23). In contrast, the minimum, maximum, and median of the cumulative catches after the fishing ban day were 0.0 oku fish in 1995, 135.4 oku fish in 1994, and 25.7 oku fish, respectively (Fig. 23). In many years, including after 2010, the cumulative catches after the day of the fishing ban exceeded 20 oku fish (Fig. 23), and the final stock abundances were below 20 oku fish (Fig. 22). Therefore, stock abundance significantly decreased after the fishing

ban, indicating that the abundance of protected adults was low.

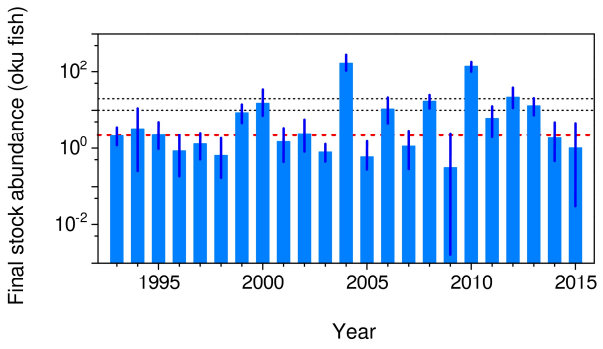

Fig. 22. The final stock abundance of the *Ammodytes japonicus* fishery in Ise Bay from 1993 to 2015. Bar: median of the Markov chain Monte Carlo samples using the integrated model; Vertical line: 90% credible interval; Bold dotted line: median of the medians; Fine dotted line: reference point (10 and 20 oku fish). Unit oku represents 100 million. The data are shown in Appendix Table 7.

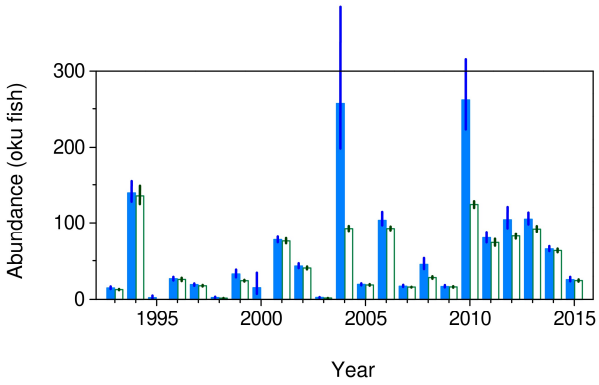

Fig. 23. The *Ammodytes japonicus* stock abundance on the day when the fishing ban was first set in the partial area of Ise Bay yearly from 1993 to 2015 and cumulative catch during the ban period. Solid bar: median of the Markov chain Monte Carlo (MCMC) samples of the stock abundance using the integrated model; Open bar: median of MCMC samples of the cumulative catch using the integrated model; Vertical line: 90% credible interval. Unit oku represents 100 million.

(j) Reproductive relationship

The maximum initial stock abundance in Ricker's model was estimated to be 416 oku fish, and the final stock abundance in the previous year was estimated to be 51 oku fish (Fig. 24a). However, the estimate of the maximum initial stock abundance using the integrated

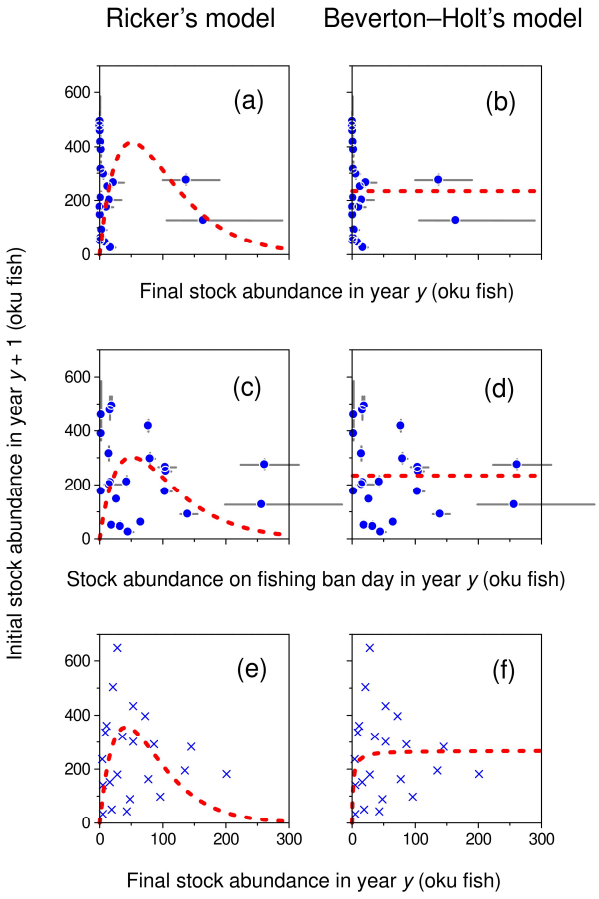

Fig. 24. Reproductive relationships between the final stock abundance in year y and the initial stock abundance in year y + 1 and between the stock abundance on the fishing ban day in year y and the initial stock abundance in year y + 1 for the *Ammodytes juponicus* fishery in Ise Bay from 1993 to 2014. (a), (b), (c), and (d) estimates using the integrated model, (e) and (f) published estimates. Dotted line in left panel: estimate using Ricker's model; Dotted line in right panel: estimate using Beverton–Holt's model; Circle: median of the Markov chain Monte Carlo samples; Vertical and horizontal lines: 90% credible interval; Cross: the published estimate. The published estimates without their credible intervals, based on Yamamoto et al. (2019). Unit oku represents 100 million.

model was 493.21 oku fish and its final stock abundance in the previous year was 0.59 oku fish (Fig. 24a). Therefore, the fit of Ricker's model was low. The equilibrium initial stock abundance estimated using the Beverton–Holt's model was 234 oku fish, and no reproductive relationship was detected (Fig. 24b). Similarly, the fit was poor for the reproductive relationship between stock abundance on the fishing ban day and the initial stock abundance estimated using the integrated model (Fig. 24c, d). The reproductive relationship based on published estimates was also unclear (Fig. 24e, f). The curves for Ricker's model were very similar regardless of the estimate used (Fig. 24a, c, e). The curves for the Beverton–Holt model were similar (Fig. 24b, d, f).

(k) Reproductive efficiency

The minimum, maximum, and median reproductive efficiencies were 0.767 in 2004, 1545.147 in 2009, and 44.062, respectively (Fig. 25). A negative correlation was observed between reproductive efficiency and final stock abundance (Fig. 26a). The magnitude of the reproductive efficiency was influenced by the abundance of the final stock (Fig. 26a). Reproductive efficiencies declined significantly in 2010 (Fig. 25); however, they fluctuated along a linear trend of $r_{300,y}$, and then had a notable decrease in 2014 (Fig. 26a). Similar downward deviations were observed in the other years (Fig. 26a). In contrast, upward deviations were observed in other years (Fig. 26a), and relative reproductive efficiencies exceeded 1.0 in 1993, 1995, 2001, 2003, 2005, and 2009 (Fig. 27). Relative reproductive efficiencies exceeding 1.0 were not observed after the 2010s (Fig. 27).

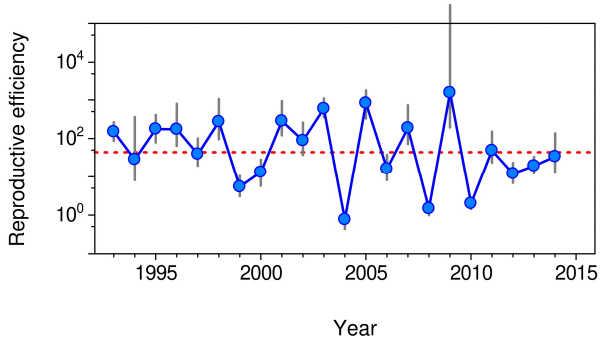

Fig. 25. Reproductive efficiency for the *Ammodytes japonicus* fishery in Ise Bay from 1993 to 2014. Circle: median of the Markov chain Monte Carlo samples using the integrated model; Vertical line: 90% credible interval. Dotted line: median of the medians.

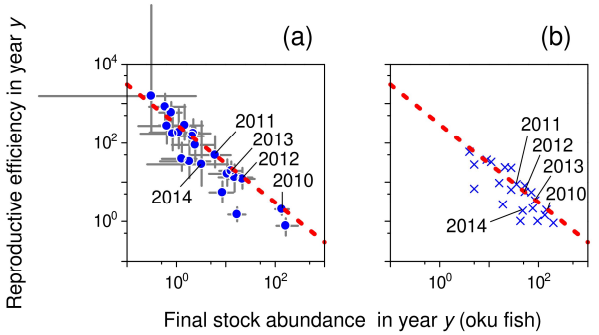

Fig. 26. Relationships between the final stock abundance and reproductive efficiency in year y for the *Ammodytes juponicus* fishery in Ise Bay from 1993 to 2014. (a) estimates using the integrated model, (b) the published estimates based on Yamamoto et al. (2019). Circle: median of the Markov chain Monte Carlo samples; Vertical line: 90% credible interval; Cross: published estimates. Published estimates without their credible intervals. Number in panel: year; Dotted line: reproductive efficiency in year y when the initial abundance in year $y+1$ becomes 300 oku fish. Unit oku represents 100 million.

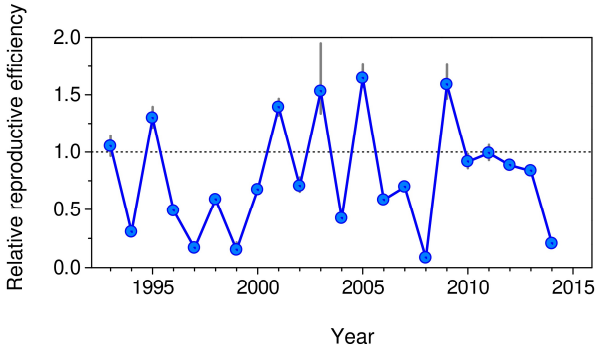

Fig. 27. The relative reproductive efficiency for the *Ammodytes japonicus* fishery in Ise Bay from 1993 to 2014. Circle: median of the Markov chain Monte Carlo samples using the integrated model; Vertical line: 90% credible interval. Dotted line: relative reproductive efficiency = 1.0.

2) Interannual trends in environmental factors and relationships between those with stock indices

(a) Condition factor

The minimum, maximum, and median of the mean condition factors were 4.05 in 2003, 4.72 in 2002, and 4.29, respectively (Fig. 28). The upper limits of the 90% credible intervals of the mean condition factors for 2004 and 2014 were below 4.2. The mean condition factor in 2015 was 4.24, and its 90% credible interval included 4.2 (Fig. 28). No long-term decreasing or increasing trends were detected in the mean condition factors (run test, p = 0.507, n = 23; Fig. 28). The correlation coefficient between the mean condition factors and the initial stock abundances was low (ρ = 0.237, p = 0.275, n = 23). No density effect that reduced the mean condition factors was detected. The minimum and maximum mean condition factors when the relative reproductive efficiencies exceeded 1.0 were 4.05 in 2003 and 4.58 in 1993, respectively (Fig. 29). The relative reproductive efficiencies were below 1.0 in 2014 and 2004, when the mean condition factors were evident below 4.2 (Fig. 29). However, no trend toward higher relative reproductive efficiency with a higher mean condition factor was observed (Fig. 29).

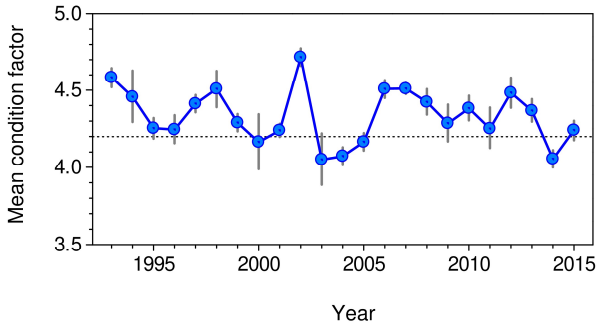

Fig. 28. The mean condition factor of caught *Ammodytes japonicus* in Ise Bay from 1993 to 2015. Circle: median of the Markov chain Monte Carlo samples using the body length body weight conversion equation; Vertical line: 90% credible interval; Dotted line: mean condition factor = 4.2.

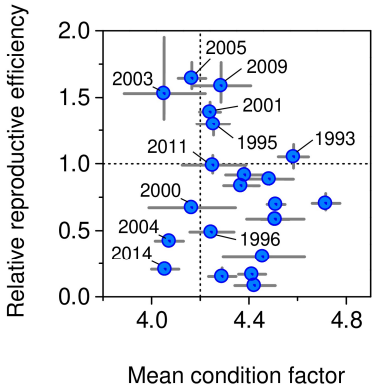

Fig. 29. Relationships between the mean condition factor and relative reproductive efficiency in the *Ammodytes japonicus* fishery in Ise Bay from 1993 to 2014. Circle: median of the Markov chain Monte Carlo samples using the integrated model and body length body weight conversion equation; Solid vertical line: 90% credible interval; Dotted vertical line: mean condition factor = 4.2; Dotted horizontal line: the relative reproductive efficiency = 1.0.

(b) Water temperature

The periods when the mean water temperatures exceeded 21 ℃ at depths of 0, 10, and 20 m in Ise Bay occurred after June, July, and July, respectively (Fig. 30). A long-term increasing trend was detected at 0 m in August (Fig. 30d; Table 5), but not at other water temperatures (Fig. 30; Table 5). However, the mean water temperatures at 10 and 20 m in July and 20 m in August with water temperatures above 21 °C positively correlated with that at 0 m in August (Table 6; Fig. 30d, g, k, l). Since 2012, the mean water temperatures at 10 m and 20 m in July has exceeded 21 °C for two consecutive years (Fig. 30g, k). No relationship was detected between relative reproductive efficiency and mean water temperature at 0 m in June and July (Fig. 31a, b). In contrast, relative reproductive efficiencies exceeding 1.0 were detected in years when the mean water temperature at 10 m in July was below 21 °C and no relative reproduction efficiencies exceeding 1.0 were detected in years when the mean water temperature at 10 m in July exceeded 21 °C (Fig. 31d). The same relationship as that at 10 m was detected for the mean water temperature at 20 m in July (Fig. 31f). The initial stock abundances in January and February negatively correlated with the mean water temperature at 0, 10, and 20 m in January and February (Fig. 32a, b, d, e, g, h).

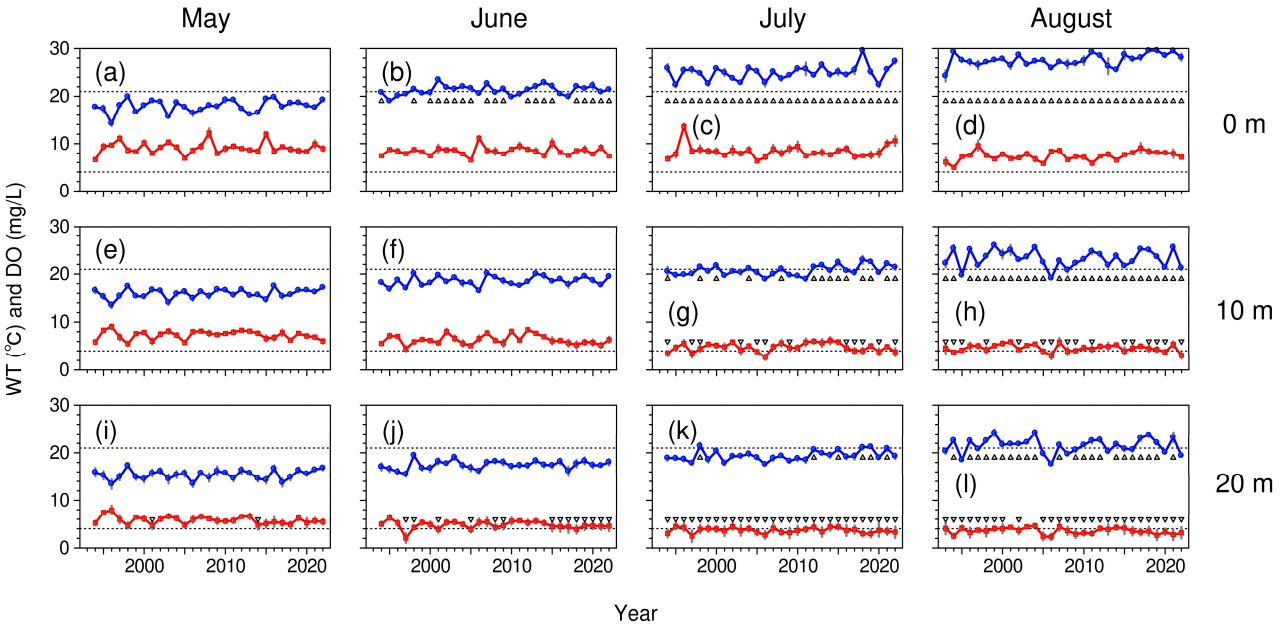

Fig. 30. The mean water temperature (WT) and mean dissolved oxygen concentration (DO) in Ise Bay from 1993 to 2022. (a), (b), (c), and (d) depth of 0 m; (e), (f), (g), and (h) depth of 10 m; (i), (j), (k), and (l) depth of 20 m; Blue circle: median of the Markov chain Monte Carlo (MCMC) samples of WT using the normal distribution model; Red rectangle: median of MCMC samples of DO using the normal distribution model; Vertical line: 90% credible interval; Upper dotted line: 21 ℃; Lower dotted line: 4 mg/L; Triangle: year when the upper credible interval of WT is above 21 ℃; Reverse triangle: year when the lower credible interval or the estimates of DO is below 4 mg/L. WT and DO were observed by the Mie Prefecture Fisheries Research Institute.

Table 5. The *p*-values of the run test for the non-random long-term trend in the mean water temperatures in Ise Bay from 1994 to 2022

Depth (m)	May	June	July	August
0	0.652	0.225	0.775	**0.011***
10	0.775	0.875	0.131	0.652
20	0.936	0.358	0.500	0.358

*: $p < 0.05$; $n = 29$; Under line: water temperatures above 21 ℃ were observed. Bold *p*-value denotes environmental conditions at the depth in the month for *Ammodytes japonicus* in Ise Bay which have evidently deteriorated over time.

Table 6. Spearman's correlation coefficients between the mean water temperature at a depth of 0 m in August and those at depths of 0, 10, and 20 m in May, June, July, and August

Month	Depth (m)	Spearman's correlation coefficient
May	0	0.349
	10	0.189
	20	0.249
June	0	−0.048
	10	−0.206
	20	−0.080
July	0	0.247
	10	**0.385***
	20	**0.375***
August	0	**1.000***
	10	0.281
	20	**0.374***

*: $p < 0.05$; $n = 29$; Under line: water temperatures above 21 ℃ were observed. Bold coefficients denote environmental conditions at the depth in the month for *Ammodytes japonicus* in Ise Bay, which have probably deteriorated over time, similar to those at 0 m in August.

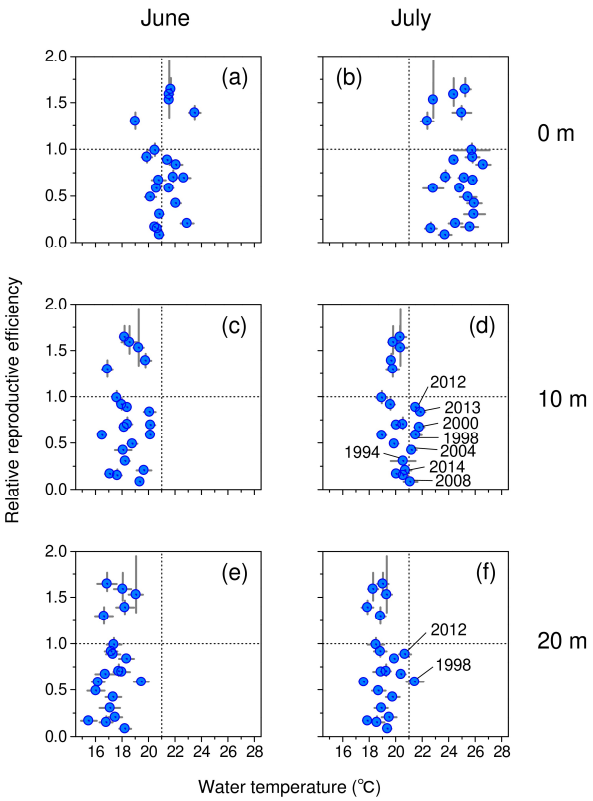

Fig. 31. Relationships between water temperature and relative reproductive efficiency of the *Ammodytes japonicus* fishery in Ise Bay from 1994 to 2014. (a) and (b) 0 m depth, (c) and (d) 10 m depth, (e) and (f) 20 m depth. Circle: median of the Markov chain Monte Carlo samples using the integrated and normal distribution models; Vertical line: 90% credible interval; Dotted vertical line: 21 ℃; Dotted horizontal line: the relative reproductive efficiency = 1.0.

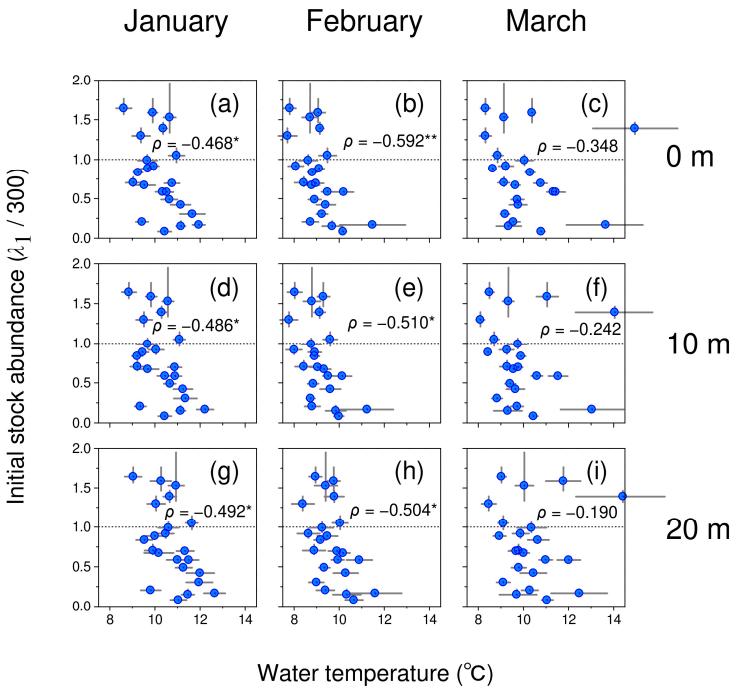

Fig. 32. Relationships between water temperature and the initial stock abundance (λ_1) of the *Ammodytes japonicus* fishery in Ise Bay from 1994 to 2014. (a), (b), and (c) 0 m depth, (d), (e), and (f) 10 m depth, (g), (h), and (i) 20 m depth. Circle: median of the Markov chain Monte Carlo samples using the integrated and normal distribution models; Vertical and horizontal lines: 90% credible interval; Dotted horizontal line: initial stock abundance = 1.0 = 300 oku fish/300 oku fish; ρ: Spearman's correlation coefficient; *: $p < 0.05$; **: $p < 0.01$; $n = 22$. Unit oku represents 100 million.

(c) Dissolved oxygen concentration

The mean DO concentrations at 10 and 20 m in Ise Bay were below 4 mg/L after July and May, respectively (Fig. 30). The mean DO at a depth of 20 m in June was occasionally below 4 mg/L, indicating a long-term decrease (Table 7; Fig. 30j). The mean DO at 20 m in July was below 4 mg/L and positively correlated with that at 20 m in June (Table 8; Fig. 30k). Relative reproductive efficiencies exceeding 1.0 were detected in years when the mean DO at 20 m in June and 10 m in July was above 4 mg/L (Fig. 33d, e).

Table 7. The *p*-values of run test for the non-random long-term trend in the mean dissolved oxygen concentrations in Ise Bay from 1994 to2022

Depth (m)	May	June	July	August
0	0.775	0.775	0.358	0.225
10	0.500	0.131	0.775	0.775
20	0.225	**0.029***	0.936	0.064

*: $p < 0.05$; $n = 29$; Under line: mean dissolved oxygen conentration below 4 mg/L were observed. Bold *p*-value denotes environmental conditions at the depth in the month for *Ammodytes japonicus* in Ise Bay which have evidently deteriorated over time.

Table 8. Spearman's correlation coefficients between the mean dissolved oxygen concentration at 20 m in June and those at depths of 0, 10, and 20 m in May, June, July, and August

Month	Depth (m)	Spearman's correlation coefficient
May	0	0.089
	10	0.718*
	20	0.621*
June	0	0.302
	10	0.766*
	20	**1.000***
July	0	0.070
	10	0.341
	20	**0.427***
August	0	−0.161
	10	0.105
	20	0.158

*: $p < 0.05$; $n = 29$; Under line: mean dissolved oxygen conentration below 4 mg/L were observed. Bold coefficients denote environmental conditions for *Ammodytes japonicus* in Ise Bay, which have probably deteriorated over time, similar to those at 20 m in June.

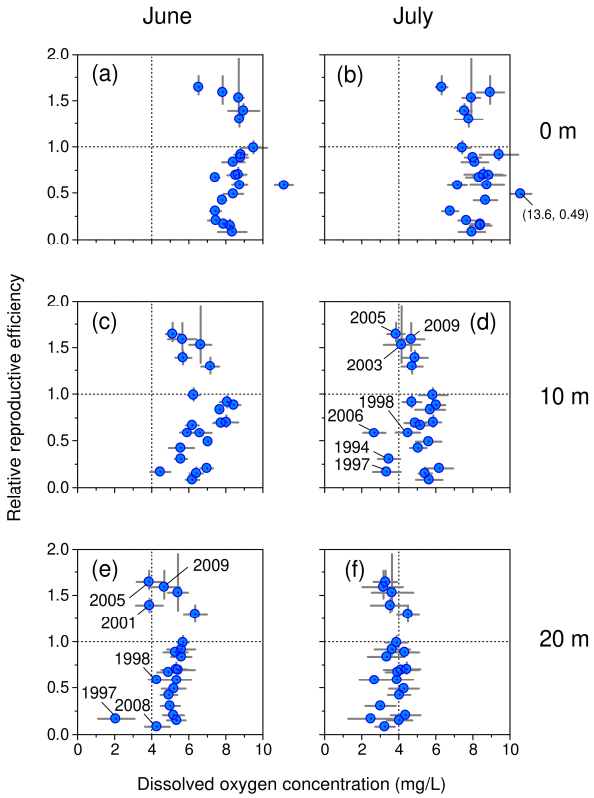

Fig. 33. Relationships between the dissolved oxygen concentration and relative reproductive efficiency of the *Ammodytes japonicus* fishery in Ise Bay from 1994 to 2014. (a) and (b) 0 m depth, (c) and (d) 10 m depth, (e) and (f) 20 m depth; Circle: median of the Markov chain Monte Carlo samples using the integrated and normal distribution models; Vertical and horizontal lines: 90% credible interval; Dotted vertical line: 4 mg/L; Dotted horizontal line: the relative reproductive efficiency = 1.0.

(d) Kuroshio path

The difference in the daily mean sea level showed considerable seasonal interannual variation before 2017 (Fig. 34b). The relative reproductive efficiencies negatively correlated with the difference in May (ρ = −0.496, p = 0.019, n = 22; Fig. 35a) but not in June (ρ = −0.386, p = 0.077, n = 22; Fig. 35b) and in July (ρ = −0.367, p = 0.093, n = 22; Fig. 35c). The initial stock abundance positively correlated with the difference in February (ρ = 0.649, p < 0.01, n = 23; Fig. 36b) and March (ρ = 0.469, p = 0.025, n = 23; Fig. 36c) but not in January (ρ = 0.212, p = 0.329, n = 23; Fig. 36a). The difference in July negatively correlated with the mean water temperature at 0, 10, and 20 m (Plate 5c, f, i). The difference in February negatively correlated with the mean water temperature at 0, 10, and 20 m (Plate 6b, e, h). The difference in March negatively correlated with the mean water temperature at 0, 10, and 20 m (Plate 6c, f, i). The difference in June positively correlated with the mean DO at 10 and 20 m (Plate 7a, c). Therefore, the Kuroshio path affected the water temperature and DO at various depths during various seasons.

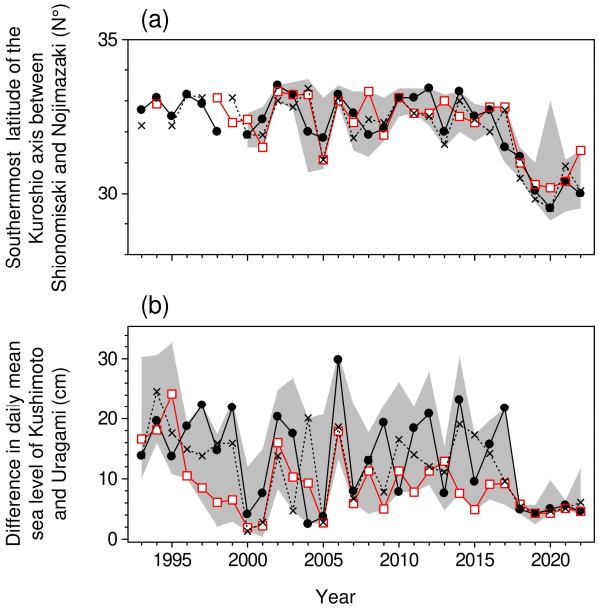

Fig. 34. The southernmost latitude of the Kuroshio axis between Shionomisaki and Nojimazaki, and difference in daily mean sea level of Kushimoto and Uragami from 1993 to 2022. (a) the Southernmost latitude, (b) difference in the daily mean sea level. Rectangle: February; Cross: May; Circle: July; Mesh: yearly range from minimum to maximum. The data were observed by the Japan Meteorological Agency.

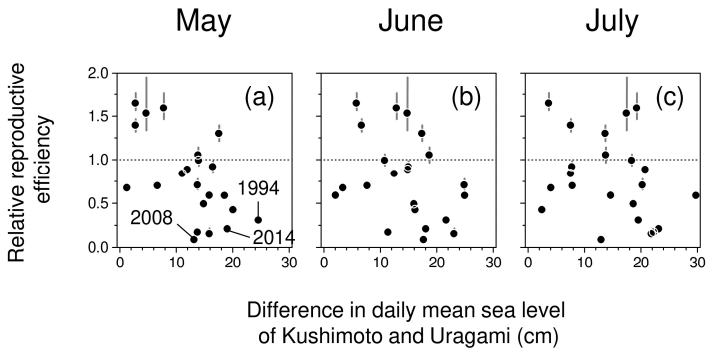

Fig. 35. Relationships between the difference in daily mean sea level of Kushimoto and Uragami immeadiately after the fishing season of the *Ammodytes japonicus* fishery in Ise Bay and the relative reproductive efficiency from 1993 to 2014. (a) May, (b) June, (c) July. Circle: median of Markov chain Monte Carlo samples using the integrated model; Vertical line: 90% credible interval; Dotted horizontal line: the relative reproductive efficiency = 1.0; Number in panel: year. The differences were observed by the Japan Meteorological Agency, which were without credible intervals.

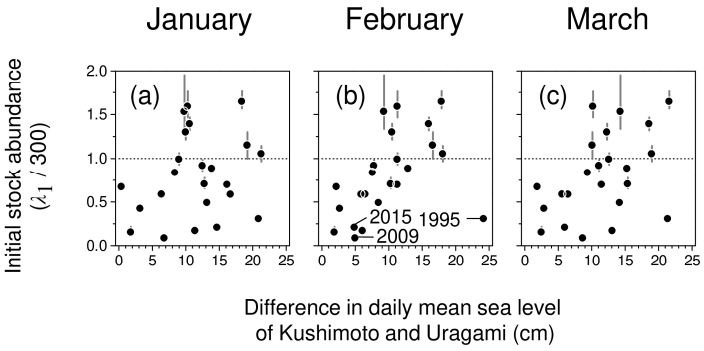

Fig. 36. Relationships between the difference in daily mean sea level of Kushimoto and Uragami immediately before the fishing season of the *Ammodytes japonicus* fishery in Ise Bay and the initial stock abundance (λ_1) from 1993 to 2015. (a) January, (b) February, (c) March. Circle: median of Markov chain Monte Carlo samples using the integrated model; Vertical line: 90% credible interval; Dotted horizontal line: initial stock abundance = 1.0 = 300 oku fish/300 oku fish; Number in panel: year. Unit oku represents 100 million. The differences were observed by the Japan Meteorological Agency, which were without credible intervals.

DISCUSSION

1. Validity of the integrated model

The MPE for bucket numbers and mean body lengths in the integrated model in this study were approximately zero (Figs. 6 and 7; Appendix Tables 2 and 3). These good fits indicated the validity of the integrated model. However, the following points should be considered.

1) Daily variation in body length selection

The selection model used in this study (Equation [37]) was assumed to be a logistic model that did not change during the fishing season. However, *A. japonicus* in Ise Bay has a higher market price for smaller body lengths (Nishimura 1993). Therefore, most fishing vessels (fisheries) possibly targeted schools with smaller body lengths during the first half of the fishing season and subsequently focused on schools with larger body lengths in the second half (Aichi Prefecture 1994). The maximum posterior prediction interval of the mean body length in 1993 was significantly more expansive than that on other days in 1993 (Fig. 7; Appendix Table 4). Although such wide intervals were not observed in years other than 1993 (Fig. 7; Appendix Table 4), size-selective fishing may have affected these estimates. In this study, the fishing gear efficiency tended to increase again during the latter half of the fishing season (Fig. 17). This may be because fishing vessels in Mie Prefecture changed their fishing methods in the latter half of the fishing season to selectively catch larger *A. japonicus* (Nakamura et al. 2017). However, in other years, an increase in fishing gear efficiency was also observed in the latter half of the fishing season for vessels in Aichi Prefecture that did not use such fishing methods. Therefore, a detailed analysis of the effects of nonlinearity on fishing gear efficiency estimates (Nishijima et al. 2019; Roa-Ureta 2012) is required.

2) Pseudo growth curve in body length

The daily growth rate of the young *A. japonicus* in Ise Bay was estimated to be 0.66–0.85 mm/day based on the relationship between otolith daily rings and body lengths (Tomiyama and Komatsu 2006). In contrast, the median peak of the daily change in the mean body length in the stock during the fishing season was 6.88 mm/day in this study. The daily changes were unnaturally large compared with the aforementioned reports, and large daily change rates were observed near the recruitment completion day (Fig. 15). Therefore, the integrated model used in this study is likely to have structural problems from the first fishing day to the day of recruitment completion. Specifically, two possible problems exist: the first is incorporating the larval transport effects. The integrated model in this study incorporated the effect of

transport into the transition probabilities of length class *i* = 1 (0–10 mm class) but not for other length classes. However, this model structure requires a short-term transition of the non-target stock from size class 0–10 mm toward larger classes if there are true transports in the larger classes. A possible countermeasure is to incorporate transport effects into other classes. However, this model structure makes it difficult to distinguish between the parameters of the selection model and those of the transport effect. The second is the segmentation of body length composition during the pre-recruitment growth phase. In the integrated model used in this study, the body length classes of the non-target stock were subdivided into 10 mm intervals. However, the Ise Bay fishery survey did not observe the non-target stock abundance and body length. Therefore, parameters before recruitment might not have been estimated adequately owing to insufficient observations. A possible countermeasure to these two problems is simplifying the model structure to combine the pre-recruitment body length classes. However, because the selection model differed yearly (Appendix Table 8), a new problem arose regarding which body length classes should be combined. Because solving the problem by only improving the model structure is challenging, a practical approach would involve research institutes conducting surveys on the abundance and body length composition of non-target stock during the fishing season.

As mentioned above, the growth from the first fishing day to the recruitment completion day in the integrated model of this study was formally constructed, making it difficult to understand its biological significance. However, the growth rates after the recruitment completion day were based on the observed body length compositions, and the mean body lengths in the stock and those of the fish caught after the recruitment completion day were in good agreement (Fig. 15). Therefore, any discussion of growth based on estimates using the integrated model should be limited to the period after the recruitment completion day.

3) Overfitting to the observed values

All observed values of the bucket numbers were within the 90% prediction intervals (Fig. 6). This may be overfitting owing to the perfect match between the number of observations of the bucket numbers and the number of parameters of fishing gear efficiency. The survey should be improved to obtain replicates of the number of buckets per prefecture per day, and the effects of overfitting should be examined. However, the parameters in the integrated model used in this study follow uninformative prior distributions. Additionally, the simulation analysis did not indicate any significant bias in the estimates obtained using the integrated model (Table 4). The effect of overfitting may have been negligible in the stock assessment of *A. japonicus* fishery in Ise Bay.

2. Properties of the integrated model

In the simulation analysis in this study, the biases of the initial and final stock abundance estimates using DeLury's model or Phiri's model were significantly larger than the true values when there were large recruits during the fishing season; this tendency was more pronounced for the final stock abundance (Table 4). As mentioned above, recruitment likely occurs during the fishing season in the *A. japonicus* fishery in Ise Bay. The integrated model analysis also confirmed that recruitment often occurred during the fishing season (Figs. 13 and 14). Therefore, the published estimates of the initial and final stock abundances using DeLury's or Phiri's model (Fig. 8a, b) may have been larger than the true values in some years. Based on their published estimates, the annual exploitation rate and reproduction efficiency (Fig. 8d, e) may also deviate significantly from the true values. Furthermore, DeLury's and Phiri's models treat the number of caught fish as known; however, these are unknown and likely have large estimation errors (Fig. 21). Note the interpretation of the estimation errors obtained from such conventional models. In contrast, in the simulation analysis of this study, the estimates of the initial stock abundance using the integrated model agreed well with the true values, even when recruitment occurred during the fishing season (Table 4). The estimates of the final stock abundance using the integrated model tended to be relatively larger, but the bias tended to be smaller than those using DeLury's or Phiri's models (Table 4). The integrated model is preferable to conventional models for estimating final stock abundance. However, regardless of

the model used, the accuracy of the estimates was affected by the sample size (Table 4; Fig. 11). In the simulation analysis of this study, large biases were identified in the datasets when the sample size (number of fishing days) was ≤ 15 days (Fig. 11). Therefore, a larger sample size was required. Because the significant overestimates had large upper limits of credible intervals (Fig. 11a, b), verifying the credible intervals of the estimates was also important. The number of fishing days in the Ise Bay *A. japonicus* fishery was ≤ 15 in 1998, 2000, 2009, and 2015 (Table 1). However, the upper limits of the credible intervals of these estimates obtained using the integrated model were small (Figs. 12 and 22). Therefore, it can be inferred that the biases owing to the small sample size were small for estimates using the integrated model in this study.

In the simulation analysis in this study, Phiri's model tended to show significantly less bias in the estimates with increasing sample size, even under large recruitment scenarios during the fishing season (Table 4). This might be because the simulation datasets used in this study were based on the *A. japonicus* fishery in Ise Bay. Therefore, recruitment during the fishing season was concentrated in the first half of the fishing season (Fig. 13), and the increase in sample size may have increased data from the second half of the fishing season when there was little recruitment. In addition, because Phiri's model enables unequal variance in the daily variation of catches, data from the second half of the fishing season may have been effectively corrected for bias. Phiri's model also tended to show a reduction in estimate bias with increasing sample size, even for scenarios with daily variations in fishing gear efficiency (Table 4). This may be because the simulations in this study assumed independent daily variations in the fishing gear efficiency over time; therefore, the accuracy improved with increasing sample size. A model that allows for unequal variance, such as Phiri's model, may be able to estimate with less bias in large sample sizes. However, the bias was large in scenario viii (Table 4). The more adverse the conditions, the larger the required sample size. Because such conditions are common in the *A. japonicus* fishery in Ise Bay, the integrated model, which is less affected by sample size, is more robust than Phiri's model.

The CPUE of the *A. japonicus* fishery in Ise Bay notably fluctuates immediately after the first fishing day (Yamada 2011). The CPUE estimated using the integrated model also fluctuated significantly immediately after the first fishing day (Fig. 21). Such large daily fluctuations are interpreted in conventional models as being due to the effects of the spatial distribution of *A. japonicus* (Yamada, 2011). In Ise Bay, surveys on the densities of *A. japonicus* larvae before the fishing season have confirmed that the distribution of larvae gradually spreads from the mouth to the inside of the bay (Miyamura and Sugino 1959; Yamada et al. 1998). In contrast, within the structure of the integrated model, catches fluctuate based on state processes related to recruitment, fishing gear efficiency, and body length composition. Recruitment and fishing gear efficiency exhibited large daily variations in the first half of the fishing season (Fig. 13 and 17). This may be attributed to intermittent recruitment during the first half of the fishing season, which increased the spatial variations in fish density and, consequently, daily variations in fishing gear efficiency. Therefore, the integrated model has a structure that allows for temporal and spatial variations.

3. Stock assessment

1) Effects of overfishing

Published estimates of the final stock abundances in 2014 and 2015 were 48 and 33 oku fish, respectively (Yamamoto et al. 2019). In contrast, the estimates obtained using the integrated model were 1.836 and 1.007 oku fish, and the upper limits of these credible intervals were well below 10 oku fish (Fig. 22). The lowest credible interval was found in 2009, and the second lowest was in 2015. These intervals overlap, indicating that 2015 might have had the lowest final stock abundance in 23 years. However, it is unlikely that the final stock abundance in 2015 was uniquely low because there were several years (1996, 1998, 2003, 2005, and 2009) when the estimates of the final stock abundance were lower than those in 2015 (Fig. 22). Therefore, explaining the low stock abundance since 2015 only by overfishing in 2014 and 2015 is challenging.

The published annual exploitation rates were approximately 80%, which is believed to be due to enhanced management increasing the final stock abundance (Nakamura et al. 2017; Yamamoto et al. 2019).

In contrast, the annual exploitation rates estimated using the integrated model in this study were higher than the published estimates, and the interannual trend was not consistent with the published estimates (Fig. 8d). Therefore, the effect of enhanced management on increasing the final stock abundance may not have been as substantial as expected. However, differences from the published estimates were observed over many years (Fig. 8d), and in some years, the annual exploitation rate was higher than that in 2015 (Fig. 20b). Therefore, the annual exploitation rate was unlikely uniquely high in 2015.

2) Validity of the reference point

As mentioned above, the final stock abundances were lower than previously assumed (Fig. 8b), and the annual exploitation rates were higher than previously assumed (Fig. 8d). Considering the intense stock utilization, what factors have contributed to the *A. japonicus* stock being sustained for over 20 years? This section addresses this question:

Most catches in the Ise Bay *A. japonicus* fishery were caught over a short period from the first fishing day (1–2 months) (Fig. 19). Therefore, the models used in this study assumed no natural mortality during the fishing season. However, *A. japonicus* stock abundance in Ise Bay, for example, has decreased because of predation by larger fish (Yamada et al. 1998; Yanagibashi et al. 1997). Ignoring this natural mortality, the initial and final stock abundances were estimated to be smaller than the true values, and the annual exploitation rates may have been overestimated. This issue is also common in published estimates using conventional models. Treating stock abundance estimates in Ise Bay, which does not account for natural mortality, as relative abundance indices appear reasonable.

As mentioned above, the published estimates of the initial and final stock abundances in Ise Bay are probably not meaningful as absolute values. Additionally, even when the published estimates were used as relative abundance indices, the trends in the final stock abundance did not coincide with those estimated using the integrated model (Fig. 8b). As a result, it was necessary to redefine the reference point based on the estimates obtained using the integrated model. However, no evident reproductive relationship was observed in the present study (Fig. 24a–d). The initial stock abundance tended to be higher when the final stock abundance was lower (Fig. 24a–d). This relationship highlights the difficulty of defining a reasonable reference point for *A. japonicus* stocks in Ise Bay. The scatterplot of reproductive relationships during 1986–1994 presented by Funakoshi et al. (1997) was very similar to that during 1993–2014 in the present study (Fig. 24a). Although we assumed Ricker's model to be a reproductive relationship in fisheries, the reference point based on these reproductive relationships may lack validity.

In this study, the stock abundance on the day the fishing ban was first implemented in the partial area was confirmed to be almost equal to the cumulative catch during subsequent days (Fig. 23). This indicates that the effect of the fishing ban was limited and that the non-target stock (*A. japonicus* in the Atsumi open sea (Tomiyama 1996)) maintained a reproductive relationship in the *A. japonicus* population in Ise Bay. Additionally, this study found an ambiguous reproductive relationship between the final and initial stock abundance in the following year (Fig. 24), suggesting the presence of stocks not targeted for fishing. Reproductive efficiency has been discussed based on the final stock abundance (Nakamura et al. 2017; Yamada 2011; Yamamoto et al. 2019). However, many of the *A. japonicus* estivating collected in Deyama in 2007 contained older fish (≥ 1 year old), making it challenging to separate age classes by their body length composition (Kamiya et al. 2008; Yamada and Sawada 2008). Therefore, the parents of the initial stock may have been yearlings and older fish. However, otolith analysis of fish estivated in the 2010s revealed that the proportion of fish older than one year was small (Uzaki and Aoyama 2012; Uzaki and Takeda 2011; Uzaki et al. 2013, 2014, 2015). The abundance of older fish, which were the main spawners up to and including the 2000s, possibly declined in the 2010s, and the stock could not recover. Such a decrease in initial stock abundance, owing to a decline in the abundance of older fish, has been reported in the Seto Inland Sea *A. japonicus* population (Akai and Yoneda 2021).

3) Reassessment of confusing cases

Confusion existed in estimating the final stock

abundance in the 1994 and 2008 stock assessments (Uzaki et al. 2010; Yamada et al. 1994). In the following section, these cases are reassessed based on the rank order of the estimates using the integrated model of this study.

(a) Reassessment in 1994

In 1994, an increase in the CPUE was observed immediately before the end of the fishing season (Yamada et al. 1994). Published estimates of the initial stock abundance for this year were estimated using DeLury's model, and the abundance was estimated to be 320 oku fish when the CPUE near the end of the fishing season was excluded and 390 oku fish when it was not excluded (Yamada et al. 1994). At that time, the cause of the increase in CPUE was unknown; therefore, the primary question was which estimate should be used to determine the final stock abundance (Yamada et al. 1994). Subsequently, detailed analyses were conducted, and the latter estimate was judged to be closer to the true abundance because a large abundance of estivating fish was found in Deyama (Yamada et al. 1995). The latter was also supported because the published estimate of the final stock abundance was 97 oku fish using Phiri's model, which ranked fourth out of 23 years (Yamada 2011; Yamamoto et al. 2019). An increase in the CPUE using the integrated model was also observed near the end of the fishing season in 1994 (Fig. 21). However, the final stock abundance using the integrated model in 1994 was estimated to be 3.24 oku fish, which ranked 10 out of 23 years (Fig. 22). Based on the estimates using the integrated model, it is unlikely that the final stock abundance in 1994 was particularly high compared to that in other years. Therefore, we must consider other reasons for the large abundance of estivating fish in 1994.

(b) Reassessment in 2008

The initial stock abundance and annual catch of *A. japonicus* fishery in Ise Bay were extremely low in 2009 (Figs. 12 and 20). Overestimation of the final stock abundance in 2008 owing to recruitment during the fishing season led to overfishing in 2008 (Uzaki et al. 2010). However, using the integrated model in this study, the final stock abundance in 2008 was estimated to be 17 oku fish, the fourth highest among 23 years (Fig. 22). Overfishing in 2008 is unlikely to have caused the low initial stock abundance observed in 2009. We must also consider other reasons for the low abundance in 2009.

One possible explanation for this confusion is that conventional models did not correct for the effects of recruitment and/or variations in fishing gear efficiency during the fishing season. Similar problems can be solved in the future using an integrated model. Another cause of confusion may be the assumption that the final stock abundance positively correlates with estivating fish abundance. This assumption is based on the results of a correlation in the 1990s (Funakoshi et al. 1997). However, its applicability since the 2000s must be examined.

4) Effects of environmental factors

In the *A. japonicus* population in the Seto Inland Sea, a decrease in condition factors owing to the deterioration of the feeding environment during the fishing season and consequent worsening of reproductive efficiency has been reported (Hashiguchi et al. 2021; Nishikawa et al. 2020). In the *A. japonicus* population in Ise Bay, a low condition factor and relative reproductive efficiency were observed in 2014 (Figs. 27 and 28). This is similar to the case in the Seto Inland Sea. However, because the same low condition factor as in 2014 was also observed in 2003 and 2004 (Fig. 28), the condition factor in 2014 was unlikely to be uniquely low. No positive correlation was observed between the condition factors and relative reproductive efficiency (Fig. 29). This correlation is evidenced by the fact that despite a standard level of condition factor in 2015 (Fig. 28), juvenile abundance in 2016 did not recover to a level sufficient to lift the ban (Hayashi et al. 2017; Yamamoto et al. 2019). Although a food shortage occurred in 2014, explaining the long-term fluctuations in *A. japonicus* stock abundance in Ise Bay solely regarding feeding environments during the fishing season is challenging.

No long-term decreasing trend in the condition factors during the fishing season was identified in this study (Fig. 28). However, a decrease in the body length of the stock was detected during the period from 1993 to 2015, after recruitment was completed (Fig. 16a). In addition, a long-term decrease in the standard deviations of the body length compositions in the stock was detected (Fig. 16b).

A positive correlation between body length and deviations in body length composition was observed in this study. In laboratory experiments, *A. japonicus* in underfed environments was observed to limit body length and increase body weight (Yamada et al. 1999a). A reduction in body length leads to decreased egg production per fish (Yamada et al. 1999a). Therefore, egg production in *A. japonicus* populations in Ise Bay may have decreased over the long term because of a lack of food. A decrease in the standard deviation of body length composition may represent a yearly reduction in spawning frequency or shortening of the spawning period. However, the correlation between the deviation in body length compositions and relative reproductive efficiency during 1993–2014 was unclear (Fig. 37). Therefore, a decrease in the mean and deviation of body length during the fishing season may have a negligible effect on stock decline.

The *A. japonicus* fishery in Ise Bay generally ends in May. Uncaught *A. japonicus* actively feed immediately before estivation, and their weight increases rapidly (Sekiguchi et al. 1976). In June and July, when the water temperature reaches 21 °C, the fish migrates to the bottom at the mouth of the bay to estivate (Itokawa 1983; Nishimura et al. 1991; Yamada 2011). Although the condition factor of fish estivating Ise Bay in the 2010s was low (Nakamura et al. 2017), no long-term decreasing trend was observed in the condition factor during the fishing season in this study (Fig. 28). This discrepancy in trend indicates that the transition period between the end of fishing and estivation was 1–2 months and that food shortages occurred during this period. Unfortunately, fisheries or surveys of *A. japonicus* in Ise Bay during this transition period were few. Discussing feeding environments based on actual conditions during the transition period is difficult. However, in this study, since 2012, the mean water temperature at 10 m in July exceeded 21 °C for two consecutive years (Fig. 30g), and a negative correlation between this water temperature and relative reproductive efficiency was confirmed (Fig. 31d). The mean water temperature at 0 m in July has been above 21 °C since the 1990s (Fig. 30c, d), indicating that this depth zone is initially unsuitable as a habitat for *A. japonicus*. In August, the water temperatures in Ise Bay have been above 21 °C since the 1990s (Fig. 30d, h, i), indicating that Ise Bay in August is initially unsuitable as a habitat for *A. japonicus*. In addition, the DO at a depth of 20 m after July has been below 4 mg/L since the 1990s (Fig. 30k, l), indicating that this depth zone after July is initially unsuitable as a habitat for *A. japonicus*. Although no studies on the vertical distribution of *A. japonicus* in Ise Bay have been conducted, in other bays, *A. japonicus* larvae are abundantly distributed at approximately 10 m when foraging for food during the daytime (Kusakabe et al. 2000; Yamashita et al. 1985). Zooplankton are densely distributed in the middle depth zone of Ise Bay (Sekiguchi 1978, 1985). The middle depth zone of Ise Bay is an important feeding ground for *A. japonicus*. However, *A. japonicus* may not have been able to feed on zooplankton during the transition period after July because of high water temperatures and low DO since the 2010s (Table 9; Fig. 30). The shortening of the transition period may also have forced *A. japonicus* to have a low condition factor. This may result in lower survival rates during estivation (Nakamura et al. 2017) and smaller body length composition variations during the following year's fishing season (Fig 16b).

The *A. japonicus* stock abundance in Ise Bay has notably declined since 2015 (Fig. 12), and the Kuroshio

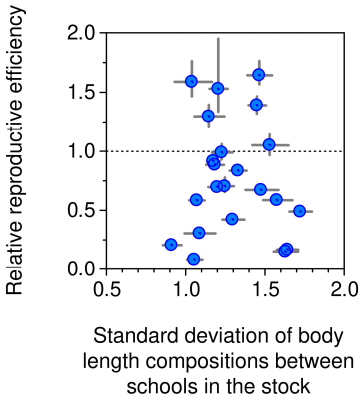

Fig. 37. A relationship between the standard deviation of body length compositions between schools in the stock and the relative reproductive efficiency in the *Ammodytes japonicus* fishery in Ise Bay from 1993 to 2014. Circle: median of the Markov chain Monte Carlo samples using the integrated model; Vertical and horizontal lines: 90% credible interval; Dotted horizontal line: the relative reproductive efficiency = 1.0. The data were based on Figs. 16 and 27.

path has changed to a large meander distant from Ise Bay since 2017 (Fig. 34a). This notable decrease does not appear to be caused by the large meandering of the Kuroshio path. However, this study confirmed that the Kuroshio path in February 2015 was similar to that of the large meander after 2017, based on the difference in the daily mean sea levels (Fig. 34b). A notable correlation was observed whereby the initial stock abundance in Ise Bay decreased during the years when the Kuroshio path in February was distant from Ise Bay. The data point in 2015 aligned well with this correlation (Fig. 36b). Although an outlier (1995) was identified in this correlation (Fig. 36b), the previous year (1994) had high water temperature and low DO in the middle depth zone in July (Fig. 30g, 31d, 33d). These environmental factors could also successfully explain the low reproductive efficiency observed in 2008, which was reassessed in the present study (Fig. 31d, 36b). Therefore, the long-term fluctuation in stock abundance can be explained by water temperature and DO in the middle depth zone during the estivation transition period and by the Kuroshio path in winter. The effects of the Kuroshio path on the initial stock abundance are particularly significant if the water temperatures were below 21 °C (ρ = 0.773; Fig. 38c). However, inconsistent cases (large initial stock abundances in DO below 4 mg/L) were identified for DO (Fig. 38d). This may have been due to the accuracy of the DO estimation and/or the validity of the reference value (4 mg/L) (Fig. 33d). Therefore, a detailed study of the effects of DO is required. The results of these effects were similar based on published estimates of initial stock abundance (Plate 8).

This study indicates that the effects of the Kuroshio path on fluctuations in *A. japonicus* stock abundance in Ise Bay may be opposite in February and May (Fig. 35a, 36b). In general, February is the time when the *A. japonicus* larvae move into Ise Bay, and young and adults move out of the bay to their estivation grounds in May. Therefore, seasonal differences in the effects of the Kuroshio path can be interpreted as reflecting the direction of transport and migration of *A. japonicus*. However, the validity of this interpretation requires further detailed analysis because the Kuroshio path has large seasonal and interannual variations (Fig. 34b) and considerably influences water quality in Ise Bay (Plates 5–7).

Table 9. Percentages of years before and after 2014 with sufficient *Ammodytes japonicus* foraging in Ise Bay

Years	Depth (m)	May	June	July	August
1994–2013	0	100 (20/20)	35 (7/20)	0 (0/20)	0 (0/20)
	10	100 (20/20)	95 (19/20)	40 (8/20)	0 (0/20)
	20	95 (19/20)	70 (14/20)	0 (0/20)	0 (0/20)
2014–2022	0	100 (9/9)	22 (2/9)	0 (0/9)	0 (0/9)
	10	100 (9/9)	100 (9/9)	0 (0/9)	0 (0/9)
	20	88 (8/9)	11 (1/9)	0 (0/9)	0 (0/9)

Number in parentheses: number of suitable years per subject year based on Fig. 30; Gray background: less than 40%.

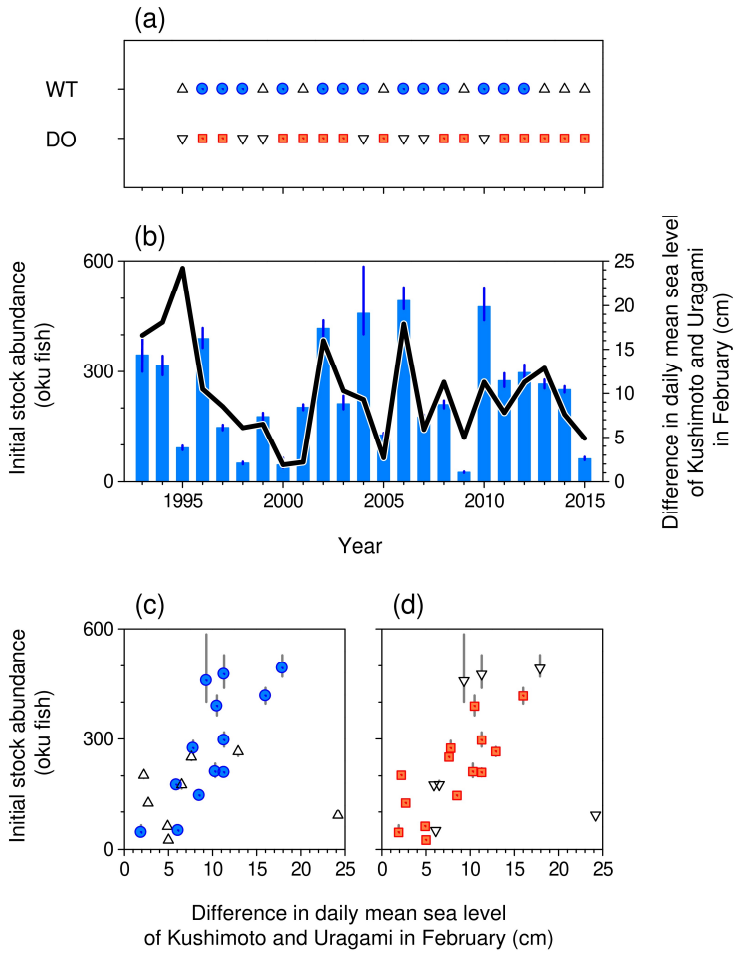

Fig. 38. (a): The water temperature (WT) and dissolved oxygen concentrations (DO) at a depth of 10 m in Ise Bay in July of the previous year from 1995 to 2015. Triangle: WT above 21 ℃; Circle: WT below 21 ℃; Reverse triangle: DO below 4 mg/L; Rectangle: DO above 4 mg/L. The data are based on Fig. 30.
(b): The initial stock abundance in the *Ammodytes japonicus* fishery in Ise bay and the differences in daily mean sea level of Kushimoto and Uragami in February from 1993 to 2015. Bar: initial stock abundance; Vertical line: 90% credible interval; Line: the difference in daily mean sea level. Unit oku represents 100 million. The data are based on Figs. 12 and 34b.
(c) and (d): Relationships between the initial stock abundance in the *A. japonicus* fishery in Ise Bay and the differences in daily mean sea level of Kushimoto and Uragami in February from 1995 to 2015. The data are based on panels a and b. Spearman's correlation coefficients in the circles and the rectangles are 0.773 ($p < 0.01$; $n = 13$) and 0.761 ($p < 0.01$; $n = 14$), respectively.

4. Prospects for the stock assessment and management

Fishing gear efficiency in the *A. japonicus* fishery in Ise Bay negatively correlated with initial stock abundance. This means determining the stock abundance only by the interannual variation of CPUE is challenging, and estimating the stock abundance yearly using certain models is necessary. However, this study indicates that the assumptions of no recruitment and constant fishing gear efficiency during the fishing season do not fit the properties of the *A. japonicus* fishery in Ise Bay. Forcing conventional models to fit data with such properties results in biased estimates. Unreasonable fitting caused confusion in past stock assessments, such as those in 1994 and 2008, as mentioned above. As it is unlikely that such a bias will occur in the estimates using the integrated model, we expect that the integrated model will be used in future stock assessments. However, the integrated model is imperfect. The fishing days of *A. japonicus* fisheries in Ise Bay positively correlated with the initial stock abundance (Fig. 39). Therefore, high accuracy is required in years when the initial stock abundance is small; however, a dilemma arises in years when the sample size is small, and estimating the stock abundance is challenging. Although this problem is not limited to integrated models, there is a risk of overestimation when sample sizes are too small, even in the integrated model. The actual catch per day was close to the reference point (Fig. 18), and the maximum catch was observed on the first fishing day (Fig. 19). If the initial stock abundance is low, the decision to prohibit fishing may be delayed. A possible countermeasure is to expand the survey of non-target stocks and improve the robustness of the model and stock management, even with a small sample size. The computation time for each year using DeLury's and Phiri's models was within tens of seconds in this study, whereas the analysis using the integrated model required several hours for each year. Therefore, a model to analyze

data from multiple years was not developed in this study. However, in the future, the use of such a model integrating data from multiple years may be effective for robust estimation (Nishijima et al. 2019). The body length to body weight conversion equation, selection model, and fishing gear efficiency in this study (Appendix Tables 6, 8, and 9) may be useful as prior distributions in future studies. Pre-fishing environmental factors (the Kuroshio path [Figs. 35 and 36] and water temperature [Figs. 31d and 32]) are likely to correlate with initial stock abundance; therefore, these surveys should also help improve the accuracy of stock assessment and management. In addition, further consideration on the fishery side is possible. For example, delaying the first fishing day or controlling the number of fishing vessels per day to increase the number of fishing days (sample size) may be effective in increasing the accuracy of the estimates (Table 4). Delaying the first fishing day until the recruitment completion day may also effectively decrease the bias of the estimates owing to recruitment during the fishing season.

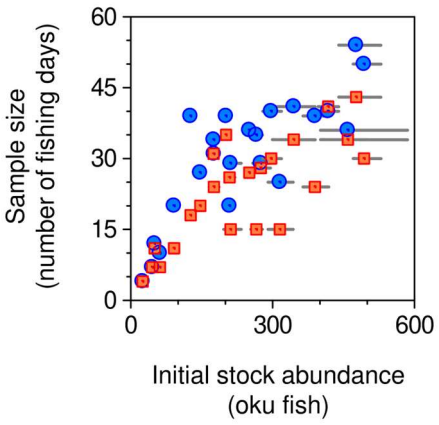

Fig. 39. Relationships between the initial stock abundance and sample size in the *Ammodytes japonicus* fishery in Ise Bay from 1993 to 2015. Circle: Mie Prefecture; Rectangle: Aichi Prefecture. Horizontal line: 90% credible interval. Unit oku represents 100 million. The data are based on Table 1 and Fig. 12.

CONCLUSIONS

Since the 2010s, the habitat of *A. japonicus* has disappeared from Ise Bay in the summer owing to high water temperatures. This disappearance and changes in the Kuroshio path after the 2010s may have caused a notable decrease in stock abundance and the inability to recover. In harsh environments, using *A. japonicus* stocks for fisheries is challenging. However, should environmental conditions improve and signs of stock recovery be observed in the future, the results of this study should inform discussions on more appropriate assessment and management by fishery stakeholders.

ACKNOWLEDGMENTS

This study results from a project by the Mie Prefecture to construct a new stock management system using ICT from 2021 to 2023. The data used in the analysis were collected over many years by the fishery cooperatives concerned in the Mie and Aichi prefectures, some of which were collected through the Fisheries Agency's stock assessment survey projects. I would like to express my deepest gratitude to all the organizations involved. I would also like to thank the staff of the Suzuka Branch of the Mie Prefecture Fisheries Research Institute for their cooperation in digitizing the vast amount of data and providing photographs. I thank Dr. Toshihiro Yamamoto of the Japan Fisheries Research and Education Agency; Motohiko Nakamura, Yuuki Shimomura, Tetsu Imaizumi, and Munehiko Uemura of the Aichi Fisheries Research Institute; Kingo Tsumoto of the Mie Prefecture Fisheries Promotion Association; Shigeyuki Hayashi and Masahiro Kuno of the Mie Prefecture Department of Agriculture, Forestry, and Fisheries; and the late Takao Ishikawa, formerly of the Mie Prefecture Fisheries Research Institute, for their guidance in the stock assessment of the *A. japonicus* fishery in Ise Bay. I thank Dr. Yasushi Tsuchihashi of the Mie Prefecture Fisheries Research Institute, Dr. Koichi Fujita of the Mie Prefecture Department of Agriculture, Forestry, and Fisheries, and Dr. Hirokatsu Yamada of the Mie Prefecture Environmental Conservation Agency for their helpful comments on the manuscript.

REFERENCES

Achiha, H. (2008). Where is the range of the bay of the Aichi Prefecture coast? Consideration of boundary of the Pacific Ocean, Ise Bay, Mikawa Bay, Chita Bay, and Atsumi Bay. Bulletin of the Aichi Fisheries Research Institute, **14**: 23–29. (in Japanese)

Aichi Prefecture (1994). Heisei 5 nendo shigenkanrigata gyogyo suishin sougou taisaku jigyo houkokusho (Koiki kaiyu shigen) [Annual report of the projects of comprehensive measures to promote fisheries that manage stock (species moving over wide areas) in 1993]: 1–45. Aichi Fisheries Research Institute, Gamagori. (in Japanese)

Akai, N. and Yoneda, M. (2021). Age-related variation in reproductive potential and influence on recruitment of western sand lance *Ammodytes japonicus* in the Seto Inland Sea, western Japan. Journal of Sea Research, **172**: 102036.

Amakawa, T. and Sekiguchi, S. (2015). Spatial Distributions of megabenthos as related to environmental characteristics in bottom waters of Ise Bay, central Japan. Bulletin on Coastal Oceanography, **53(1)**: 97–110.

Beverton, R. J. H. and Holt, S. J. (1957). On the dynamics of exploited fish populations. Her Majesty's Stationery Office, London.

DeLury, D. B. (1947). On the estimation of biological populations. Biometrics, **3(4)**: 145–167.

Fujita, K. (2002). Study on the relationship between the variation of the Kuroshio path to the south of Japan and the sea level difference between Kushimoto and Uragami. Bulletin of Fisheries Research Division, Mie Prefectural Science and Technology Promotion Center, **10**: 1–50.

Fujita, K., Nakanishi, N., and Maruyama, T. (2006). Annual report, **2005**: 106–107. Fisheries Research Division, Mie Prefectural Science and Technology Promotion Center, Shima. (in Japanese)

Fujita, K., Nakanishi, N., Maruyama, T., and T. Iwade, S. (2007). Annual report, **2006**: 104–105. Fisheries Research Division, Mie Prefectural Science and Technology Promotion Center, Shima. (in Japanese)

Fujiwara, M., Iwade, S., Hodokawa, K., and Mizutani, A. (2011). Annual report, **2010**: 89–90. Mie Prefecture Fisheries Research Institute, Shima. (in Japanese)

Fujiwara, M., Iwade, S., Hodokawa, K., and Oki, T. (2010). Annual report, **2009**: 92–93. Mie Prefecture Fisheries Research Institute, Shima. (in Japanese)

Fujita, K., Iwade, S., Oki, T, and Takagi, I. (2009). Annual report, **2008**: 83–84. Mie Prefecture Fisheries Research Institute, Shima. (in Japanese)

Fujiwara, M., Iwade, S., and Shimizu, Y. (2012). Annual report, **2011**: 71–72. Mie Prefecture Fisheries Research Institute, Shima. (in Japanese)

Fujiwara, M. and Shimizu, Y. (2013). Annual report, **2012**: 91–92. Mie Prefecture Fisheries Research Institute, Shima. (in Japanese)

Funakoshi, S. (1991). Isewan no ikanago no shigenkanri [Resource management of Ikanago in Ise Bay]. Fisheries Promotion, **283**: 1–58. Tokyo Fisheries Promotion Foundation, Tokyo. (in Japanese)

Funakoshi, S., Nakamura, M., Yanagibashi, S., and Tomiyama, M. (1997). Studies on the reproduction mechanisms of Japanese sandeel for the basis of the resource management system for Ikanago fisheries in and around Ise Bay. Bulletin of the Aichi Fisheries Research Institute, **4**: 11–22. (in Japanese with English abstract)

Gelman, A., J. B. Carlin and H. S. Stern, D. B. Dunson, A. Vehtari and D. B. Rubin (2013). Bayesian data analysis (3rd edition). Chapman and Hall/CRC.

Hashiguchi, S., Nishikawa, T., Uozumi, K., Furusawa, K., Mori, A., Imao. K., and Tanda, M. (2021). Causal factors of interannual decrease in stomach content index (SCI) of juvenile western sand lance *Ammodytes japonicus* in Harima-Nada, eastern Seto Inland Sea, Japan. Bulletin of the Japanese Society of Fisheries Oceanography, **85(1)**: 24–32. (in Japanese with English abstract)

Hayashi, B. (1985). Annual report, **1983**: 245–247. Fisheries Research Institute of Mie, Hamajima. (in Japanese)

Hayashi, S., Iwade, S., and Fujishima, H. (2014). Annual report, **2013**: 87–88. Mie Prefecture Fisiheries Research Institute, Shima. (in Japanese)

Hayashi, S., Iwade, S., and Katsuta, K. (2016). Annual report, **2015**: 97–98. Mie Prefecture Fisheries Research Institute, Shima. (in Japanese)

Hayashi, S., Iwade, S., Matsuoka, S., and Fujishima, H.

(2015). Annual report, **2014**: 5-22–5-23. Mie Prefecture Fisheries Research Institute, Shima. (in Japanese)

Hayashi, S., Yamada, D., and Katsuta, K. (2017). Annual report, **2016**: 90. Mie Prefecture Fisheries Research Institute, Shima. (in Japanese)

Itokawa, S. (1978a). Annual report, **1976**: 151–156. Mie Prefectural Ise Bay Fisheries Experimental Station, Suzuka. (in Japanese)

Itokawa, S. (1978b). Annual report, **1976**: 156–164. Mie Prefectural Ise Bay Fisheries Experimental Station, Suzuka. (in Japanese)

Itokawa, S. (1983). Annual report, **1983**: 65–80. Mie Prefectural Ise Bay Fisheries Experimental Station, Suzuka. (in Japanese)

Kakuta, I. (2006). Deoxygenation of enclosed coastal sea area and technologies for environmental improvement. Bulletin of the Society of Sea Water Science, Japan, **60(4)**: 238–242. (in Japanese)

Kamiya, N., Nakanishi, N., and Iwade, S. (2008). Annual report, **2007**: 91–92. Fisheries Research Division, Mie Prefectural Science and Technology Promotion Center, Shima. (in Japanese)

Kusakabe, T., Nakajima, M., Sano, M., and Watanabe, K. (2000). The influence of light intensity on the vertical distribution and feeding of Japanese sand lance *Ammodytes personatus* larvae in Osaka Bay. Nippon Suisan Gakkaishi, **66(4)**: 713–718. (in Japanese with English abstract)

Miyamura, M. and Sugino, T. (1959). Isewansan Ikanago (*Ammodytes personatus* Girard) ni tsuite. I sanranba, sanranki, chishi no ido [Ikanago (*Ammodytes personatus* Girard) in Ise Bay. I spawning ground, spawning season, migration of larvae]. Ise Bay Division, Mie Prefectural Fisheries Experimental Station, **1**: 1–9. (in Japanese)

Moriyasu, S. (1958). On the fluctuation of the Kuroshio south of Honshu (4) (The influence of the oceanographic conditions upon the monthly mean sea level). The Journal of the Oceanographical Society of Japan, **14(3)**: 1–8.

Mukai, R., Bando, M., and Kaikomaru crews (1988). Annual report, **1987**: 96–106. Aichi Fisheries Research Institute, Gamagori. (in Japanese)

Nakamura, M., Uemura, M., Hayashi, S., Yamada, T., Yamamoto, T. (2017). Ecology and Fishery Resources of Japanese Sand Lance *Ammodytes japonicus* in Ise Bay. Fisheries Biology and Oceanography in the Kuroshio, **18**: 3–15.

Nakajima, H., Sakaguchi, M., Yamada, H. (1986). Annual report, **1984**: 9–10. Mie Prefecture Fisheries Research Institute, Hamajima. (in Japanese)

Narita, T., Hanyu, K, and Sekiguchi, H. (2002). Relationships among oceanographic conditions, plankton biomass and commercial catch yields in Ise Bay, central Japan (Preliminary). Bulletin of Plankton Society of Japan, **49(2)**: 127–135. (in Japanese with English abstract)

Nishijima, S., Suzuki, S. Ichinokawa, M., and Okamura, H. (2019). Integrated multi-timescale modeling untangles anthropogenic, environmental, and biological effects on catchability. Canadian Journal of Fisheries and Aquatic Sciences, **76(11)**: 2045–2056.

Nishikawa, T., Y. Nakamura, S. Okamoto, and H. Ueda (2020). Interannual decrease in condition factor of the western sand lance *Ammodytes japonicus* in Japan in the last decade: Evidence for food-limited decline of the catch. Fisheries Oceanography, **29(1)**: 52–55.

Nishimura, A. (1993). Annual report, **1992**: 81–85. Mie Prefecture Fisheries Research Institute, Hamajima. (in Japanese)

Nishimura, A., Fujita, K., and Tsuchihashi, Y. (1991). Annual report, **1990**: 46–56. Mie Prefecture Fisheries Research Institute, Hamajima. (in Japanese)

Nishimura, A., Yamada, H., and Tsuchihashi, Y. (1993). Annual report, **1992**: 68–80. Mie Prefecture Fisheries Research Institute, Hamajima. (in Japanese)

Phiri, H., K. Shirakihara and T. Yamakawa (1999). A generalized DeLury's method based on Taylor's Power Law and its application to a pelagic species in southern Lake Tanganyika. Fisheries science, **65(5)**: 717–720.

R Core Team (2024). R: A language and environment for statistical computing. R Foundation for Statistical Computing. https://www.r-project.org/.

Ricker, W. E. (1954). Stock and recruitment. J. Fish. Res. Bd. Can., 11(5), 559–623.

Roa-Ureta, R. H. (2012). Modelling in-season pulses of recruitment and hyperstablility-hyperdepletion in the *Loligo gahi* fishery around the Falkland Islands with generalized depletion models. ICES Journal of Marine Science, **69(8)**: 1403–1415.

Sekiguchi, H. (1978). Biology of cladocerans and copepods in Ise Bay, central Japan-1. Seasonal cycles of the dominant species. Bulletin of the Faculty of Fisheries, Mie University, **5**: 13–23.

Sekiguchi, H. (1985). Biology of cladocerans and copepods in Ise Bay-2. Vertical distribution of neritic copepods in relation to their life histories. Bulletin of the Faculty of Fisheries, Mie University, **12**: 1–12.

Sekiguchi, H., M. Nagoshi, K. Horiuchi and N. Nakanishi (1976). Feeding, fat deposits and growth of sand-eels in Ise Bay, central Japan. Bulletin of the Japanese Scientific Fisheries, **42(8)**: 831 – 835.

Signorell, A. (2024). DescTools: Tools for Descriptive Statistics. R package version 0.99.54. https://CRAN.R-project.org/package=DescTools.

Stan Development Team (2024). RStan: The R interface to Stan. R package version 2.32.6. https://mc-stan.org/.

Taylor, R. (1961). Aggregation, variance and the mean. Nature, **189**: 732–735.

Tsumoto, K., Fujita, K., Mie Prefecture Tsu Agriculture, Fisheries and Commerce Depertment, and Aichi Fisheries Research Institute (2005). Annual report, **2004**: 96–98. Fisheries Research Division, Mie Prefectural Science and Technology Promotion Center, Shima. (in Japanese)

Tsumoto, K. and Itokawa, S. (1989). Annual report, **1988**: 18–21. Mie Prefecture Fisheries Research Institute, Hamajima. (in Japanese)

Tokai, T. and Mtsuhashi, T. (1998). SELECT model for estimating selectivity curve from comparative fishing experiments. Bulletin of the Japanese Society of Fisheries Oceanography, **62(3)**: 235–247. (in Japanese with English abstract)

Tomiyama, M. (1996). Atsumi gaikai no Ikanago [*Ammodytes japonicus* in Atsumi Outer Sea]. Fisheries Biology and Oceanography in the South-Western Waters of Japan, **12**: 59–60. (in Japanese)

Tomiyama, M. (2002). Shigenhyouka taisei kakuritsu suishin jigyo houkokusyo [Report on the project to promote the establishment of a stock assessment system]: 32–46. Japan Fisheries Resource Conservation Association, Tokyo. (in Japanese)

Tomiyama, M. (2003). Stock recovery of Japanese sandeels (GIRARD) *Ammodytes personatus* in Ise bay during the fishing season of 2001. Bulletin of the Aichi Fisheries Research Institute, **10**: 37–44. (in Japanese with English abstract)

Tomiyama, M. and Komatsu, T. (2006). Effects of temperature on growth and recruitment during early life history of the Japanese sandeel in Ise Bay. Bulletin of the Japanese Society of Fisheries Oceanography, **70(2)**: 114–121. (in Japanese with English abstract)

Tomiyama, M. Lesage, C., and Komatsu, T. (2005). Practice of sandeel fisheries management in Ise Bay toward responsible and sustainable fisheries. Global Environmental Research, **9(2)**: 139–149.

Tomiyama, M. and Nakamura, M. (1998). Annual report, **1997**: 84–86. Aichi Fisheries Research Institute, Gamagori. (in Japanese)

Uzaki, N. and Aoyama, T. (2012). Annual report, **2011**: 102–103. Aichi Fisheries Research Institute, Gamagori. (in Japanese)

Uzaki, N., Aoyama, T., Osawa, H., Shiota, H., Kabeya, N., Matsumoto, T., Matsuzawa, T., and Furuhashi, T. (2013). Annual report, **2012**: 68–69. Aichi Fisheries Research Institute, Gamagori. (in Japanese)

Uzaki, N., Fujiwara, M., and Katayama, S. (2010). Approaches and issues on fisheries management of Pacific sandeel, *Ammodytes personatus*, in Ise Bay and Mikawa Bay. Fisheries biology and oceanography in the Kuroshio, 11: 25–28.

Uzaki, N., Kato, T., Oasawa, H., Shiota, H., Kabeya, N., Matsumoto, T., Matsuzawa, T., and Furuhashi, T. (2014). Annual report, **2013**: 70–71. Aichi Fisheries Research Institute, Gamagori. (in Japanese)

Uzaki, N. and Takeda, K. (2011). Annual report, **2010**: 92–93. Aichi Fisheries Research Institute, Gamagori. (in Japanese)

Uzaki, N., Sawada, T., and Kato, T. (2015). Annual report,

2014: 97– 99. Aichi Fisheries Research Institute, Gamagori. (in Japanese)

Yamada, H. (2011). Studies on the mechanisms of recruitment determination of Japanese sand lance *Ammodytes personatus* in Ise Bay. Bulletin of Mie Prefecture Fisheries Research Institute, **20**: 1–77.

Yamada, H., Mizuno, T., Sakaguchi, K., Ishikawa, T., Mie Prefecture Tsu Agriculture, Fisheries and Commerce Department, and Aichi Fisheries Research Institute (2001). Annual report, **2000**: 77–80. Fisheries Research Division, Mie Prefectural Science and Technology Promotion Center, Hamajima. (in Japanese)

Yamada, H., Nishimura, A., Tsuchihashi, Y., and Kuno, M. (1999a). Nutritional condition and reproductive potential of sand lance *Ammodytes personatus* in Ise Bay. Bulletin of the Japanese Society of Fisheries Oceanography, **63(3)**: 22–29. (in Japanese with English abstract)

Yamada, S. and Sawada, T. (2008). Annual report, **2007**: 97–98. Aichi Fisheries Research Institute, Gamagori. (in Japanese)

Yamada, H., Tsumoto, K., and Kuno, M. (1998). Cannibalistic mortality of larval sand eel *Ammodytes personatus* by adults in Ise Bay central Japan. Nippon Suisan Gakkaishi, **64(5)**: 807–814. (in Japanese with English abstract)

Yamada, H., Tsumoto, K., Ikeda, T., and Ishikawa, T. (1994). Annual report, **1993**: 73–78. Mie Prefecture Fisheries Research Institute, Hamajima. (in Japanese)

Yamada, H., Tsumoto, K., Kuno, M., and Ishikawa, T. (1995). Annual report, **1994**: 76–82. Mie Prefecture Fisheries Research Institute, Hamajima. (in Japanese)

Yamada, H., Yamakawa, T., Kuno, M., Ishikawa, T., Mie Prefecture Tsu Agriculture, Fisheries and Commerce Department, and Aichi Fisheries Research Institute (1999b). Annual report, **1998**: 62–66. Fisheries Research Division, Mie Prefectural Science and Technology Promotion Center, Hamajima. (in Japanese)

Yamamoto, T., Sakaji, H., and Kuroki, H. (2019). Stock assessment and evaluation for *Ammodytes japonicus* in Ise and Mikawa Bay, **2018**: 1637–1651. Marine fisheries stock assessment and evaluation for Japanese waters. Japan Fisheries Agency and Japan Fisheries Research and Education Agency, Tokyo.

Yamashita, Y, D. Kitagawa, and T. Aoyama. (1985). Diel vertical migration and feeding rhythm of the larvae of the Japanese sand-eel *Ammodytes personatus*. Bulletin of the Japanese Society of Scientific Fisheries, **51(1)**: 1–5.

Yanagibashi, S., Funakoshi, S., Mukai, R., and Nakamura, M. (1997). Mechanisms of the maturation and spawning of Japanese sandeel *Ammodytes personatus* GIRARD in and around Ise Bay with special reference to their survival during the estivation period. Bulletin of the Aichi Fisheries Research Institute, **4**: 23–31. (in Japanese with English abstract)

Yoshida T, Shimohira Y, Rinno H, Yokouchi K, and Akiyama H (2006). Criteria for the determination of a large meander of the Kuroshio based on its path information. Oceanographic Society of Japan, **15**: 499–507. (in Japanese with English abstract)

SUPPLEMENT A

Simulated data with small recruitment during the fishing season were generated by setting φ_1 to values in 2004 when the annual recruitment rate was the smallest from 1993 to 2015 (Table A1; Fig. 14). Simulated data with large recruitment during the fishing season were generated by setting φ_1 to values in 1996, when the annual recruitment rate was approximately 0.825, the median from 1993 to 2015 (Table A1; Fig. 14).

Simulated data without variations in fishing gear efficiency were generated by setting σ_η to zero (Table A1). Simulated data with variations in the fishing gear efficiency were generated by setting σ_η to 0.856, which was the median between 1993 and 2015 (Table A1; Appendix Table 9). Simulated data with a small sample size were generated by setting η_0 to −6.08, which was the median from 1993 to 2015 (Table A1; Appendix Table 9). Simulated data with a large sample size were generated by setting η_0 to −7.19, which was a mean of the median and the maximum value during 1993–2015 to be for convenience close to the actual sample size (Table A1; Appendix Table 9). The initial stock abundance was set at 211 oku fish, and simulation data were generated until the day the true final stock abundance fell below 2.2 oku fish owing to fishing. The 2.2 oku fish were the median of the final stock abundance from 1993 to 2015 (Fig. 22; Appendix Table 7). Because the median of the actual ratio of fishing days to fishing season was 0.47, fishing days were randomly set for each dataset at this probability. Based on the fishing data for each year in Mie Prefecture, the slope and intercept of a single regression model with the fishing day as the explanatory variable (t) and the number of fishing vessels at fishing day t as the dependent variable (X_t) were estimated to have a median slope of −0.45 and a median intercept of 80. The numbers of fishing vessels in Mie Prefecture in each dataset were assumed to be random numbers following Poisson distributions with estimates using this regression equation as the expected values. The numbers of fishing vessels for Aichi Prefecture in each dataset were random numbers that followed Poisson distributions, with the expected value obtained by dividing the estimates of the regression equation for Mie Prefecture by 0.55. However, because the lowest CPUE in actual fishing was 30 kg per vessel, fishing was terminated if the mean CPUE in both prefectures fell below 30 kg per vessel. Because the median of the actual sampling rates of fishing vessels for body length composition was 0.2, the number of vessels sampled in each dataset were random numbers following this probability. The number of caught fish, measured in terms of body length, was 100 per vessel. For the other parameters, the median of the actual values from 1993 to 2015 was used (Table A1). The variations in the state and observation processes were assumed to follow the probability distribution presented in the text.

As shown in Equation (10), the estimation of stock abundance using DeLury's and Phiri's models in the *Ammodytes japonicus* fishery in Ise Bay assumes that the mean weights $\overline{w}_{t,\mathrm{Mie}}$ and $\overline{w}_{t,\mathrm{Aichi}}$ of the caught fish are known. However, actual observations often contain missing data. In published assessments, if values were observed before and after the missing date, the mean of those values was used instead of the missing value; if no values were observed before or after, the values of the adjacent observation date were used. In addition, some treatments did not follow these rules, and the method of providing them was unclear. Therefore, in the estimation of stock abundance using the conventional models, the estimated value $\hat{\overline{w}}_t$ by the following equation was assigned to the missing data, and the $\overline{w}_{t,\mathrm{Mie}}$ was substituted with $\overline{w}_{t,\mathrm{Aichi}}$.

$$\hat{\overline{w}}_t = \exp(b_2 + b_3\, t), \qquad \text{(A-1)}$$

where b_2 and b_3 are obtained by fitting the log-transformed simple regression model of Equation (A-1) to the observed values of $\overline{w}_{t,\mathrm{Mie}}$ in Equation (10) using the least-squares method in each dataset.

Table A1. Conditions and their setting of parameters to generate simulation data

	Scenario							
Condition	i	ii	iii	iv	v	vi	vii	viii
Recruitment	Small				Large			
Variation in fishing gear efficiency	None		Some		None		Some	
Sample size	Large	Small	Large	Small	Large	Small	Large	Small
Parameter	Setting of value in each scenario							
$\varphi_{1,1}$	0.018				0.699			
$\varphi_{2,1}$	0.002				0.069			
$\varphi_{3,1}$	0.073				0.158			
$\varphi_{4,1}$	0.868				0.067			
$\varphi_{5,1}$	0.038				0.007			
$\varphi_{6,1}$	0.001				0.000			
$\varphi_{7,1}$	0.000				0.000			
$\varphi_{8,1}$	0.000				0.000			
$\varphi_{9,1}$	0.000				0.000			
$\varphi_{10,1}$	0.000				0.000			
$\varphi_{11,1}$	0.000				0.000			
σ_η	0.000		0.856		0.000		0.856	
η_0	−7.19	−6.08	−7.19	−6.08	−7.19	−6.08	−7.19	−6.08
λ_1	211							
ω_0	2							
ω_1/σ_ω	0.48							
ω_2/σ_ω	−1.04							
ω_3/σ_ω	−1.36							
ω_4/σ_ω	−0.51							
ω_5/σ_ω	−0.19							
ω_6/σ_ω	0.03							
ω_7/σ_ω	0.28							
ω_8/σ_ω	0.65							
ω_9/σ_ω	1.01							
$\omega_{10}/\sigma_\omega$	0.56							
$\omega_{11}/\sigma_\omega$	0.00							
σ_ω	4.1							
σ_τ	3.76							
μ_1	25.2							
σ_l	2.81							
σ_ζ	1.23							
γ_1	−14.3							
γ_2	3.46							
$\sigma_{\log\bar{W}}$	0.08							

Recruitment, variation in fishing gear efficiency, and sample size were controlled by $\varphi_{i,1}$, σ_η, and η_0, respectively. i indicates the number of size classes. σ_η, σ_ω, σ_τ, σ_ζ, and $\sigma_{\log\bar{W}}$ represent root of σ_η^2, σ_ω^2, σ_τ^2, σ_ζ^2, and $\sigma_{\log\bar{W}}^2$, respectively.

SUPPLEMENT B

The water temperature and DO from 1993 to 2022 used in the analysis of this study were observed by Mie Prefecture Fisheries Research Institute using the system manufactured by Sea-Bird Scientific (Fig. 2). These observations were conducted monthly during the downcasting of the instruments from the sea surface to the sea bottom and upcasting from the sea bottom to the sea surface at each measurement point. However, data were not recorded during downcasting for some years (mainly from 1996 to 2002). Therefore, in this study, I estimated these missing values by the Bayesian method, assuming that the value of the bathymetric series i on observation t ($\delta_{i,t}$) for each measurement point follows a following multivariate normal distribution:

$$\begin{bmatrix}\delta_{1,t}\\ \delta_{2,t}\\ \vdots\\ \delta_{7,t}\end{bmatrix} \sim \mathrm{MultiNormal}\left(\begin{bmatrix}\mu_1\\ \mu_2\\ \vdots\\ \mu_7\end{bmatrix}, \begin{bmatrix}\sigma_1^2 & \sigma_1\sigma_2 & \cdots & \sigma_1\sigma_7\\ \sigma_2\sigma_1 & \sigma_2^2 & \cdots & \sigma_2\sigma_7\\ \vdots & \vdots & \ddots & \vdots\\ \sigma_7\sigma_1 & \sigma_7\sigma_2 & \cdots & \sigma_7^2\end{bmatrix}\right), \tag{B-1}$$

where the bathymetric series numbers i = 1–3 represent depths of 0, 10, and 20 m on downcasting. i = 4–6 represent depths of 0, 10, and 20 m on the upcasting, respectively. i = 7 represents a depth of 1 m immediately above the sea bottom. Series of 20 m (i = 3 and 6) were excluded for the shallow water points. The μ_i represents the mean value in series i, $\sigma_i\sigma_j$ represents the covariance between series i and series j. The σ_i^2 represents $\sigma_i\sigma_i$.

In this study, if available, the observed values on the downcasting were used; if observations on the downcasting were missing, the median values of the MCMC samples were used as estimates of the values. The estimation showed a slight difference in water temperature values between downcasting and upcasting; however, for DO, the values for upcasting were lower than those for downcasting.

Appendix Table 1. Fishing ban dates in a partial fishing area in the *Ammodytes japonicus* fishery in Ise Bay from 1993 to 2015

Year	First fishing date	Fishing ban date in a partial area of Ise Bay			Last fishing date
		First area	Second area	Third area	
1993	February 12	April 18			May 9
1994	February 27	March 26			April 29
1995	March 29				May 14
1996	March 3	April 14	April 24		May 19
1997	March 6	April 2	April 11		April 30
1998	February 22	March 23			March 30
1999	March 7	April 4	April 9		May 13
2000	March 6	April 1			March 31
2001	March 6	March 25	March 27		May 24
2002	February 24	April 30			May 30
2003	February 22	April 6			April 29
2004	March 4	April 4	April 16		May 28
2005	March 8	April 3	April 10	April 24	May 29
2006	March 9	May 9			June 18
2007	February 27	April 8			April 30
2008	March 2	March 23	April 13		April 30
2009	March 8	March 13	March 16		March 25
2010	March 3	April 11	April 25		June 9
2011	March 11	March 31	April 21		May 26
2012	March 8	April 13			June 7
2013	February 28	March 21	April 1	April 21	June 2
2014	March 2	March 26	April 13		May 15
2015	March 6	March 15	March 22	April 12	March 31

Modified unpublished data collected by the Aichi Prefecture Fisheries Institute. The ban areas varied annually.

Appendix Table 2. Mean percentage error and root mean square percentage error for the bucket numbers using the integrated model for the *Ammodytes japonicus* fishery in Ise Bay from 1993 to 2015

Year	Bucket numbers in Mie Prefecture				Bucket numbers in Aichi Prefecture			
	MPE		RMSPE		MPE		RMSPE	
	Median	PPP	Median	PPP	Median	PPP	Median	PPP
1993	−0.5	0.47	6.7	0.52	−0.4	0.53	6.7	0.48
1994	−0.9	0.48	10.1	0.52	−1.0	0.57	9.9	0.41
1995	−0.2	0.48	4.7	0.50	−0.2	0.51	4.6	0.51
1996	−1.8	0.49	14.0	0.51	−1.8	0.53	13.9	0.44
1997	−0.7	0.47	8.1	0.52	−0.6	0.55	7.9	0.46
1998	−0.3	0.48	6.5	0.49	−0.4	0.52	6.5	0.50
1999	−0.6	0.46	8.3	0.54	−0.7	0.54	8.2	0.48
2000	−0.5	0.48	5.8	0.50	−0.3	0.50	5.8	0.49
2001	−1.1	0.47	10.4	0.50	−1.1	0.54	10.4	0.46
2002	−1.2	0.51	11.3	0.46	−1.2	0.59	11.3	0.33
2003	−3.0	0.48	17.9	0.46	−2.5	0.65	17.5	0.31
2004	−0.5	0.54	7.6	0.48	−0.6	0.46	7.6	0.54
2005	−0.5	0.49	7.4	0.51	−0.5	0.53	7.3	0.49
2006	−0.7	0.48	8.2	0.50	−0.7	0.51	8.1	0.51
2007	−0.3	0.49	6.0	0.49	−0.3	0.54	6.0	0.40
2008	−0.3	0.54	5.7	0.50	−0.4	0.46	5.8	0.50
2009	−0.5	0.48	5.4	0.51	−0.2	0.50	5.4	0.50
2010	−1.4	0.55	12.9	0.48	−1.5	0.48	12.9	0.46
2011	−2.4	0.46	16.6	0.53	−2.4	0.56	16.6	0.45
2012	−1.9	0.52	14.8	0.49	−1.9	0.52	14.6	0.51
2013	−0.9	0.50	9.5	0.51	−0.7	0.51	9.3	0.49
2014	−0.7	0.43	8.5	0.52	−0.7	0.59	8.4	0.43
2015	−0.4	0.49	5.9	0.50	−0.3	0.51	5.8	0.50

MPE, mean percentage error; RMSPE, root mean square percentage error; Median, median based on the Markov chain Monte Carlo (MCMC) samples (n = 2000); PPP, posterior predictive p-value based on the MCMC samples (n = 2000).

Appendix Table 3. Mean percentage error and root mean square percentage error for the mean body length using the integrated model for the *Ammodytes japonicus* fishery in Ise Bay from 1993 to 2015

Year	MPE		RMSPE	
	Median	PPP	Median	PPP
1993	0.0	0.72	1.5	0.74
1994	0.0	0.71	1.8	0.70
1995	0.0	0.66	1.5	0.41
1996	0.0	0.78	1.8	0.31
1997	0.0	0.78	1.7	0.11
1998	0.0	0.73	1.9	0.33
1999	0.0	0.81	1.6	0.15
2000	0.0	0.73	1.8	0.22
2001	0.0	0.78	1.6	0.18
2002	0.0	0.81	1.4	0.19
2003	0.0	0.75	1.6	0.05
2004	0.0	0.88	1.4	0.09
2005	0.0	0.81	1.5	0.04
2006	0.0	0.76	1.5	0.22
2007	0.0	0.87	1.2	0.29
2008	0.0	0.79	1.9	0.04
2009	0.0	0.72	1.0	0.36
2010	0.0	0.81	1.9	0.12
2011	0.0	0.77	1.7	0.21
2012	0.0	0.79	1.3	0.15
2013	0.0	0.83	1.9	0.08
2014	0.0	0.77	1.9	0.04
2015	0.0	0.82	1.7	0.14

MPE, mean percentage error; RMSPE, root mean square percentage error; Median, median based on the Markov chain Monte Carlo (MCMC) samples (n = 2000); PPP, posterior predictive p-value based on the MCMC samples (n = 2000).

Appendix Table 4. Standardized 90% prediction intervals of the mean body length of fish caught in the *Ammodytes japonicus* fishery in Ise Bay from 1993 to 2015 and percentages of schools whose mean body length was included in the prediction interval

Year	Standardized prediction interval				*M*	Percentage
	n	Minimum	Median	Maximum		
1993	33	0.19	0.33	1.07	125	71
1994	23	0.18	0.33	0.49	112	73
1995	15	0.19	0.23	0.36	111	65
1996	32	0.24	0.40	0.54	323	78
1997	27	0.26	0.35	0.48	295	77
1998	11	0.31	0.39	0.52	175	71
1999	26	0.16	0.26	0.54	264	80
2000	7	0.35	0.37	0.41	127	75
2001	32	0.17	0.26	0.50	380	75
2002	31	0.09	0.18	0.43	503	82
2003	22	0.22	0.26	0.30	313	76
2004	26	0.16	0.23	0.33	259	88
2005	19	0.18	0.26	0.41	229	79
2006	40	0.11	0.17	0.34	419	76
2007	28	0.11	0.19	0.40	373	85
2008	19	0.23	0.27	0.40	293	79
2009	4	0.13	0.16	0.19	75	72
2010	45	0.17	0.20	0.46	532	81
2011	27	0.14	0.20	0.38	255	76
2012	33	0.13	0.15	0.28	397	79
2013	31	0.16	0.27	0.47	401	82
2014	28	0.09	0.18	0.27	274	73
2015	10	0.18	0.23	0.33	121	82

The prediction intervals were standardized by the median of the Markov chain Monte Carlo samples of the mean body length using the integrated model in each interval: the standardized prediction interval = (prediction interval 95% point − prediction interval 5% point)/median. *n*: number of the intervals shown in Fig. 7; *M*: school number observed its mean body length shown in Fig. 7.

Appendix Table 5. Scenarios of recruitment, variation in fishing gear efficiency, and sample size to generate datasets in simulation, and summary of estimates using the integrated, DeLury's, and Phiri's models in each scenario

	Scenario							
	i	ii	iii	iv	v	vi	vii	viii
(a) Condition to generate simulation data								
Recruitment	Small				Large			
Variation in fishing gear efficiency	None		Some		None		Some	
Sample size	Large	Small	Large	Small	Large	Small	Large	Small
(b) Initial stock abundance								
Median of ratios of initial stock abundance estimate to its true value in each model								
Integrated model	0.99	0.99	0.99	0.98	1.00	0.98	0.99	0.99
DeLury's model	0.98	0.97	0.97	0.99	1.13	1.17	1.11	1.09
Phiri's model	0.97	0.96	0.98	1.04	1.00	1.05	1.01	1.14
Percentage of true initial stock abundances included in 90% high-density interval of the estimate in each model								
Integrated model	73	86	78	87	85	86	88	93
DeLury's model	25	23	74	70	50	98	89	100
Phiri's model	1	7	21	54	36	81	51	70
(c) Final stock abundance								
Median of ratios of the final stock abundance estimate to its true value in each model								
Integrated model	1.01	1.00	0.87	1.08	1.00	1.03	1.29	1.35
DeLury's model	2.21	2.15	1.97	1.90	9.92	22.69	13.32	15.77
Phiri's model	1.02	1.09	1.32	7.71	1.83	9.29	3.28	20.64
Percentage of true final stock abundances included in 90% high-density interval of estimate in each model								
Integrated model	95	96	96	94	91	94	94	97
DeLury's model	81	98	95	90	35	96	94	99
Phiri's model	98	95	97	99	63	79	76	86

Medians and percentages were obtained based on 100 datasets in each scenario. Estimate: mode. The high-density intervals were calculated using the function 'density' with the default setting in R.

Appendix Table 6. The coefficients of the body length-to-weight conversion equation for the *Ammodytes japonicus* fishery in Ise Bay from 1993 to 2015

Year	Intercept coefficient (γ_1)			Slope coefficient (γ_2)			Standard deviation ($\sigma_{\log\bar{W}}$) × 100		
	CI 5%	Estimate	CI 95%	CI 5%	Estimate	CI 95%	CI 5%	Estimate	CI 95%
1993	−14.4	−14.2	−14.1	3.42	3.45	3.49	5.95	6.70	7.60
1994	−14.8	−14.5	−14.3	3.45	3.52	3.58	8.87	9.93	11.29
1995	−13.7	−13.6	−13.4	3.23	3.27	3.31	4.24	4.71	5.31
1996	−14.5	−14.3	−14.2	3.42	3.46	3.50	12.47	13.29	14.21
1997	−14.7	−14.6	−14.4	3.48	3.51	3.55	7.25	7.98	8.82
1998	−14.5	−14.3	−14.2	3.42	3.47	3.52	6.02	6.60	7.29
1999	−14.2	−14.1	−13.9	3.36	3.40	3.43	7.64	8.27	9.01
2000	−14.4	−14.1	−13.8	3.32	3.40	3.48	5.25	6.11	7.15
2001	−14.4	−14.2	−14.0	3.38	3.43	3.48	9.55	10.17	10.91
2002	−15.1	−15.0	−14.9	3.61	3.63	3.66	10.38	10.93	11.51
2003	−14.1	−13.8	−13.5	3.24	3.32	3.40	15.53	16.57	17.75
2004	−14.0	−13.9	−13.7	3.30	3.34	3.37	6.99	7.51	8.09
2005	−13.6	−13.4	−13.3	3.20	3.25	3.29	6.73	7.32	7.96
2006	−14.7	−14.6	−14.5	3.51	3.54	3.56	7.58	8.02	8.51
2007	−14.6	−14.5	−14.4	3.49	3.51	3.53	5.64	5.97	6.35
2008	−14.9	−14.7	−14.6	3.51	3.55	3.59	5.41	5.78	6.20
2009	−14.1	−13.8	−13.4	3.24	3.32	3.41	5.16	5.87	6.78
2010	−14.8	−14.6	−14.4	3.48	3.53	3.58	11.70	12.29	12.94
2011	−14.5	−14.3	−14.0	3.37	3.44	3.51	14.43	15.50	16.73
2012	−15.5	−15.3	−15.0	3.62	3.68	3.74	13.06	13.83	14.74
2013	−15.0	−14.9	−14.7	3.55	3.59	3.62	8.79	9.30	9.85
2014	−14.7	−14.6	−14.4	3.46	3.49	3.53	7.76	8.34	8.98
2015	−14.5	−14.3	−14.2	3.41	3.46	3.50	5.47	6.06	6.81

Equation: log(mean body weight) = $\gamma_1 + \gamma_2 \times$ log(mean body length); Estimate: median of the Markov chain Monte Carlo samples using the equation; CI: credible interval.

Appendix Table 7. The initial stock abundance and the final stock abundance of the *Ammodytes japonicus* fishery in Ise Bay from 1993 to 2015

Year	Initial stock abundance (λ_1)			Final stock abundance (N_{T+1})		
	CI 5%	Estimate	CI 95%	CI 5%	Estimate	CI 95%
1993	299	345	390	1.19	2.10	3.59
1994	290	315	343	0.256	3.236	11.138
1995	85.7	91.5	97.7	0.960	2.200	4.925
1996	364	390	419	0.187	0.840	2.266
1997	140	147	154	0.510	1.288	2.550
1998	46.7	50.4	54.3	0.170	0.641	1.835
1999	166	176	187	4.66	8.57	14.10
2000	37.0	45.4	64.8	7.17	15.11	34.43
2001	194	202	210	0.442	1.469	3.420
2002	396	418	440	0.812	2.410	5.714
2003	197	211	234	0.449	0.788	1.278
2004	401	459	585	106	164	289
2005	121	127	132	0.280	0.590	1.516
2006	470	493	529	4.57	10.72	21.44
2007	169	175	182	0.287	1.116	2.910
2008	199	209	220	11.2	17.0	25.0
2009	23.7	25.1	27.3	0.00165	0.31001	2.47230
2010	440	477	529	100	137	190
2011	258	275	295	1.96	6.08	12.64
2012	279	297	319	11.5	21.7	38.5
2013	254	265	278	7.39	12.94	20.60
2014	243	251	260	0.467	1.836	4.855
2015	58.3	61.8	67.4	0.0297	1.0070	4.5954

Estimate: median of the Markov chain Monte Carlo samples using the integrated model; CI: credible interval; Unit: oku fish (100 million fish).

Appendix Table 8. The selection model coefficients in the *Ammodytes japonicus* fishery in Ise Bay from 1993 to 2015

Year	Body length with selection probability 0.50 (μ_l)			Range from selection probability 0.25 to 0.75 (σ_l)		
	CI 5%	Estimate	CI 95%	CI 5%	Estimate	CI 95%
1993	16.8	21.0	24.8	0.781	2.529	3.972
1994	16.0	18.3	20.2	0.556	1.774	2.687
1995	17.1	21.8	25.3	0.772	2.552	4.694
1996	24.2	25.2	26.1	3.47	3.88	4.33
1997	26.9	27.8	28.7	4.12	4.57	5.08
1998	9.05	15.58	19.87	0.165	1.478	3.355
1999	16.7	20.7	24.5	0.708	2.331	3.784
2000	20.5	29.6	33.5	1.93	4.43	7.02
2001	27.7	28.8	30.2	5.16	5.62	6.14
2002	24.6	25.0	25.5	3.63	3.89	4.15
2003	27.9	28.6	29.3	4.22	4.64	5.08
2004	9.05	15.33	19.14	0.423	2.657	5.924
2005	34.0	34.9	35.7	6.06	6.52	6.92
2006	18.2	19.0	19.9	2.37	2.81	3.21
2007	25.2	25.8	26.4	3.33	3.62	3.94
2008	24.2	26.3	28.6	3.84	4.79	6.03
2009	27.6	32.4	35.3	0.144	0.878	2.431
2010	7.14	11.49	14.42	0.477	1.423	2.192
2011	25.8	26.9	27.9	4.88	5.28	5.73
2012	8.42	15.03	16.88	0.140	1.191	2.417
2013	15.6	16.8	17.8	0.573	1.713	2.516
2014	28.7	29.3	29.8	3.54	3.98	4.42
2015	26.4	29.3	31.4	0.488	1.567	2.379

Estimate: median of the Markov chain Monte Carlo samples using the integrated model; CI: credible interval; Unit: mm.

Appendix Table 9. Mean fishing gear efficiency and its daily variations of the *Ammodytes japonicus* fishery in Ise Bay from 1993 to 2015

Year	Mean fishing gear coefficient ($\exp(\eta_0)\ 10^3$)			Standard deviation of the daily fishing gear efficiencies on log scale (σ_η)		
	CI 5%	Estimate	CI 95%	CI 5%	Estimate	CI 95%
1993	1.73	2.10	2.55	0.537	0.639	0.767
1994	2.33	3.17	4.49	0.844	1.046	1.320
1995	1.19	1.86	2.80	0.641	0.796	1.051
1996	1.69	2.29	3.05	0.970	1.144	1.354
1997	1.78	2.30	2.94	0.678	0.814	0.989
1998	1.82	2.71	4.02	0.585	0.757	1.007
1999	0.568	0.727	0.935	0.547	0.658	0.801
2000	0.960	1.421	2.110	0.170	0.245	0.374
2001	1.75	2.22	2.83	0.861	0.992	1.165
2002	2.23	3.04	4.10	1.26	1.45	1.68
2003	5.56	7.06	8.98	0.528	0.649	0.814
2004	0.119	0.184	0.249	0.392	0.455	0.532
2005	4.46	5.98	8.07	0.878	1.038	1.255
2006	1.41	1.78	2.25	0.845	0.965	1.104
2007	3.16	4.25	5.70	1.09	1.26	1.49
2008	1.22	1.63	2.11	0.462	0.545	0.664
2009	6.68	13.87	36.17	0.500	0.936	1.956
2010	0.236	0.301	0.373	0.332	0.379	0.436
2011	2.31	3.04	3.97	0.755	0.902	1.089
2012	0.697	0.946	1.274	0.734	0.856	1.008
2013	1.76	2.17	2.63	0.466	0.556	0.669
2014	3.08	4.06	5.33	1.01	1.19	1.41
2015	5.85	9.57	16.96	0.774	1.072	1.598

Estimate: median of the Markov chain Monte Carlo samples using the integrated model; CI: credible interval.

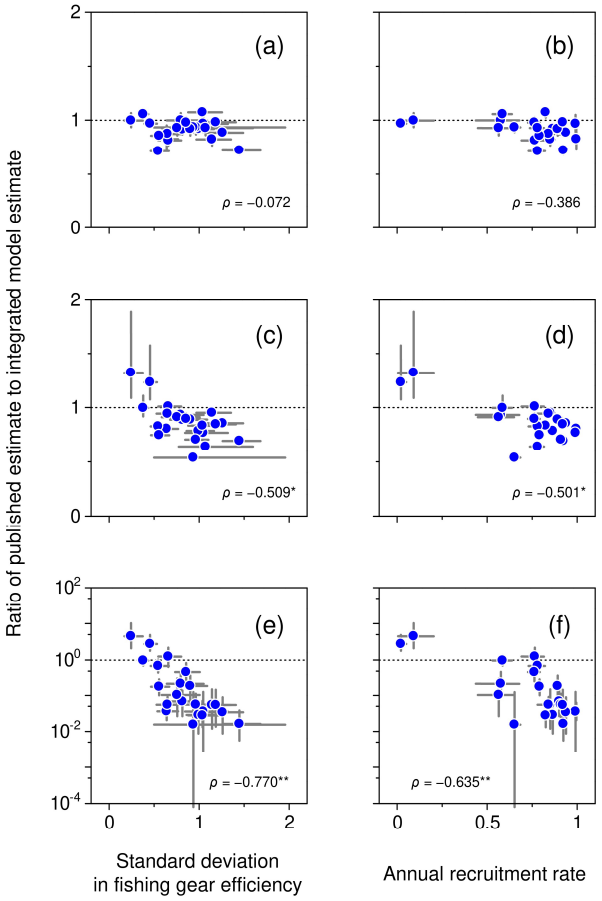

Plate 1. Effects of daily variation in fishing gear efficiencies and annual recruitment rates during the fishing season on ratio of the published estimates to the initial and final stock abundance estimates using the integrated model. (a) and (b) annual catch, (c) and (d) annual exploitation rate, (e) and (f) reproductive efficiency. Circle: median of the Markov chain Monte Carlo samples using the integrated model; Vertical and horizontal lines: 90% credible interval; ρ: Spearman's correlation coefficient; *: $p < 0.05$; **: $p < 0.01$; $n = 23$. The standard deviation denotes σ_η in the text.

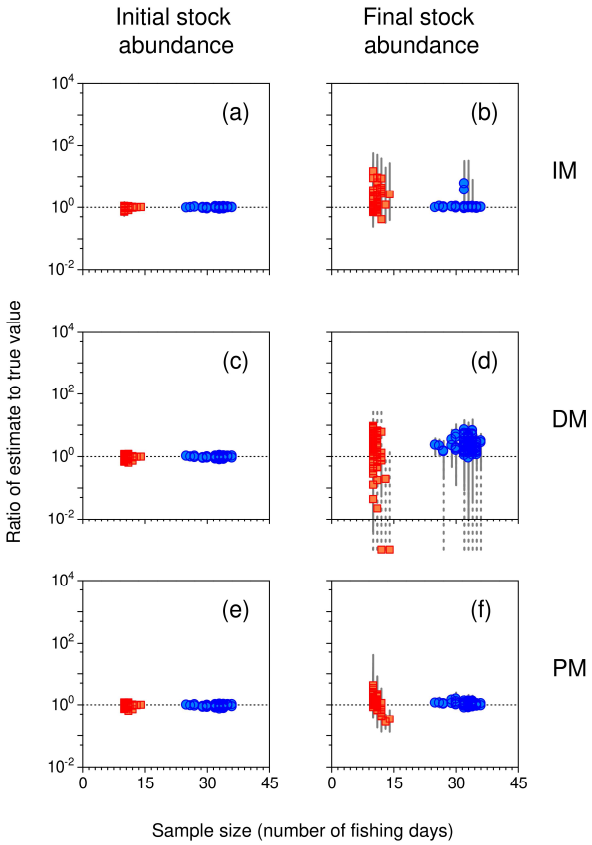

Plate 2. Relationships between sample size and ratio of stock abundance estimate to its true value in simulations. The simulation conditions were set up with a small recruitment rate and no variation in fishing gear efficiency (Scenarios i and ii in Table 4). (a) and (b) estimates using the integrated model (IM), (c) and (d) estimates using DeLury's model (DM), (e) and (f) estimates using the Phiri's model (PM). Rectangle: median of the Markov chain Monte Carlo (MCMC) samples of the ratio for the small sample size (Scenario ii in Table 4); Circle: median of MCMC samples of the ratio for a large sample size (Scenario i in Table 4); Rectangle outside frame: median of the ratio less than 0; Solid vertical line: 90% credible interval; Dotted vertical line: 90% credible interval with lower limit less than 0. Horizontal dotted line: ratio = 1.0 (unbiased).

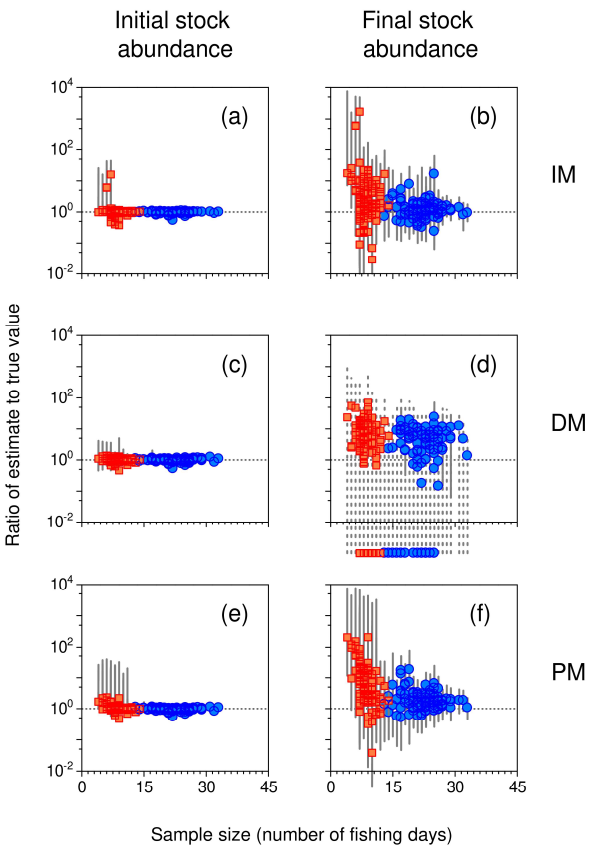

Plate 3. Relationships between sample size and ratio of stock abundance estimate to its true value in simulations. The simulation conditions were set up with a small recruitment rate and some variation in fishing gear efficiency (Scenario iii and iv in Table 4). (a) and (b) estimates using the integrated model (IM), (c) and (d) estimates using DeLury's model (DM), (e) and (f) estimates using Phiri's model (PM). Rectangle: median of the Markov chain Monte Carlo (MCMC) samples of the ratio for the small sample size (i.e., scenario iv in Table 4); Circle: median of MCMC samples of the ratio for the large sample size (Scenario iii in Table 4); Circle and rectangle outside frame: median of the ratio less than 0; Solid vertical line: 90% credible interval; Dotted vertical line: 90% credible interval with lower limit less than 0. Horizontal dotted line: ratio = 1.0 (unbiased).

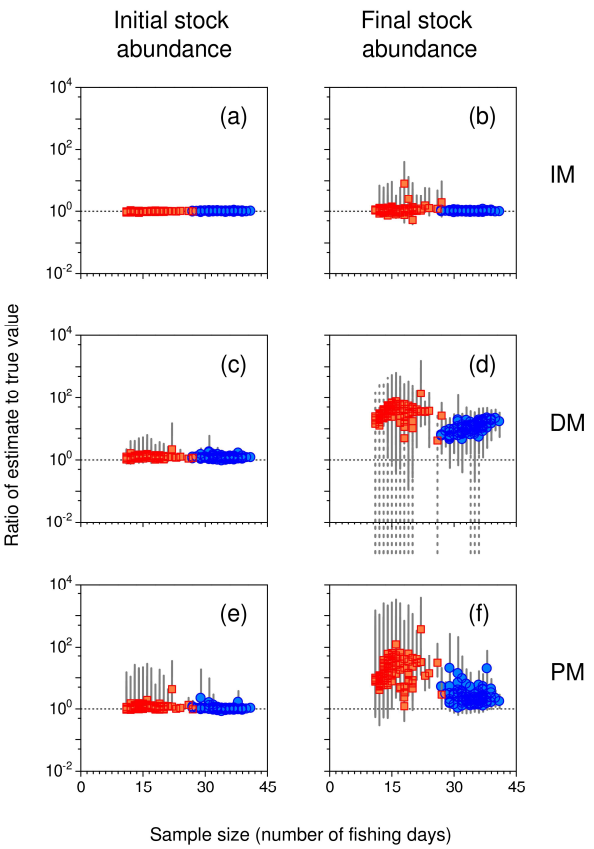

Plate 4. Relationships between sample size and ratio of stock abundance estimate to its true value in simulations. The simulation conditions were set up with large recruitment rate and no variation in fishing gear efficiency (Scenarios v and vi in Table 4). (a) and (b) estimates using the integrated model (IM), (c) and (d) estimates using the DeLury's model (DM), (e) and (f) estimates using Phiri's model (PM). Rectangle: median of the Markov chain Monte Carlo (MCMC) samples of the ratio for the small sample size (Scenario vi in Table 4); Circle: median of MCMC samples of the ratio for the large sample size (Scenario v in Table 4); Solid vertical line: 90% credible interval; Dotted vertical line: 90% credible interval with lower limit less than 0. Horizontal dotted line: ratio = 1.0 (unbiased).

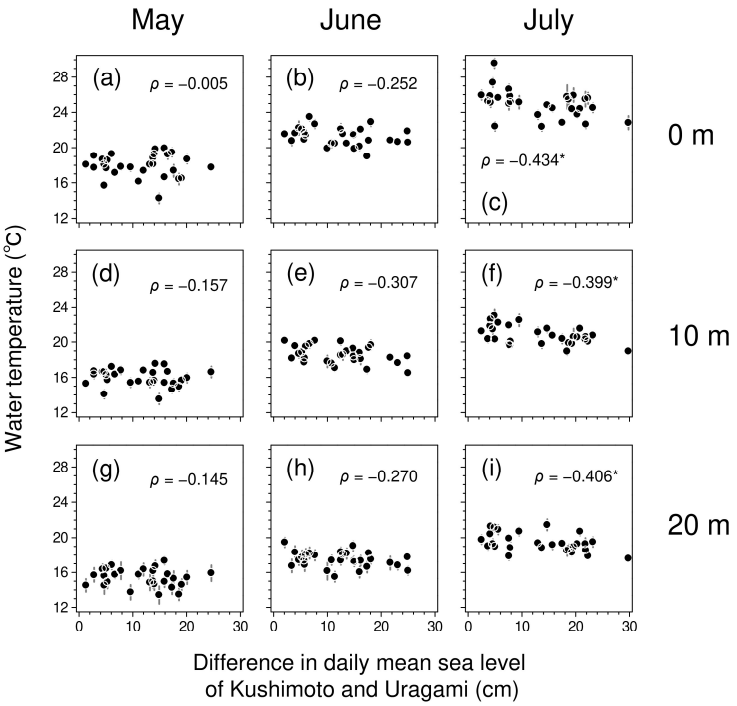

Plate 5. Relationships between the difference in daily mean sea level of Kushimoto and Uragami and the mean water temperature in Ise Bay from 1994 to 2022. (a), (b), and (c) 0 m depth; (d), (e), and (f) 10 m depth; (g), (h), and (i) 20 m depth. Circle: median of Markov chain Monte Carlo samples using the normal distribution model; Vertical line: 90% credible interval; ρ: Spearman's correlation coefficient; *: $p < 0.05$; $n = 29$. The differences were observed by the Japan Meteorological Agency, which were without credible intervals.

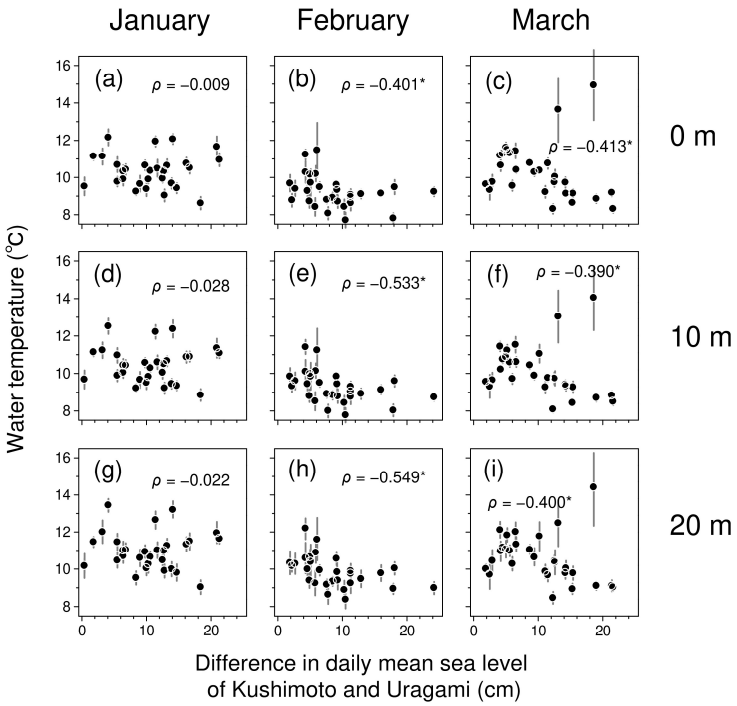

Plate 6. Relationships between the difference in daily mean sea level of Kushimoto and Uragami and the water temperature in Ise Bay from 1994 to 2022. (a), (b), and (c) 0 m depth; (d), (e) and (f) 0 m depth; (g), (h), and (i) 20 m depth. Circle: median of Markov chain Monte Carlo samples using the normal distribution model; Vertical line: 90% credible interval; ρ: Spearman's correlation coefficient; *: $p < 0.05$; $n = 29$. The differences were observed by the Japan Meteorological Agency, which were without credible intervals.

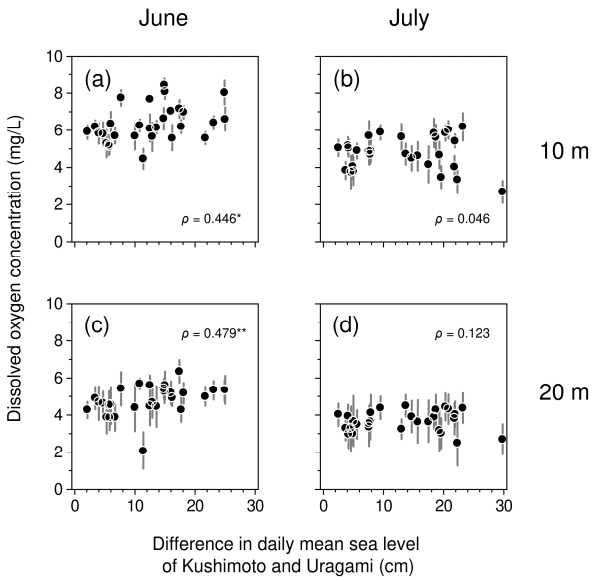

Plate 7. Relationships between the mean dissolved oxygen concentration in Ise Bay and the difference in daily mean sea level of Kushimoto and Uragami from 1994 to 2022. (a) and (b) 10 m depth, (c) and (d) 20 m depth. Circle: median of Markov chain Monte Carlo samples using the normal distribution model; Vertical line: 90% credible interval; ρ: Spearman's correlation coefficient; *: $p < 0.05$; **: $p < 0.01$; $n = 29$. The differences were observed by the Japan Meteorological Agency, which were without credible intervals.

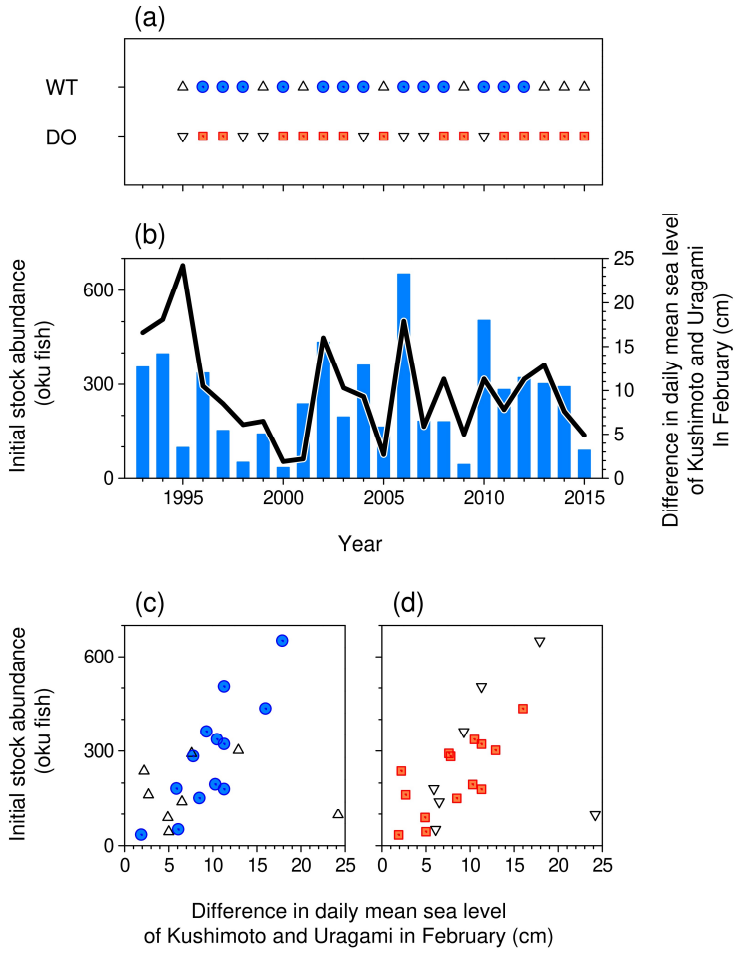

Plate 8. (a): The water temperature (WT) and dissolved oxygen concentrations (DO) at a depth of 10 m in Ise Bay in July of the previous year from 1995 to 2015. Triangle: WT above 21 ℃; Circle: WT below 21 ℃; Reverse triangle: DO below 4 mg/L; Rectangle: DO above 4 mg/L. The data are based on Fig. 30.

(b): The initial stock abundance in the *Ammodytes japonicus* fishery in Ise bay and the differences in daily mean sea level of Kushimoto and Uragami in February from 1993 to 2015. Bar: the published estimates of initial stock abundance; Line: the difference in daily mean sea level. Unit oku represents 100 million. The data are based on Yamamoto et al (2019) and Fig. 34b.

(c) and (d): Relationships between the initial stock abundance in the *A. japonicus* fishery in Ise Bay and the differences in daily mean sea level of Kushimoto and Uragami in February from 1995 to 2015. The data are based on panels a and b. Spearman's correlation coefficients in the circles and the rectangles are 0.762 ($p < 0.01$; $n = 13$) and 0.706 ($p < 0.01$; $n = 14$), respectively.

要　約

1. 伊勢湾のイカナゴの資源評価として，(1) 漁期中加入と漁具能率の日変動の影響を加味した資源量推定モデル（統合型モデル）の開発，(2) 統合型モデルを用いた初期資源尾数と残存資源尾数の再推定とそれらの公表値との比較，(3) 資源変動に対する環境要因（肥満度（餌環境），水温，溶存酸素濃度，黒潮流路）の影響の解析，(4) 資源評価・管理の展望，に取り組んだ。
2. 公表値の推定に利用されてきた DeLury のモデルや Phiri らのモデルは，伊勢湾のイカナゴ漁のように漁期中加入や漁具能率の日変動がある条件下では，残存資源尾数を過大推定する傾向があった。一方，本研究の統合型モデルは，そのような条件下でも偏りが小さい傾向があった。
3. 残存資源尾数の公表値は多くの年において管理目標値（20 億尾）を上回っていたが，統合型モデルによるそれら推定値は多くの年において 20 億尾を下回った。また，イカナゴ資源は 2015 年以降急減したが，それより前のいくつかの年の残存資源尾数は 2014 年と 2015 年のものより少なかった。加えて，統合型モデルを用いた資源尾数の推定値に対する Ricker 型や Beverton–Holt 型の再生産関係のモデルの当てはまりは悪く，適正な管理目標値を見出すことができなかった。現行の管理目標値は見直しが必要と考えられる。
4. 資源変動に対する水温と黒潮流路の影響が確認された。2010 年代以降の伊勢湾のイカナゴ資源の減少・低迷は，高水温化や黒潮流路の変化によるものと考えられる。
5. 現行の資源評価・管理方策では，資源量の推定精度の低さ，強い漁獲圧，不明瞭な再生産関係の影響により，期待した効果が得られない可能性がある。将来，環境が好転し資源の回復傾向が認められた場合には，本研究の結果を踏まえて，評価・管理方策を見直すことが望ましい。